MAGNETO-MECHANICAL DYNAMICS AT THE NANOSCALE

MAGNETO-MECHANICAL DYNAMICS AT THE NANOSCALE

Proefschrift

ter verkrijging van de graad van doctor
aan de Technische Universiteit Delft,
op gezag van de Rector Magnificus prof. ir. K. C. A. M. Luyben,
voorzitter van het College voor Promoties,
in het openbaar te verdedigen op dinsdag 20 december 2011 om 10:00 uur

door

Stefan BRETZEL

Diplom Physiker, Universität Konstanz,
geboren te Friedrichshafen, Duitsland.

Dit proefschrift is goedgekeurd door de promotor:

Prof. dr. ir. G. E. .W. Bauer

Samenstelling van de promotiecommissie:

Rector Magnificus	voorzitter
Prof. dr. ir. G. E. W. Bauer	Technische Universiteit Delft, promotor
Prof. dr. S. Maekawa	Tohoku University and JAEA, Japan
Prof. dr. T. Rasing	Radboud University Nijmegen
Prof. dr. A. G. G. M. Tielens	Universiteit Leiden
Prof. dr. ir. H. S. J. van der Zant	Technische Universiteit Delft
Dr. Y. M. Blanter	Technische Universiteit Delft
Dr. S. T. B. Gönnenwein	Bayerische Akademie der Wissenschaften, Duitsland
Prof. dr. Yu. V. Nazarov	Technische Universiteit Delft (reservelid)

CONTENTS

1

INTRODUCTION

1.1 MAGNETISM

Magnetism is probably the physical phenomenon that has captivated people's fascination the longest. It was first observed in terms of the attractive force that lodestone, a mineral rich in magnetite, exerted on iron. One of the first accounts of the attractive force of lodestone in Western literature was written by the pre-socratic philosopher Thales of Miletus (approx. 624 BC - 546 BC) and was later discussed by Socrates, as reported in the Platonic dialogue "Ion"[1].

The first application of magnetism is the compass used for navigation. Although its exact date of invention is unknown, it is usually credited to the Chinese. In 121 AD the first Chinese reference occurs that mentions the fact that lodestone can be used to magnetize a needle [1]. However, the actual use of a compass by the Chinese is only recorded much later and the first description of the actual use of a compass is thus attributed to Alexander Neckam (1157-1217), who mentions in his *De naturis rerum* a pivoted needle used by sailors to keep their course – a compass [2]. The compass is not only the first example of an application of magnetic phenomena, but also an example for a magneto-mechanical system, viz. a system in which the mechanical and magnetic degrees of freedom are coupled. Such systems are the focus of this thesis.

In the framework of classical electrodynamics, the magnetic moment is defined as the lowest order contribution to the multipole expansion of the magnetic field caused by a current distribution [3], as is demonstrated below. The Biot-Savart law states that a local current density distribution $\vec{j}$ creates a magnetic flux

density:

$$\vec{B}(\vec{x}) = \frac{1}{c}\int \mathrm{d}^3x'\, \vec{j}(\vec{x}') \times \frac{(\vec{x}-\vec{x}')}{|\vec{x}-\vec{x}'|^3} = \frac{1}{c}\nabla \times \int \mathrm{d}^3x'\, \frac{\vec{j}(\vec{x}')}{|\vec{x}-\vec{x}'|}\,. \tag{1.1}$$

In the case of steady state currents, *i.e.* when $\nabla\cdot\vec{j}=0$, the two Maxwell's equations for the magnetic flux density read

$$\nabla\cdot\vec{B}=0 \quad \text{and} \quad \nabla\times\vec{B}=\frac{4\pi}{c}\vec{j}. \tag{1.2}$$

Since $\nabla\cdot\vec{B}=0$, a vector potential $\vec{A}$ with $\vec{B}=\nabla\times\vec{A}$ can be introduced. The vector potential created by a current distribution $\vec{j}$ is of the form

$$\vec{A}(\vec{x}) = \frac{1}{c}\int \mathrm{d}^3x'\, \frac{\vec{j}(\vec{x}')}{|\vec{x}-\vec{x}'|} + \nabla\psi\,, \tag{1.3}$$

where ψ is an arbitrary scalar function that can be freely chosen. Using the Coulomb gauge, $\nabla\cdot\vec{A}=0$, Eq. (1.2) yields

$$\Delta\vec{A} = -\frac{4\pi}{c}\vec{j}\,, \tag{1.4}$$

i.e. the components of $\vec{A}$ in Cartesian coordinates fullfill the Poisson equation. Using

$$\Delta\frac{1}{|\vec{x}-\vec{x}'|} = -4\pi\delta(\vec{x}-\vec{x}') \tag{1.5}$$

and Eq. (1.3) in Eq. (1.4) one finds $\Delta\psi=0$. Since $\Delta\psi=0$ has to hold true in all space, it needs to vanish identically. Thus, one finds the vector potential generated by a current distribution to be

$$\vec{A}(\vec{x}) = \frac{1}{c}\int \mathrm{d}^3x'\, \frac{\vec{j}(\vec{x}')}{|\vec{x}-\vec{x}'|} \tag{1.6}$$

when the Coulomb gauge, $\nabla\cdot\vec{A}=0$, is used.

The magnetic moment is now introduced by performing a series expansion of the vector potential $\vec{A}(\vec{x})$ created by a local current distribution in a small volume V', that is far from the observer at $\vec{x}$. We can expand the denominator in Eq. (1.6) as

$$\frac{1}{|\vec{x}-\vec{x}'|} = \frac{1}{|\vec{x}|} + \frac{\vec{x}\cdot\vec{x}'}{|\vec{x}|^3} + \cdots\,. \tag{1.7}$$

Since for steady state currents $\nabla\cdot\vec{j}=0$ the zeroth order term in the expansion of $\vec{A}(\vec{x})$, Eq. (1.6), drops out and we are left with

$$\vec{A}(\vec{x}) = \frac{1}{c|\vec{x}|^3}\int \mathrm{d}^3x'\, \vec{j}(\vec{x}')(\vec{x}\cdot\vec{x}') + \cdots = -\frac{\vec{x}}{2c}\times\int \mathrm{d}^3x'\left[\vec{x}'\times\vec{j}(\vec{x}')\right] + \cdots\,. \tag{1.8}$$

The magnetic moment $\vec{\mu}$ can now be defined as

$$\vec{\mu} = \frac{1}{2c} \int \mathrm{d}^3 x' \, \vec{x}' \times \vec{j}(\vec{x}') \,. \tag{1.9}$$

The force acting on a current distribution $\vec{j}$ in a magnetic field reads

$$\vec{F} = \frac{1}{c} \int \mathrm{d}x'^3 \, \vec{j}(\vec{x}') \times \vec{B}(\vec{x}') \,. \tag{1.10}$$

If the magnetic field varies slowly over the region with non-zero current distribution, one can employ a Taylor expansion for the magnetic field, *e.g.* the i-th component may be expanded as $B_i(\vec{x}) = B_i(\vec{x})|_{\vec{x}=0} + \vec{x} \cdot \nabla B_i|_{\vec{x}=0} + \dots$. The force then reads

$$\vec{F} = \frac{1}{c} \int \mathrm{d}x'^3 \, \vec{j}(\vec{x}') \times \left[(\vec{x}' \cdot \nabla) \vec{B}(0) \right] + \dots = \nabla \times \left[\vec{B}(0) \times \vec{m} \right] + \dots = \nabla(\vec{m} \cdot \vec{B}(0)) + \dots \,. \tag{1.11}$$

The force can also be interpreted as the negative gradient of a potential energy U, *i.e.* $\vec{F} = -\mathrm{grad}\, U$ and therefore

$$U = -\vec{m} \cdot \vec{B} \,. \tag{1.12}$$

It was first suggested by Ampère [4] that ferromagnets can be interpreted as molecules of circulating currents. As we have seen in Eq. (1.9), a local current distribution gives rise to a magnetic moment $\vec{\mu}$. This "molecular current hypothesis" was later, in 1854, expanded by Weber [1] and provided a first theory on the origin of the magnetic moment.

1.2 GYROMAGNETISM: BARNETT AND EINSTEIN-DE HAAS EFFECTS

The definition of the magnetic moment $\vec{\mu}$, Eq. (1.9), gives rise to a close relationship with the angular momentum $\vec{L}$. Suppose the current distribution is given by a number of charged particles with charges q_i, masses M_i and velocities $\vec{v}_i$ located at $\vec{x}_i$. The current distribution then reads

$$\vec{j}(\vec{x}) = \sum_i q_i \vec{v}_i \delta(\vec{x} - \vec{x}_i) \tag{1.13}$$

and the magnetic moment is given by

$$\vec{\mu} = \frac{1}{2c} \sum_i q_i (\vec{x}_i \times \vec{v}_i) = \sum_i \frac{q_i}{2 M_i c} \vec{L}_i \,, \tag{1.14}$$

where in the last step we have used the expression $\vec{L}_i = M_i(\vec{x}_i \times \vec{v}_i)$ for the orbital angular momentum of the ith particle. If all particles have the same charge to mass ratio, *i.e.* $q_i/M_i = e/M$, one can relate the magnetic moment to the total orbital angular momentum of the current distribution:

$$\vec{\mu} = \frac{e}{2Mc} \sum_i \vec{L}_i = \frac{e}{2Mc} \vec{L} = \gamma \vec{L}. \tag{1.15}$$

As a consequence of Eq. (1.15), a coupling between the magnetic and mechanical degrees of freedom exists. Such gyromagnetic effects were looked for – albeit without success – already by Maxwell in 1861 [5, §575]. However, only the work by Barnett [6] resp. Einstein and de Haas [7] in 1915 led to a first determination of the gyromagnetic constant γ, which was found to be by a factor of $g \approx 2$ larger than the classically expected value of $e/(2Mc)$. This anomalous g-factor provided a first hint at the quantum nature of the electron magnetic moment or spin.

1.2.1 THE EINSTEIN-DE HAAS EFFECT

The Einstein-de Haas effect is the label for the mechanical rotation of a body that is induced by changing its magnetization. This effect was first sought after by Owen Willans Richardson in 1908 [8], but Albert Einstein and Johannes Wander de Haas reported a first determination of the gyromagnetic ratio using this method in 1915 [7].

The Noether theorem states that rotational symmetry implies the conservation of the total angular momentum. Now let us consider a free magnet located in a magnetic field along its symmetry axis. If the magnetization is now changed from – say – being oriented antiparallel to the magnetic field to parallel orientation, a mechanical rotation of the magnetic body is induced as the total angular momentum in direction of the magnetic field needs to be conserved. This is the key idea of Einstein's and de Haas' experiment, whose experimental setup is sketched in Fig. 1.1: A ferromagnetic body is suspended from a thin wire. By applying a magnetic field pulse along the symmetry axis, the body is magnetized and thus inducing the body to move. In the absence of mechanical damping and torsion the motion would be a uniform rotation due to the conservation of the total angular momentum, whereas otherwise a damped torsional motion is observed. Einstein and de Haas could now determine the gyromagnetic ratio by bringing the coupled magnetic and mechanical degrees of freedom in resonance.

Let us denote the mechanical angular momentum in the direction of the symmetry axis with $L_{\parallel} = I_{\parallel}\dot{\phi}$, where $I_{\parallel}$ is the moment of inertia of the body and ϕ the rotation angle, and the magnetic moment with $M_{\parallel}$. The mechanical equation of
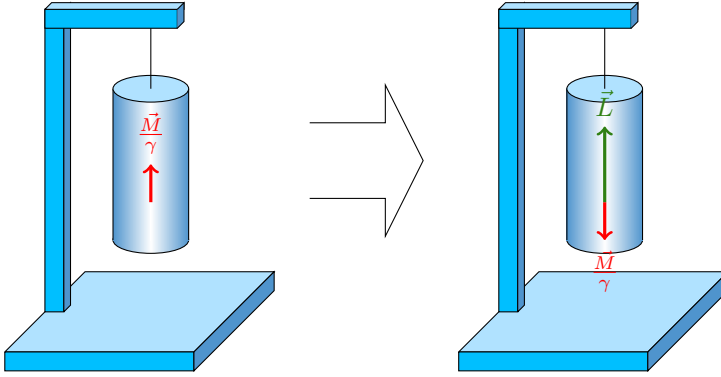
FIGURE 1.1: The Einstein-de Haas effect refers to the mechanical rotation of a suspended body induced by changing its magnetization.

motion reads

$$\dot{L}_\parallel = T - 2I_\parallel \kappa \dot{\phi} - I_\parallel \left(\frac{\Theta}{I_\parallel} \right)^2 \phi, \qquad (1.16)$$

where κ is the damping constant of the mechanical motion, Θ the torsion constant of the wire and T a torque, that reflects the conservation of the total angular momentum of the coupled mechanical and magnetic degrees of freedom. Therefore,

$$\dot{M}_\parallel = -\gamma T. \qquad (1.17)$$

As a consequence, in the absence of torsion and damping, a uniform rotation is induced by inducing a magnetic moment in the body since then $\gamma \dot{L}_\parallel + \dot{M}_\parallel = 0$. Einstein and de Haas assumed that by applying a pulsed magnetic field, the magnetization of the body, $M_\parallel$ switches from $+\delta M$ to $-\delta M$ and vice versa. Assuming this is repeated with frequency ω, we can expand T in a Fourier series. Taking only the lowest harmonic in the expansion into account,

$$T = 2\delta M \cos(\omega t), \qquad (1.18)$$

which leads to a solution $\phi = |A| \cos(\omega t - \psi)$ with phase angle

$$\tan \psi = \frac{2\omega\kappa}{\omega_0^2 - \omega^2}, \qquad (1.19)$$

FIGURE 1.2: A schematic of the experiment conducted by Beth [10]. The dashed lines show the path of the linearly polarized light, while the straight lines the path of circularly polarized light. The different colors denote the two different polarizations which differ by an angle of $\pi/2$. All in all, a photon that traverses the setup deposits an angular momentum of $4\hbar$ in the suspended $\lambda/2$-plate, which is shown in gray in the figure.

where $\omega_0 = \Theta/I_\parallel$ is the resonance frequency, and amplitude
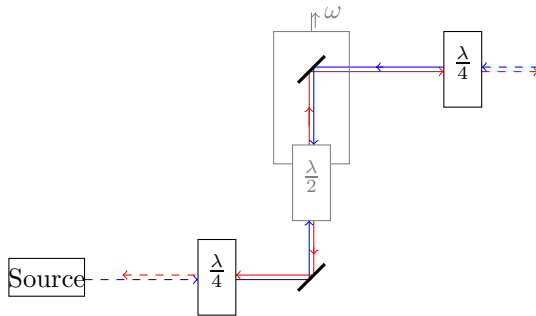
$$|A| = \frac{2\delta M}{I_\parallel \gamma \sqrt{(\omega_0^2 - \omega^2)^2 + 4\omega^2 \kappa^2}} . \qquad (1.20)$$

By employing the resonant enhancement, Einstein and de Haas inferred the gyromagnetic ratio γ from the observed maximal amplitude. Einstein's and de Haas' initially published g-factor was close to one – as expected by classical electrodynamics when the charge is carried by electrons (see section 1.2). In fact, as de Haas later admitted [9] they had taken two sets of measurements, one yielding a g-factor of 1.02 and another yielding 1.45. The latter was dismissed by the two investigators as being due to disturbances in the experimental setup and thus one of the first evidences of the anomalous g-factor of the electron spin went unnoticed.

An optical experiment that is similar in spirit to the Einstein-de Haas experiment was devised by Beth [10], which is shown in Fig. 1.2. A linearly polarized light beam is left circularly polarized by a $\lambda/4$-plate, *i.e.* a photon has angular momentum $-\hbar$ when entering the measurement apparatus. A suspended $\lambda/2$-plate changes the the polarization from left- to right-circular polarized, *i.e.* $-2\hbar$ angular momentum is transferred to the suspended $\lambda/4$-plate and causes it to rotate (due to conservation of total angular momentum). The light beam is sent through another $\lambda/4$ and reflected back, so that another $-2\hbar$ angular momentum is transferred to the suspended $\lambda/2$-plate. This experiment is in the same spirit as the
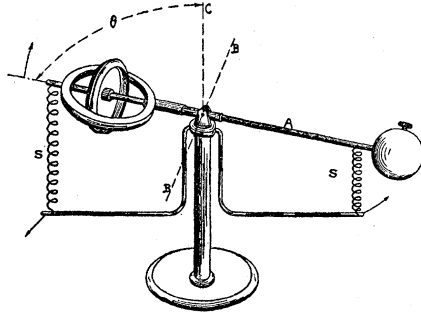
FIGURE 1.3: Barnett explained magnetization by rotation with the following classical analogy: One may consider the magnetic moment $\vec{\mu}$ as the wheel of a gyroscope oriented in some direction A. If this gyroscopic wheel is spun around an axis C, the wheel will align itself more with the axis of impressed rotation C. Restoring torques in the rotating frame of reference may be modelled by springs (S). This picture was taken from [13].

Einstein-de Haas experiment in that it proves that quantum mechanical angular momentum can be converted to mechanical angular momentum.

1.2.2 THE BARNETT EFFECT

First attempts to observe magnetization induced by mechanical rotation of the body – the Barnett effect – were made by Barnett in 1909 [11]. However, it took another six years before quantitative results on this issue were obtained [6] – almost simultaneously with Einstein's and de Haas' work on rotation induced by magnetization.

In order to explain the Barnett effect, we need to distinguish two frames of reference: the laboratory frame of reference fixed in space and a body frame of reference, which are linked by a rotation matrix $\mathbf{R}$ such that

$$\vec{a}_{\text{body}} = \mathbf{R}\vec{a}_{\text{lab}}. \tag{1.21}$$

In addition, the time-derivatives in laboratory and body frame of reference are linked by the Euler equations [12], *i.e.*

$$\dot{\vec{a}}_{\text{lab}} = \mathbf{R}^{-1} \left[\dot{\vec{a}}_{\text{body}} + \vec{\omega}_{\text{body}} \times \vec{a}_{\text{body}} \right], \tag{1.22}$$

where $\vec{\omega}_{\text{body}}$ denotes the rotation axis.

We now assume that the magnetic moment $\vec{\mu}$ is rotated around the $\vec{z}_{\text{lab}}$ axis with a fixed frequency Ω. Barnett [6, 13] made the following classical analogy (see

Fig. 1.3). We can model the magnetic moment $\vec{\mu}$ as the wheel of a gyroscope, whose rotation axis we assume to be the $\vec{z}_{\mathrm{body}}$ axis. In the rotating frame, the angular momentum $\vec{L}_{\mathrm{body}}$ obeys

$$\dot{\vec{L}}_{\mathrm{body}} = \vec{L}_{\mathrm{body}} \times \vec{\omega}_{\mathrm{body}} + \vec{T}_{\mathrm{body}}, \tag{1.23}$$

where $\vec{T}_{\mathrm{body}}$ denotes a restoring torque. If it were not for this restoring torque, a gyroscopic wheel on which an external rotation frequency Ω around an axis $\vec{z}_{\mathrm{Lab}}$ is impressed should align itself with the impressed axis of rotation. In a steady state, *i.e.* when $\dot{\vec{L}}_{\mathrm{body}} = 0$ we have

$$0 = \vec{\mu}_{\mathrm{body}} \times \left(\frac{\vec{\omega}_{\mathrm{body}}}{\gamma} \right) + \vec{T}_{\mathrm{body}}, \tag{1.24}$$

where $\gamma \vec{L}_{\mathrm{body}} = \vec{\mu}_{\mathrm{body}}$. The first term in Eq. (1.24) can be interpreted as the torque of a "Barnett gauge field"

$$\vec{B}_{\mathrm{body}} = \frac{\vec{\omega}_{\mathrm{body}}}{\gamma} \tag{1.25}$$

on the magnetic moment $\vec{\mu}_{\mathrm{body}}$. The magnetic moment aligns itself more parallel to the axis of rotation if $\gamma > 0$ and more antiparallel to it if $\gamma < 0$.

Experimentally, Barnett verified in 1915 [6] for rotating ferromagnets, which were rotated with frequencies of up to $\nu = \omega/(2\pi) = 50$ Hz, that the magnetic flux density is proportional to the frequency of rotation as stated by (1.25). The proportionality is

$$\frac{\hbar}{g\mu_B} = \frac{3.1 \cdot 10^{-11} \text{ Ts}}{2\pi}.$$

So even for the maximum frequencies achieved in Barnett's experiment, the magnetic flux density through the rotating ferromagnet was orders of magnitudes lower than the magnetic field of the earth, which is of the order of 50 μT.

1.3 EFFECTIVE MAGNETIC FIELD

The first law of thermodynamics demands that for any reversible change of a closed system

$$\mathrm{d}U + \mathrm{d}E_{\mathrm{pot}} = \delta W + \delta Q, \tag{1.26}$$

where $\mathrm{d}U$ refers to the variation of internal energy U, $\mathrm{d}E_{\mathrm{pot}}$ is the change in the potential energy, δW is the work performed and δQ is the heat absorbed by the system. The second law of thermodynamics states that

$$\mathrm{d}S \geq \frac{\delta Q}{T}, \tag{1.27}$$

where dS is the change of entropy and the equal sign holds true for reversible processes.

Let dV be a small volume of magnetic material with magnetization density $\vec{M}$. Furthermore, let us define $\vec{\mathcal{M}} = \vec{M}dV$ so that $\vec{\mathcal{M}}$ is the magnetic moment contained in dV. In an external magnetic field $\vec{H}_{\text{ext}}$ one finds

$$\mathrm{d}E_{\text{pot}} = \vec{\mathcal{M}} \cdot \mathrm{d}\vec{H}_{\text{ext}} + \vec{H}_{\text{ext}} \cdot \mathrm{d}\vec{\mathcal{M}} \tag{1.28}$$

and the work performed on the system when the magnetization is changed by d$\vec{\mathcal{M}}$ is given by

$$\delta W = \vec{H}_{\text{ext}} \cdot \mathrm{d}\vec{\mathcal{M}} \,. \tag{1.29}$$

For systems where the temperature T is constant rather than the entropy S, one can introduce appropriate thermodynamic potentials such as the Helmholtz free energy $F(\vec{\mathcal{H}}_{\text{ext}}, T) = U - TS$ or the Gibbs free energy $G(\vec{M}, T) = F + \vec{\mathcal{M}} \cdot \vec{H}_{\text{ext}}$. One finds with the first and second law of thermodynamics

$$\mathrm{d}F \leq -\vec{\mathcal{M}} \cdot \mathrm{d}\vec{H}_{\text{ext}} - S\mathrm{d}T \,, \tag{1.30}$$

where the equal sign holds for reversible processes. At constant external magnetic field and temperature d$F \leq 0$, which means that if constraints are removed the Helmholtz free energy will decrease to a minimum. In the following let us consider the different terms contributing to the Helmholtz free energy functional.

One of the basic properties of ferromagnets is the presence of uniformly magnetized domains due to the presence of an exchange interaction that penalizes deformations in the magnetization. In the isotropic case, the contribution to the free energy caused by exchange interaction must consist of an even power series of the gradients of the magnetization components [14], *i.e.*

$$F_{\text{exchange}} = \int_{\Omega} \mathrm{d}V A \left[(\nabla m_x)^2 + (\nabla m_y)^2 + (\nabla m_z)^2 \right] , \tag{1.31}$$

where A denotes the exchange constant. A first microscopic derivation of this energy was provided by Heisenberg [15], who considered localized spins on a lattice.

The coercivity of ferromagnets can be expressed in terms of easy directions (or planes) that minimize the free energy due to an effective crystal magnetic field. For a uniaxial anisotropy, the contribution to the free energy to lowest order in Θ, where Θ is the angle between the magnetization and the anisotropy axis, reads [16]

$$F_{\text{an}} = \int_{\Omega} \mathrm{d}V K_1 \sin^2 \Theta \,. \tag{1.32}$$

For $K_1 > 0$, the anisotropy axis is an easy axis, whereas for $K_1 < 0$ it is a hard axis, *i.e.* the magnetization in equilibrium is perpendicular to it.

The contribution to the free energy by magnetic dipolar interactions is given by

$$F_{\mathrm{m}} = -\frac{1}{2} \int_{\Omega} \mathrm{d}V \vec{M} \vec{H}_{\mathrm{m}}, \qquad (1.33)$$

where $\vec{H}_{\mathrm{m}}$ denotes the magnetostatic field. According to Maxwell's equations in magnetized media [3]

$$\nabla \cdot \vec{H}_{\mathrm{m}} = -4\pi \nabla \cdot \vec{M} \qquad (1.34)$$

in the volume Ω with constant magnetization density and $\nabla \cdot \vec{H}_{\mathrm{m}} = 0$ outside of Ω and

$$\nabla \times \vec{H}_{\mathrm{m}} = 0 \qquad (1.35)$$

everywhere. At the surface $\partial \Omega$ of Ω, the conditions

$$\vec{n} \cdot [\vec{H}_{\mathrm{m}}]_{\partial\Omega} = \vec{n} \cdot \vec{M} \quad \text{and} \quad \nabla \times [\vec{H}_{\mathrm{m}}]_{\partial\Omega} = 0 \qquad (1.36)$$

must be fulfilled. In the last equation, $\vec{n}$ denotes an outward pointing unit vector that is perpendicular to the surface of Ω. In a uniformly magnetized ellipsoid, the field inside the ellipsoid can be written as [14]

$$\vec{H}_{\mathrm{m}} = -\mathbf{D}\vec{M}, \qquad (1.37)$$

where $\mathbf{D}$ is the demagnetization tensor with trace 4π.

The external field $\vec{H}_{\mathrm{ext}}$ contributes to the Helmholtz free energy as

$$F_{\mathrm{ext}} = -\int_{\Omega} \mathrm{d}V \vec{M} \cdot \vec{H}_{\mathrm{ext}}. \qquad (1.38)$$

The free energy is now given by $F = F_{\mathrm{exchange}} + F_{\mathrm{an}} + F_{\mathrm{m}} + F_{\mathrm{ext}}$. In the following we write $\vec{M} = M_s \vec{m}$, i.e. $\vec{m}$ is the unit vector of magnetization direction. At equilibrium with constant external field $\vec{H}_{\mathrm{ext}}$ and temperature, the free energy is minimal according to Eq. (1.30). The ground state configuration can be found by imposing the constraint that the variation of the free energy vanishes for variations $\delta\vec{m}$ of the unit-magnetization vector $\vec{m}$, i.e. $|\vec{m} + \delta\vec{m}| = 1$. Denoting the volume density of the Helmholtz free energy F with f, one finds

$$\delta F = \int_{\Omega} \mathrm{d}V \frac{\partial f}{\partial \vec{m}} \delta \vec{m}. \qquad (1.39)$$

The variation of the unit magnetization vector can be written as $\delta\vec{m} = \vec{m} \times \delta\vec{\theta}$, where $\delta\vec{\theta}$ represents an elementary rotation by the angle $\delta\theta$. Then

$$\delta F = \int_{\Omega} \mathrm{d}V \delta\vec{\theta} \left[\frac{\partial f}{\partial \vec{m}} \times \vec{m} \right] = \int_{\Omega} \mathrm{d}V \delta\vec{\theta} \left[\vec{m} \times \vec{H}_{\mathrm{eff}} \right], \qquad (1.40)$$

implying that at equilibrium $\vec{m} \times \vec{H}_{\mathrm{eff}} = 0$.

1.4   LANDAU-LIFSHITZ-GILBERT EQUATION

We now turn to discuss the undamped equations of motion of a quantum spin with operator $\vec{\hat{S}}$ in a magnetic field $\vec{B}$. For a spin-1/2 particle $\vec{\hat{S}} = \hbar \vec{\hat{\sigma}}/2$, where $\vec{\hat{\sigma}}$ is the vector of Pauli-matrices. Disregarding the orbital degrees of freedom, the Hamiltonian $\hat{H}$ is simply given by the dipolar interaction $\hat{H} = \mu_B \hat{\sigma} \cdot \vec{B}$. The Heisenberg equation of motion for the spin-1/2 particle then reads [17]

$$i\hbar \frac{\mathrm{d}\vec{\hat{S}}}{\mathrm{d}t} = 2i\mu_B \vec{B} \times \vec{\hat{S}}. \tag{1.41}$$

The change of angular momentum per unit-time on the right hand side is the torque exerted on the particle spin. As it was experimentally established by Barnett resp. Einstein and de Haas, the magnetic moment $\vec{\mu}$ of an electron is related to its angular momentum by

$$\vec{\mu} = \gamma \vec{L}, \tag{1.42}$$

where $\gamma = g\mu_B/\hbar < 0$ is the gyromagnetic ratio and $g \approx 2$. Thus, Eq. (1.41) is the equation of motion of a magnetic moment. By replacing the the operators in Eq. (1.41) by expectation values, we obtain an equation of motion of for the classical magnetization [18].

   As shown in the previous section, the interactions of the magnetization with the environment give rise to an effective magnetic field, which leads to the Landau-Lifshitz (LL) equation of motion for the magnetization:

$$\frac{\mathrm{d}\vec{M}}{\mathrm{d}t} = \gamma \vec{M} \times \vec{H}_{\mathrm{eff}}. \tag{1.43}$$

Various microscopic processes govern the interaction of the individual magnetic moments with the environment, which lead to dissipation or energy transfer from the magnetic system to the environment. This transfer can be incorporated into the equation by means of an additional damping term, leading to the well-known phenomenological Landau-Lifshitz-Gilbert equation [18, 19]

$$\frac{\partial \vec{M}}{\partial t} = \gamma \vec{M} \times \vec{H}_{\mathrm{eff}} - \frac{\alpha \hat{\gamma}}{M_s} \vec{M} \times \frac{\partial \vec{M}}{\partial t}, \tag{1.44}$$

where the damping parameter $\alpha > 0$ and $\hat{\gamma} = \gamma/|\gamma|$ denotes the sign of the gyromagnetic constant. A closely related equation was proposed by Landau and Lifshitz beforehand [20]. In order to arrive at a correct description of the dynamics with large damping, Gilbert derived the damping torque using a Lagrangian description augmented by a Rayleigh dissipation functional [18]. For small damping parameters
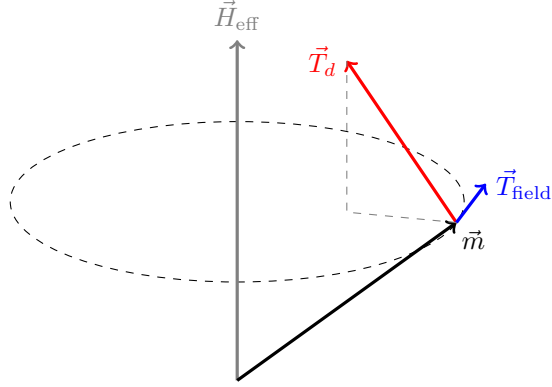
FIGURE 1.4: The effective magnetic field $\vec{H}_{\text{eff}}$ exerts a torque $\vec{T}_{\text{field}} = -\gamma \vec{m} \times \vec{H}_{\text{eff}}$ on the magnetic moment (shown in blue), whereas the Gilbert damping term exerts a torque $\vec{T}_{\text{d}} = \alpha \vec{m} \times \dot{\vec{m}}$ (shown in red) that tends to align the magnetic moment with the direction of $\vec{H}_{\text{eff}}$.

α, the two forms of damping torque, *i.e.* the Gilbert and Landau-Lifshitz forms, are equivalent.

It is easy to see by multiplying Eq. (1.44) by $\vec{M}$, that

$$\frac{\mathrm{d}}{\mathrm{d}t}|\vec{M}|^2 = 0 \tag{1.45}$$

and thus for all t the LLG equation conserves the modulus of the magnetization,

$$|\vec{M}(\vec{r},t)| = |\vec{M}(t_0,\vec{r})| = M_s. \tag{1.46}$$

A consequence is, that all magnetization dynamics described by the Landau-Lifshitz-Gilbert equation at position $\vec{r}$ takes place on a sphere with radius $|\vec{M}| = M_s$.

By scalar multiplication of the Landau-Lifshitz-Gilbert equation, Eq. (1.44), with $\gamma \vec{H}_{\text{eff}} - \text{sig}(\gamma)\alpha/M_s \partial \vec{M}/\partial t$, one finds

$$\frac{\partial \vec{M}}{\partial t} \cdot \left(\gamma \vec{H}_{\text{eff}} - \frac{\alpha}{M_s} \text{sig}(\gamma) \frac{\partial \vec{M}}{\partial t} \right) = 0. \tag{1.47}$$

With this we find for the time-derivative of the free energy F

$$
\begin{aligned}
\frac{\mathrm{d}}{\mathrm{d}t}F &= \int_{\Omega}\mathrm{d}V\left[\frac{\delta f}{\delta\vec{M}}\frac{\partial\vec{M}}{\partial t}+\frac{\delta f}{\delta\vec{H}_{\mathrm{a}}}\frac{\partial\vec{H}_{\mathrm{ext}}}{\partial t}\right]=\int_{\Omega}\mathrm{d}V\left[-\vec{H}_{\mathrm{eff}}\frac{\partial\vec{M}}{\partial t}-\vec{M}\cdot\frac{\partial\vec{H}_{\mathrm{a}}}{\partial t}\right] \\
&= -\int_{\Omega}\mathrm{d}V\left[\frac{\alpha}{M_s|\gamma|}\left(\frac{\partial\vec{M}}{\partial t}\right)^2+\vec{M}\cdot\frac{\partial\vec{H}_{\mathrm{ext}}}{\partial t}\right]
\end{aligned}
\tag{1.48}
$$

where f denotes the energy density. Since $\alpha > 0$, this implies that the free energy is a monotonously decreasing function in time if the external field $\vec{H}_{\mathrm{ext}}$ is constant in time.

1.5 NANOMECHANICAL SYSTEMS

Refining fabrication processes and increased understanding of the involved materials has enabled the microelectronics industry to continuously shrink the size of the electronic elements used on computer chips. By employing the same techniques, researchers managed to produce mechanical elements – beams, cantilevers and membranes – with ever smaller size, giving rise to the field of micro-electro-mechanical-systems (MEMS) and with further miniaturization to nano-electro--mechanical-systems (NEMS). NEMS can have high resonance frequencies ω_0 beyond 1 GHz and quality factors $Q \sim 10^3 - 10^5$ [21].

The coupled magnetovibrational dynamics of a cantilever with a ferromagnetic single-domain tip has been studied by Kovalev et al. [22–24] (see Fig. 1.5). Here, a constant magnetic field $\vec{H}_c$ is oriented along the y-axis of the cantilever. In addition, an oscillating field $\vec{H}_{osc}$ along the x-axis as well as the crystal anisotropy and demagnetization fields contribute to the effective magnetic field $\vec{H}_{eff}$. When the ferromagnetic tip is of length $\Delta L \ll L$, where L denotes the length of the cantilever, the magnetovibrational coupling may be treated as a boundary condition to the mechanical equation of motion [22]. The magnetic susceptibility $\chi_\omega = (m_x/H_{osc})_\omega$, which is the linear response of the magnetization in x-direction to an oscillating field H_{osc} in the same direction, reads

$$
\frac{\chi_\omega}{\gamma^2 M_s V}=\left[\frac{\omega^2-\omega_m^2}{H_A+H_0+\nu M_s}+\frac{\omega^2 GL\tan(kL)}{2kc^2(H_A+\nu M_s+H_0(1-GL\tan(kL)/2kc^2))}\right]^{-1},
\tag{1.49}
$$

where H_A is the crystalline anisotropy, c the transverse velocity of sound, V the volume of the cantilever and $k = \omega/c$ the wave number. ν describes the demagnetizing dipolar field and $\omega_m^2 = \gamma(H_A+\nu M_s)\gamma H_A$ is the unperturbed magnetic resonance frequency.
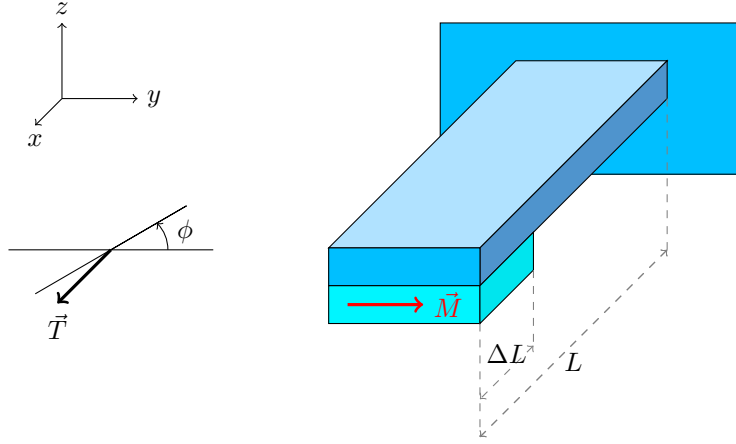
FIGURE 1.5: A nano-cantilever with a magnetic tip exhibits coupled magneto-mechanical dynamics.

The Einstein-de Haas effect in a NiFe film, which was deposited on a sillicon microcantilever of $200\mu\text{m} \times 20\mu\text{m} \times 600\text{nm}$ size was observed by Wallis et al. [25], yielding a magnetomechanical g-factor of 1.82.

An electrical equivalent of Beth's experiment [10] has been performed by Zolfa-gharkani et al. [26]: They observed the spin-flip torque by nanomechanical means. To this end, they fabricated a nanomechanical device consisting of a suspended nanowire, which contained a ferromagnetic/normal metal in its middle. If a current is driven through the wire, a non-equilibrium spin accumulation $\delta m = \mu_B \Delta N$, where μ_B is the Bohr magneton and ΔN the number of non-equilibrium spins, is created at the interface of normal-metal to ferromagnet. ΔN is given by

$$\Delta N = \frac{I_s}{e}\tau_{sf}, \tag{1.50}$$

where τ_{sf} denotes the spin relaxation time and $I_s = I_\uparrow - I_\downarrow = P(I_\uparrow + I_\downarrow)$, with $P = (I_\uparrow - I_\downarrow)/(I_\uparrow + I_\downarrow)$, denotes the spin-polarized current. The decaying spin current exerts a torque on the lattice ammounting to

$$T = \frac{\hbar}{2}\frac{I_s}{e}, \tag{1.51}$$

which was shown to be mechanically detectable in a suspended structure.

1.6   THIS THESIS

In Chapter 2, we carry out a theoretical feasibility study concerning the observability of the Barnett effect in magnetic nanostructures and thin films. To this end, we modify the Landau-Lifshitz-Gilbert equation in order to take into account that magnetization is damped only when moving in a frame of reference that co-rotates with the lattice. We find, that in order to observe the Barnett effect in thin films of permalloy or GaMnAs with the magneto-optical Kerr effect, rotation frequencies that are on the brink or beyond the experimentally feasible ones are required since a relatively strong shape anisotropy field has to be overcome. We also assess the observability of the Barnett effect in a magnetic wire containing a domain wall.

In Chapter 3, we present the linear response matrix for a sliding domain wall in a rotatable magnetic nanowire, which is driven out of equilibrium by mechanical torque and/or applied magnetic field. Applying Onsager's reciprocity relation, we find a unified description of the Barnett effect – magnetization by rotation – and Einstein-de Haas effect – mechanical rotation induced by magnetization.

In Chapter 4 we study the alignment of rapidly rotating cosmic dust grains with respect to a magnetic field. This system is an example of the interplay between the two gyromagnetic effects – the Barnett and Einstein-de Haas effect. In addition, the alignment of cosmic dust grains is an important issue in astronomy, as aligned dust grains cause a polarization of starlight which paves the way to starlight polarimetry. The latter allows for the mapping of cosmic magnetic fields, which play an important role in the evolution of our universe. In particular, we discuss the alignment of a single dust grain by setting up the coupled magneto-mechanical equations of motion taking the conservation of the total angular momentum into account.

In Chapter 5 we discuss the magnetization of a free electron gas by rotation. We find that the eigenstates of the rotating electron gas resembles the Landau levels one finds for a free electrong gas subjected to a magnetic field. However, in the case of a rotating electron gas, the radial motion of the electron is not quantized as in the case of an applied external magnetic field.

REFERENCES

[1] E. C. Stoner, *Magnetism and Matter* (Methuen & Co., London, 1934).

[2] A. D. Aczel, *The riddle of the compass: the invention that changed the world* (Harcourt Books, San Diego, 2001).

[3] J. D. Jackson, *Classical Electrodynamics* (John Wiley & Sons, Inc., 1962).

[4] J. R. Hofman, *André-Marie Ampère* (Cambridge University Press, Cambridge, 1986).

[5] J. C. Maxwell, *A Treatise on Electricity and Magnetism* (Clarendon Press, Oxford, 1873).

[6] S. J. Barnett, *Magnetization by Rotation*, Phys. Rev. **6**, 239 (1915).

[7] A. Einstein and J. W. de Haas, *Experimental Proof of the Existence of Ampere's Molecular Currents*, Proceedings of the Koninklijke Akademie van Wetenschappen te Amsterdam **18 I**, 696 (1916).

[8] O. W. Richardson, *A Mechanical Effect Accompanying Magnetization*, Phys. Rev. (Series I) **26**, 248 (1908).

[9] A. Pais, *Subtle is the Lord* (Oxford University Press, 2005).

[10] R. A. Beth, *Mechanical Detection and Measurement of the Angular Momentum of Light*, Phys. Rev. **50**, 115 (1936).

[11] S. J. Barnett, *On Magnetization by Angular Acceleration*, Science **30**, 413 (1909).

[12] L. D. Landau and E. M. Lifshitz, *Mechanics* (Butterworth Heinemann, 1976), 3rd ed.

[13] S. J. Barnett, *Gyromagnetic and Electron-Inertia Effects*, Rev. Mod. Phys. **7**, 129 (1935).

[14] W. F. Brown jr., *Magnetostatic Principles in Ferromagnetism* (North Holland Publishing Company, Amsterdam, 1962).

[15] W. Heisenberg, *Zur Theorie des Ferromagnetismus*, Zeitschrift für Physik A Hadrons and Nuclei **49**, 619 (1928).

[16] L. Landau and E. Lifshitz, *Electrodynamics of Continous Media* (Pergamon Press, Oxford, 1984).

[17] A. Messiah, *Quantum Mechanics, Vol. 1 and 2* (Dover, Mineola, 1999).

[18] T. Gilbert, *A phenomenological theory of damping in ferromagnetic materials*, Magnetics, IEEE Transactions on **40**, 3443 (2004).

[19] T. Gilbert, *A Lagrangian formulation of the gyromagnetic equation of the magnetic field (Abstract Only)*, Physical Review **100**, 1243 (1955).

[20] L. Landau and E. Lifshitz, *On the Theory of the Dispersion of Magnetic Permeability in Ferromagnetic Bodies*, Phys. Z. Sowjetunion **8**, 153 (1935).

[21] K. L. Ekinci and M. L. Roukes, *Nanoelectromechanical Systems*, Review of Scientific Instruments **76**, 061101 (2005).

[22] A. A. Kovalev, G. E. W. Bauer, and A. Brataas, *Magnetovibrational coupling in small cantilevers*, Appl. Phys. Lett. **83**, 1584 (2003).

[23] A. A. Kovalev, G. E. W. Bauer, and A. Brataas, *Nanomechanical Magnetization Reversal*, Phys. Rev. Lett. **94**, 167201 (2005).

[24] A. A. Kovalev, G. E. W. Bauer, and A. Brataas, *Magnetomechanical Torques in Small Magnetic Cantilevers*, Japanese Journal of Applied Physics **45**, 3878 (2006).

[25] T. M. Wallis, J. Moreland, and P. Kabos, *Einstein-de Haas effect in a NiFe film deposited on a microcantilever*, Appl. Phys. Lett. **89**, 122502 (2006).

[26] G. Zolfagharkhani, A. Gaidarzhy, P. Degiovanni, S. Kettemann, P. Fulde, and P. Mohanty, *Nanomechanical detection of itinerant electron spin flip*, Nature Nanotechnology **3**, 720 (2008).

2

BARNETT EFFECT IN THIN MAGNETIC FILMS AND NANOSTRUCTURES

The Barnett effect refers to the magnetization induced by rotation of a demagnetized ferromagnet. We describe the location and stability of stationary states in rotating nanostructures using the Landau-Lifshitz-Gilbert equation. The conditions for an experimental observation of the Barnett effect in different materials and sample geometries are discussed.

At the dawn of quantum mechanics, the Barnett [2, 3] effect (magnetization induced by rotation) confirmed that magnetization is associated with angular momentum. Furthermore, Barnett measured the gyromagnetic ratio of electrons in ferromagnets and the anomalous g-factor of the electron for the first time. The Barnett effect can be understood in terms of a rotating gyroscopic wheel, that aligns itself with the axis of rotation until a stationary state in the rotating frame of reference is achieved. Since angular momentum $\vec{L}$ is associated with magnetization $\vec{M} = -\gamma\vec{L}$, with $\gamma = g\mu_B/\hbar = g|e|/2m$ being the gyromagnetic ratio, mechanical rotation induces a net magnetization antiparallel to the axis of rotation. The torque acting on the magnetization in the rotating frame of reference is equivalent to a torque due to the presence of a gauge magnetic field

$$\vec{H}_{\text{rot}} = -\gamma^{-1}\vec{\omega}. \tag{2.1}$$

There has recently been a renewed interest in the coupling of magnetization with mechanical motion, for example in mechanically detected ferromagnetic resonance spectroscopy measurements [4]. A nano-magnetomechanical system consisting of a cantilever and a thin magnetic film shows coupled magnetovibrational modes [5, 6]. Furthermore, the nanomechanical current-driven spin-flip torque at the normal-metal/ferromagnet interface of a suspended nanowire has been detected [7].

In Barnett's original experiments, rotation frequencies of $\omega \lesssim 500$ Hz generated a change of the magnetic field of the order of 10^{-4} Gauss in macroscopic samples. Although in nanostructures detecting such small fields may become more challenging, a range of powerful techniques have recently been developed, which could be utilized for the purpose. To date, very small changes in the magnetization can be measured using the magneto-optical Kerr effect, Faraday spectroscopy, superconducting quantum interference devices (SQUID's) or Hall micromagnetometry [8]. Therefore, we present here a theoretical feasibility study of the Barnett effect in magnetic thin films and nanostructures. Our focus is the dynamics in magnetic thin films and nanoclusters, which we study by means of the Landau-Lifshitz-Gilbert (LLG) equation for the magnetization vector $\vec{m}$:

$$\dot{\vec{m}} = -\gamma\vec{m} \times \vec{H}_{\text{eff}} + \alpha\,\vec{m} \times \dot{\vec{m}}\big|_{\text{Lat}}\,, \tag{2.2}$$

where $\vec{H}_{\text{eff}}$ is the effective magnetic field, $\vec{m}$ is the unit vector of magnetization and α the dimensionless damping constant. We can separate the dynamics caused by the rotation of the system as a whole from the dynamics in the rotating frame of reference by the transformation $\vec{m} = R(\phi)\vec{m}_R$ and $\vec{H}_{\text{eff}} = \mathbf{R}(\phi)\vec{H}_{\text{eff}}^R$, where $\mathbf{R}(\phi)$ is a unitary matrix describing the rotation by a time-dependent angle $\phi(t)$ around the axis of rotation and $\vec{m}_R$ ($\vec{H}_{\text{eff}}^R$) denote the magnetization (effective magnetic field)

in the rotating frame of reference. The damping is caused by the magnetization motion relative to the lattice:

$$\vec{m} \times \dot{\vec{m}}\big|_{\text{Lat}} = \mathbf{R}(\phi(t))\left(\vec{m}_R \times \dot{\vec{m}}_R\right). \tag{2.3}$$

In the rotating frame of reference Eq. (2.2) becomes

$$\dot{\vec{m}}_R = \vec{m}_R \times \left(-\gamma \vec{H}^R_{\text{eff}} + \dot{\phi}(t)\vec{e}_z + \alpha \dot{\vec{m}}_R\right). \tag{2.4}$$

In this derivation, we have tacitly assumed that the Hamiltonian transforms trivially under rotation, *i.e.* rotation only generates the gauge Zeeman field Eq. (2.1) in the rotating frame of reference. [Note that if rotation stems from a rotating field [9–11] rather than the lattice, we would have to use a different form of damping, *viz.* $\vec{m} = \mathbf{R}(\phi)\vec{m}_R$ in $\vec{m} \times \dot{\vec{m}}$. Then the right hand side of Eq. (2.4) contains an additional term $\alpha\omega\vec{m}_R \times \vec{e}_z$ and the stationary states of Eq. (2.4) depend on the damping constant α.]

Following Barnett [2], we are looking for stationary state solutions in the rotating frame of reference, *i.e.*, solutions $\vec{m}_R$ for which $\dot{\vec{m}}_R = 0$, at constant angular velocity $\dot{\phi}(t) = \omega = \text{const.}$. From Eq. (2.4) it follows that the stationary states obey:

$$0 = \vec{m}_R \times \left(-\gamma \vec{H}^R_{\text{eff}} + \omega\vec{e}_z\right). \tag{2.5}$$

Here the magnetization in the lab frame of reference precesses around the axis of rotation (z-axis) at a fixed angle. We analyze the stability of the stationary states in spherical coordinates, *i.e.*,

$$\vec{m}_R = (\sin\theta\cos\phi, \sin\theta\sin\phi, \cos\theta) \tag{2.6}$$

by linearizing the set of equations resulting from Eq. (2.4) for small deviations $(\delta\theta, \delta\phi)$ from the equilibrium (rotating-frame) positions (θ_n, ϕ_n). When $\vec{H}_{\text{eff}} = 0$, *e.g.*, in a spherical particle without crystal anisotropy, the stationary states are given by $\pm\vec{e}_z$. Clearly the stationary state at $\vec{e}_z$ is unstable and $-\vec{e}_z$ is stable.

For a film with free energy $F = DM_z^2/2$, *i.e.*, $D > 0$ refers to a easy-plane magnetization and $D < 0$ to an easy-axis magnetization parallel to the axis of rotation, $\vec{H}_{\text{eff}}$ is given by $\vec{H}_{\text{eff}} = -M_s\text{diag}\{0,0,D\}\vec{m}$, where diag$\{\dots\}$ refers to a diagonal matrix with entries 0 and D and M_s refers to the saturation magnetization. Without limiting generality, we consider the case that $\omega > 0$. By using Eq. (2.6) in Eq. (2.4):

$$\dot{\theta} = -\alpha\dot{\phi}\sin\theta = \frac{\alpha}{1+\alpha^2}\left(\omega + \gamma M_s D\cos\theta\right)\sin\theta. \tag{2.7}$$

Thus, the stationary states are given by $\sin\theta_1 = 0$ and, if $\omega \leq \gamma M_s|D|$, by

$$\cos\theta_2 = -\frac{\omega}{\gamma M_s D}. \tag{2.8}$$

These fixed points do not depend on the coordinate ϕ due to the axial symmetry. For small deviations $\delta\theta$ from $\theta = 0, \pi$, the linearized Eq. (2.7) yields

$$\delta\dot{\theta} = \frac{\alpha}{1 + \alpha^2} \left(\gamma M_s D \pm \omega\right) \delta\theta, \qquad (2.9)$$

where the $+ (-)$ sign refers to the steady state at $\theta = 0$ ($\theta = \pi$). For $\omega < \gamma M_s |D|$ there are additional stationary states $\cos\theta = -\omega/\gamma M_s D$. For small deviations $\delta\theta$ from $\arccos(-\omega/\gamma M_s D)$ the linearized Eq. (2.7) reads

$$\delta\dot{\theta} = \frac{\alpha}{1 + \alpha^2} \frac{\omega^2 - \gamma^2 M_s^2 D^2}{\gamma M_s D} \delta\theta. \qquad (2.10)$$

We can now identify three different regimes: $\omega > \gamma M_s |D|$, $\omega < \gamma M_s |D|$ and $D < 0$ or $D > 0$ (regions I, II and III in Fig. 2.1a). If $\omega > \gamma M_s |D|$, $i.e.$, region I in Fig. 2.1a, one sees from Eq. (2.9) that the stationary state $\theta = 0$ ($\theta = \pi$) is unstable (stable). See cartoon I in Fig. 2.1b. When $\omega < \gamma M_s |D|$, additional steady states given by Eq. (2.8) exist. If also $D < 0$ (region II in Fig. 2.1a), $i.e.$, easy axis anisotropy, it follows from Eq. (2.9) that $\theta = 0, \pi$ are stable and from Eq. (2.10) that $\cos\theta_2 = -\omega/\gamma M_s D$ are unstable stationary states (see cartoon II in Fig. 2.1b). However, if $D > 0$ (region III in Fig. 2.1a), $i.e.$, easy plane anisotropy, according to Eqs. (2.9) resp. (2.10) $\theta = 0, \pi$ are unstable and $\cos\theta_2 = -\omega/\gamma M_s D$ are stable stationary states (see cartoon III in Fig. 2.1b).

To summarize, in a system with in plane magnetization, $i.e.$, $D > 0$, the stable stationary states acquire a z component by rotation. The rotation acts like a magnetic field along the magnetic hard axis. Fig. 2.2 shows the z-component (component along the axis of rotation) of the magnetization in the stationary state in the ω vs. $\gamma M_s D$ plane. In this regime the magnetization displays a hysteresis loop when ω is cycled. The larger $\gamma M_s D$, the slower the transients become.

Limit cycles do not exist, since when ω is constant, we find for the time-derivative of the free energy $\dot{F}\gamma/M_s = -\alpha(\dot{\vec{m}}_R)^2$. In other words, the magnetization approaches its stationary state.

When the axis of rotation no longer coincides with the anisotropy axis of the crystal, the rotational symmetry around the axis of rotation is broken. As a consequence, only a finite number of fixed points exists. For an autonomous system on the unit sphere such as the LLG equation with time-independent effective field, it follows from the Poincare index theorem [12, 13] that the number of (un)stable fixed points minus the number of saddles must be equal to two. A magnetic needle along the y-axis, $i.e.$, $\vec{H}_{\text{eff}} = M_s \text{diag}\{0, D, 0\}\vec{m}$ spun around the z axis exhibits four stationary states when $\omega < \gamma M_s |D|$: $\theta_{1,2} = 0, \pi$ and $\cos\theta_{3,4} = -\omega/\gamma M_s D$, $\cos\phi_{3,4} = 0$. If $D > 0$, then $\theta_1 = 0$ is an unstable and $(\theta_{3,4}, \phi_{3,4})$ stable stationary states whereas

(a)

I

II

III

0    $\gamma M_s D$

ω

(b)
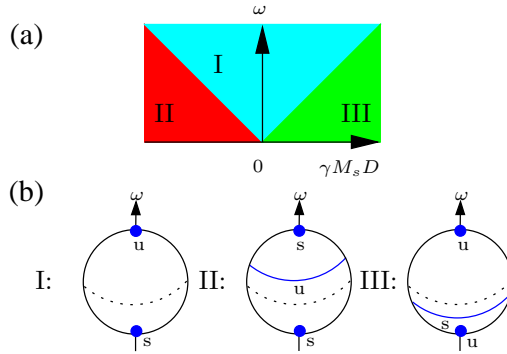
I: II: III:

FIGURE 2.1: I, II and III indicate regions in the $(\omega, \gamma M_s D)$ plane with stable and unstable stationary states located at $\mp \vec{e}_z$, respectively, (region I), stable stationary states at $\pm \vec{e}_z$ and unstable stationary states located at a fixed angle $\theta = \arccos(-\omega/\gamma M_s D)$ in the upper half plane (region II) and stable stationary states located in the lower half plane and unstable stationary states at $\pm \vec{e}_z$ (region III).
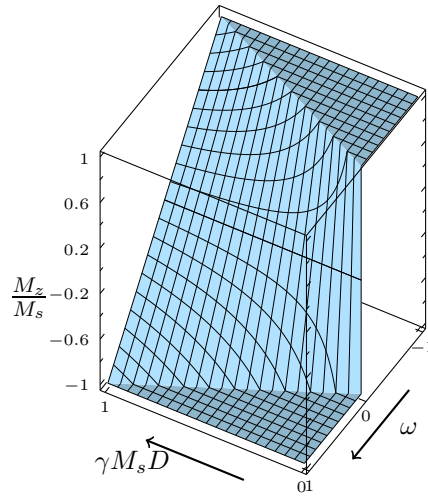
FIGURE 2.2: The z component of the magnetization for the easy-plane configuration, *i.e.*, $D > 0$, in the rotation frequency ω vs. anisotropy field $\gamma M_s D$ plane. Both x and y axes are scaled by the same frequency unit.

$\theta_2 = \pi$ is a saddle point. In the opposite case, *i.e.*, $D < 0$, $(\theta_{3,4}, \phi_{3,4})$ are unstable and $\theta_2 = \pi$ is stable, whereas $\theta_1 = 0$ is a saddle point.

For typical magnetic materials, the critical frequencies to fully rotate the magnetization from in-plane to perpendicular-to-plane orientation are inaccessibly high: $\omega \sim 200$ GHz for permalloy with $M_s \sim 1000$ emu/cm^3 and $D \sim 4\pi$, and $\omega \sim 4$ GHz for a GaMnAs film [14] with $M_s \sim 15$ emu/cm^3 and $D \sim 4\pi$. However, to identify the Barnett effect, it is sufficient to observe small changes in the z component of the magnetization: $M_z = -\omega/\gamma D$. For example, in metals polar magneto-optic Kerr spectroscopy is reported to be sensitive to magnetic moment changes down to $\sim 10^{-15}$ emu at a spot diameter of 0.5 μm [15]. For a 10 nm thick permalloy film ($D \sim 4\pi$) this corresponds to a change in the magnetization of $M_z \sim 1$ emu/cm^3 which is achieved by a rotation frequency of $\omega \gtrsim 200$ MHz. A Kerr angle of 0.3 deg has been measured when the magnetization of GaMnAs is fully aligned perpendicular to the axis of rotation by an external magnetic field [14]. Together with a reported angular resolution in polar Kerr measurements [16] of $\sim 10^{-4}$ deg this yields a required rotation frequency of a few MHz. However, since the cubic anisotropy is important in GaMnAs [14], the above number serves as a lower bound for the frequency estimate. The Barnett effect can be observed at lower spinning rates by choosing a material with small anisotropies. The perpendicular anisotropy in thin magnetic films can be tuned by the layer thickness to cancel the shape anisotropy [17–20].

The Barnett effect can be also used to move domain walls. Consider a wire along the y axis, which contains a transverse Bloch wall in the xz plane. When the wire is rotated around the z axis, the Bloch domain wall moves with a velocity [21] $v = \lambda_w \omega/\alpha$, where λ_w is the width of the transverse Bloch domain wall. For $\lambda_w \sim 100$ nm and $\alpha \sim 10^{-2}$ this yields $v \sim (10 \text{ m/s}) \cdot (\omega/\text{MHz})$.

It might be easier to observe the Barnett effect by vibration rather than rotation, but the mechanical vibration amplitude $\delta\varphi$ then becomes an additional control parameter. The magnetization response is enhanced when the harmonic vibration and FMR frequencies coincide. At this magnetopolariton mode [5], a z component of the magnetization is excited in a needle in the xy plane that oscillates around the z axis. Assuming a vibration amplitude $\delta\varphi$ (rad), M_z oscillates with an amplitude $M_s\delta\varphi/2\alpha$.

In the ideal case of zero anisotropy only the temperature-induced thermal activation of the magnetization has to be overcome in order to observe a Barnett effect, which sets the lower bound on frequency according to $V M_s \omega \gtrsim \gamma k_B T$. For a spherical particle with diameter d and saturation magnetization M_s this yields a minimum frequency of about 500 MHz at $T = 1$ K, $M_s = 10$ emu/cm^3 and $d = 10$ nm. For a 10 nm thick film with $M_s = 10$ emu/cm^3 and area $A = 1$ μm^2 with compensating form and crystal anisotropies, the required rotation frequency is about 25 kHz.

In conclusion, we discussed the Barnett effect in magnetic nanostructures, which gives a handle to manipulate magnetization by mechanical means. We find that the rotation frequencies necessary to fully switch magnetizations in conventional materials are very high and beyond present experimental possibilities. However, the Barnett effect can be observed via partial magnetization of very soft materials, rotation-induced domain-wall motion, and vibrations close to magnetic resonance frequencies.

REFERENCES

[1] S. Bretzel, G. E. W. Bauer, Y. Tserkovnyak, and A. Brataas, *Barnett Effect in Magnetic Thin Films and Nanostructures*, Applied Physics Letters **95**, 122504 (2009).

[2] S. J. Barnett, *Magnetization by Rotation*, Phys. Rev. **6**, 239 (1915).

[3] S. J. Barnett, *Gyromagnetic and Electron-Inertia Effects*, Rev. Mod. Phys. **7**, 129 (1935).

[4] D. Rugar, C. S. Yannoni, and J. A. Sidles, *Mechanical detection of magnetic resonance*, Nature **360**, 563 (1992).

[5] A. A. Kovalev, G. E. W. Bauer, and A. Brataas, *Magnetovibrational coupling in small cantilevers*, Applied Physics Letters **83**, 1584 (2003).

[6] T. M. Wallis, J. Moreland, and P. Kabos, *Einstein-de Haas effect in a NiFe film deposited on a microcantilever*, Appl. Phys. Lett. **89**, 122502 (2006).

[7] G. Zolfagharkhani, A. Gaidarzhy, P. Degiovanni, S. Kettemann, P. Fulde, and P. Mohanty, *Nanomechanical detection of itinerant electron spin flip*, Nature Nanotechnology **3**, 720 (2008).

[8] A. K. Geim, S. V. D. abd J. G. S. Lok, I. V. Grigorieva, J. C. Maan, L. T. Hansen, and P. E. Lindelof, *Ballistic Hall micromagnetometry*, Appl. Phys. Lett. **71**, 2379 (1997).

[9] C. Serpico, M. d'Aquino, G. Bertotti, and I. Mayergoyz, *Analysis of quasiperiodic Landau-Lifshitz-Gilbert dynamics*, Journal of Magnetism and Magnetic Materials **272–276**, 734 (2004).

[10] M. d'Aquino, Ph.D. thesis, Universita degli Studi di Napoli (2004).

[11] N. A. Sinitsyn, V. V. Dobrovitski, S. Urazhdin, and A. Saxena, *Geometric control over the motion of magnetic domain walls*, Phys. Rev. B **77**, 212405 (2008).

[12] L. Perko, *Differential Equations and Dynamical Systems*, Texts in Applied Mathematics 7 (Springer-Verlag, 1991).

[13] G. Bertotti, C. Serpico, and I. D. Mayergoyz, *Nonlinear Magnetization Dynamics under Circularly Polarized Field*, Phys. Rev. Lett. **86**, 724 (2001).

[14] R. Lang, A. Winter, H. Pascher, H. Krenn, X. Liu, and J. K. Furdyna, *Polar Kerr effect studies of* $Ga_{1-x}Mn_xAs$ *epitaxial films*, Phys. Rev. B **72**, 024430 (2005).

[15] M. Cormier, J. Ferré, A. Mougin, J.-P. Cromières, and V. Klein, *High resolution polar Kerr magnetometer for nanomagnetism and nanospintronics*, Rev. Sci. Instrum. **79**, 033706 (2008).

[16] D. A. Allwood, G. Xiong, M. D. Cooke, and R. P. Cowburn, *Magneto-optical Kerr effect analysis of magnetic nanostructures*, Journal of Physics D: Applied Physics **36**, 2175 (2003).

[17] A. Shen, H. Ohno, F. Matsukura, Y. Sugawara, N. Akiba, T. Kuroiwa, A. Oiwa, A. Endo, S. Katsumoto, and Y. Iye, *Epitaxy of (Ga,Mn)As, a new diluted magnetic semiconductor based on GaAs*, J. Cryst. Growth **175/176**, 1069 (1997).

[18] G. H. O. Daalderop, P. J. Kelly, and F. J. A. den Broeder, *Prediction and confirmation of perpendicular magnetic anisotropy in Co/Ni multilayers*, Phys. Rev. Lett. **68**, 682 (1992).

[19] Y. B. Zhang, J. A. W. P. He, J. X. Shen, R. D. Kirby, and D. J. Sellmyer, *Magnetic and magneto-optic properties of sputtered Co/Ni multilayers*, J. Appl. Phys **75**, 6495 (1994).

[20] G. N. Phillips, K. O'Grady, and J. C. Lodder, *Magnetization reversal at elevated temperatures in Co/Pt multilayer thin films*, Journal of Physics D: Applied Physics **34**, 2960 (2001).

[21] N. L. Schryer and L. R. Walker, *The motion of* $180°$ *domain walls in uniform dc magnetic fields*, Journal of Applied Physics **45**, 5406 (1974).

3

COUPLED MAGNETO-MECHANICAL DYNAMICS IN A SUSPENDED FERROMAGNETIC WIRE

We present the linear response matrix for a sliding domain wall in a rotatable magnetic nanowire, which is driven out of equilibrium by mechanical torque and applied magnetic field. Applying Onsager's reciprocity relation, we find a unified description of the Barnett effect – magnetization by rotation – and Einstein-de Haas effect – mechanical rotation induced by magnetization.

3.1 INTRODUCTION

In 1915, two experimental works on gyromagnetic effects were published: While Einstein and de Haas [2] demonstrated that reversing the magnetic moment of a ferromagnetic cylinder leads to mechanical rotation, Barnett [3] demonstrated that mechanical rotation of a demagnetized ferromagnet creates a net magnetization along the rotation axis. The latter work provided first evidence of the anomalous g-factor of the electron and therefore of the electron spin. Both effects are governed by the same gyromagnetic tensor [4]. Interest in the coupling of magnetic and mechanical degrees of freedom has recently been revived in the field of micro-electro-mechanical systems (MEMS) and nano-electro-mechanical systems (NEMS). Kovalev *et al.* [5–7] studied theoretically the coupled magneto-mechanical dynamics of a cantilever with a ferromagnetic tip while Ketteman *et al.* [8] provided a theoretical study of the torque exerted by a decaying spin-current on a mounted wire. Experimentally, the Einstein-de Haas effect in a magnetic cantilever was studied by Wallis *et al.* [9] while Zolfagharkani *et al.* [10] reported the first detection of the mechanical torque induced by the decay of a spin-current. This latter experiment can be interpreted as a variation of the experiment performed by Beth [11], where the mechanical torque induced by circularly polarized light on a suspended $\lambda/2$-plate was measured. In the previous chapter, Chapter 2, we presented a theoretical feasibility study on the Barnett effect in magnetic nanostructures. In particular, we estimated the domain-wall velocity in a rotating one-dimensional magnetic nanowire.

In this chapter, we investigate in linear response the dynamics of magneto-mechanical system consisting of a rotatable magnetic nanowire containing a sliding domain wall. To this end, we first review nonequilibrium thermodynamics in the next section before discussing our magneto-mechanical element.

3.2 NONEQUILIBRIUM THERMODYNAMICS

In this section, we review nonequilibrium thermodynamics following [12]. The second law of thermodynamics dictates that the entropy S is maximal in equilibrium. When considering small deviations of the n state variables $a_i = A_i - \bar{A}_i$ from their equilibrium values $\bar{A}_i$, we can thus write the fluctuations of the entropy ΔS from their equilibrium value as

$$\Delta S = -\frac{1}{2} \sum_{i=1}^{n} \sum_{k=1}^{n} \hat{g}_{ik} a_i a_k \leq 0, \tag{3.1}$$

where the matrix of coefficients $\hat{g}$ is positive definite and symmetric. The conjugate variable or force associated with the fluctuating state variable a_i can be de-

fined by

$$X_i = T\frac{\partial S}{\partial a_i} = -T\sum_{k=1}^{n} \hat{g}_{ik}a_k,\tag{3.2}$$

where T denotes the equilibrium temperature. The fluctuations A_i will relax to their equilibrium values $\bar{A}_i$ according to

$$J_i = \dot{a}_i = \sum_{k=1}^{n} \hat{L}_{ik}X_k,\tag{3.3}$$

where $\hat{L}$ is the response matrix. The system responses J_i are called fluxes, rates etc.

The entropy generation rate reads

$$\dot{S} = -\sum_i \dot{a}_i \sum_k \hat{g}_{ik}a_k = \frac{1}{T}\sum_i J_i X_i = \frac{1}{T}\sum_{i,k} \hat{L}_{ik}^{-1}X_k X_i.\tag{3.4}$$

Onsager [13] discovered a symmetry property of the response matrix elements, which is due to the microscopic time-reversal symmetry:

$$\hat{L}_{ik}(\vec{H}_{\text{ext}}, \vec{m}) = \epsilon_i \epsilon_k \hat{L}_{ki}(-\vec{H}_{\text{ext}}, -\vec{m}),\tag{3.5}$$

where $\epsilon_i = 1$ if the state variable a_i is even under time reversal and $\epsilon_i = -1$ otherwise. The time-reversal (anti)symmetry in the presence of external magnetic field $\vec{H}_{\text{ext}}$ and equilibrium magnetic ordering of unit length $\vec{M}(\vec{r})$, which parametrizes the position-dependent direction of the magnetization, has been made explicit. The inverse of the response matrix $\hat{L}$, for which

$$X_i = \sum_{k=1}^{n} \hat{L}_{ik}^{-1}J_k,\tag{3.6}$$

has the same Onsager symmetry property, *i.e.*

$$\hat{L}_{ik}^{-1}(\vec{H}_{\text{ext}}, \vec{m}) = \epsilon_i \epsilon_k \hat{L}_{ki}^{-1}(-\vec{H}_{\text{ext}}, -\vec{m}).\tag{3.7}$$

3.3 MAGNETOMECHANICAL ELEMENT

The standard model system for studying domain wall motion is a quasi-one-dimensional magnetic nanowire with easy-axis anisotropy that contains a transverse domain wall. In the following, we study the coupled magneto-mechanical dynamics of such a wire when it is mounted in such way that it can rotate freely around its symmetry axis. Furthermore, we choose the tail-to-tail topology rather than the head-to-head topology. The system we are studying is depicted in Fig. 3.1.
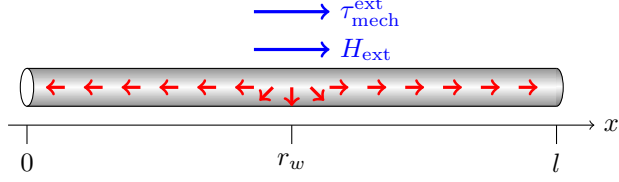
FIGURE 3.1: A magnetic nanowire of length l is mounted in such a way that it can rotate around the x-axis. A tail-to-tail domain wall is located in the wire at position r_w. A magnetic field H_{ext} and a torque $\tau^{\text{ext}}_{\text{mech}}$ can be applied along x.

The equation of motion of the magnetization in the lattice frame of reference $M_s\vec{m}(x,t)$, where M_s is the constant saturation magnetization and $\vec{m}$ a unit vector, is governed by the Landau-Lifshitz-Gilbert equation appended by a Barnett gauge field term as we have discussed in Chapter 2:

$$\dot{\vec{m}} = -\gamma\vec{m}\times\vec{H}_{\text{eff}} + \alpha\vec{m}\times\dot{\vec{m}} + \vec{m}\times\vec{x}\dot{\phi}, \tag{3.8}$$

where $\gamma > 0$ is the modulus of the gyromagnetic ratio and $\dot{\phi}$ the angular velocity of the wire rotating around the $\vec{x}$-axis. The effective field $\vec{H}_{\text{eff}}$ is the functional derivative of the free energy F with respect to the magnetization, which has contributions from the applied, anisotropy and exchange fields:

$$\vec{H}_{\text{eff}} = -\frac{\delta F[\vec{m}]}{M_s\delta\vec{m}(\vec{r})} = \vec{x}(H_{\text{ext}} + Km_x) - K_\perp m_z\vec{z} + A_{\text{ex}}\nabla^2\vec{m}, \tag{3.9}$$

where the unit vector of magnetization $\vec{m} = (m_x, m_y, m_z)$ can be parametrized as $\vec{m} = (\cos\theta, \sin\theta\cos\psi, \sin\theta\sin\psi)$. $K > 0$ and $K_\perp > 0$ are the anisotropy constants and A_{ex} is the exchange stiffness. In the absence of pinning the Walker ansatz [14],

$$\ln\tan\frac{\theta(x,t)}{2} = -\frac{x - r_w(t)}{\lambda_w} \quad\text{and}\quad \psi(x,t) = \psi(t), \tag{3.10}$$

provides a solution for a domain wall with time-dependent postion r_w and squared width $\lambda_w^2 = A_{\text{ex}}/(K + K_\perp\sin^2\psi)$. The angle ψ describes the tilt of the magnetization with respect to the $x-z$-plane, which vanishes at equilibrium. In the case of sufficiently small, steady state driving forces the polar angle ψ is constant. Consequently, it is not treated as a dynamical variable in what follows. Using the Walker ansatz, Eq. (3.10), in the Landau-Lifshitz-Gilbert equation, Eq. (3.8), one finds

$$\dot{r}_w = \frac{\lambda_w}{\alpha}(\dot{\phi} - \gamma H_{\text{ext}}), \quad K_\perp\sin 2\psi = -\frac{2(\dot{\phi} - \gamma H_{\text{ext}})}{\alpha\gamma}. \tag{3.11}$$

The Walker ansatz yields solutions which are valid up to a critical threshold at which $|\sin 2\psi_w| = 1$. To linear order in the driving field, the domain-wall width λ_w can be approximated by its equilibrium value $\lambda_w = \sqrt{A_{\text{ex}}/K}$.

Let us now focus on the mechanical degree of freedom of the wire, which is governed by the damped oscillator equation:

$$I\ddot{\phi} + \beta^{\text{mech}}\dot{\phi} = \tau^{\text{mech}}, \tag{3.12}$$

where I designates the moment of inertia of the wire, β^{mech} the mechanical damping parameter and τ^{mech} the total mechanical torque acting on the $\vec{x}$-axis. The combined, *i.e.* mechanical and magnetic, angular momentum of a freely rotating wire with cross-section A along its symmetry axis $\vec{x}$ is given by

$$L_x = -\frac{AM_s}{\gamma}(l - 2r_w) + I\dot{\phi}, \tag{3.13}$$

which is dissipated to the environment at a rate $\dot{L}_x = -\beta^{\text{mech}}\dot{\phi}$. This leads us to a Einstein-de Haas torque, induced by the moving domain wall, of

$$\tau^{\text{mech}}_{\text{EdH}} = -\frac{2AM_s}{\gamma}\dot{r}_w. \tag{3.14}$$

In the following we limit our discussion to overdamped systems, *i.e.* we limit the discussions to frequencies smaller than β^{mech}/I. In this case the angular acceleration $\ddot{\phi}$ and the moment of inertia drop out of the problem. The rotation velocity $\dot{\phi}$ is then directly proportional to the total torque $\tau^{\text{mech}} = \tau^{\text{mech}}_{\text{ext}} + \tau^{\text{mech}}_{\text{EdH}}$, *i.e.*

$$\beta^{\text{mech}}\dot{\phi} = \tau^{\text{mech}}_{\text{ext}} - \frac{2AM_s}{\gamma}\dot{r}_w. \tag{3.15}$$

In the following, we will show that the above results are consistent with Onsager's reciprocity principle and the second law of thermodynamics. Disregarding thermal effects, we may switch from the entropy S to the free energy F:

$$F(r_w, \phi) = F_w + F_\phi = (2r_w - l)AM_sH_{\text{ext}} + E(\phi), \tag{3.16}$$

where $E(\phi)$ is the mechanical energy that governs the external torque: $\tau^{\text{mech}}_{\text{ext}} = -\partial_\phi E(\phi)$, l is the total length of the wire and the domain-wall position r_w is measured with respect to the left end of the wire. We omit the internal energy of the domain wall, which below the Walker threshold may be treated as a rigid particle-like massless object specified by its position. The conjugate forces associated with r_w and ϕ are

$$X_w = -\frac{\partial F}{\partial r_w} = -2AM_sH_{\text{ext}} \tag{3.17}$$

and

$$X_\phi = -\frac{\partial F}{\partial \phi} = \tau^{\text{ext}}_{\text{mech}}. \tag{3.18}$$

Using Eqs. (3.11) and (3.15) we find the energy dissipation to be

$$T\dot{S} = -\dot{F} = -2AM_s H_{\text{ext}} \dot{r}_w + \tau^{\text{mech}}_{\text{ext}} \dot{\phi} = \frac{2\alpha A M_s}{\gamma \lambda_w} \dot{r}_w^2 + \beta^{\text{mech}} \dot{\phi}^2 \geq 0, \tag{3.19}$$

which is positive definite. By rewriting the equations of motion, Eqs. (3.11) and (3.15), we find that the cross terms obey Onsager's symmetry

$$\left(1 + \frac{2AM_s}{\gamma} \frac{\lambda_w}{\alpha\beta^{\text{mech}}}\right)\begin{pmatrix} \dot{\phi} \\ \dot{r}_w \end{pmatrix} = \begin{pmatrix} \frac{1}{\beta^{\text{mech}}} & -\frac{\lambda_w}{\alpha\beta^{\text{mech}}} \\ \frac{\lambda_w}{\alpha\beta^{\text{mech}}} & \frac{\lambda_w \gamma}{2\alpha A M_s} \end{pmatrix}\begin{pmatrix} X_\phi \\ X_w \end{pmatrix}. \tag{3.20}$$

We note, that the antisymmetry of the off-diagonal terms stems from Onsagers's reciprocity, which relates here the response of the tail-to-tail domain wall to that of its time-reversed partner, a head-to-head domain wall. The inverse of Eq. (3.20) reads

$$\begin{pmatrix} X_\phi \\ X_w \end{pmatrix} = \begin{pmatrix} \beta^{\text{mech}} & \frac{2AM_s}{\gamma} \\ -\frac{2AM_s}{\gamma} & \frac{2AM_s}{\gamma}\frac{\alpha}{\lambda_w} \end{pmatrix}\begin{pmatrix} \dot{\phi} \\ \dot{r}_w \end{pmatrix}. \tag{3.21}$$

We may rewrite Eq. (3.20) as

$$\begin{pmatrix} \dot{\phi} \\ \dot{r}_w \end{pmatrix} = \begin{pmatrix} \frac{1}{\tilde{\beta}^{\text{mech}}} & -\frac{\lambda_w}{\tilde{\alpha}\beta^{\text{mech}}} \\ \frac{\lambda_w}{\tilde{\alpha}\beta^{\text{mech}}} & \frac{\lambda_w \gamma}{2\tilde{\alpha} A M_s} \end{pmatrix}\begin{pmatrix} X_\phi \\ X_w \end{pmatrix} = \begin{pmatrix} L_{\phi,\phi} & L_{\phi,w} \\ L_{w,\phi} & L_{ww} \end{pmatrix}\begin{pmatrix} X_\phi \\ X_w \end{pmatrix}, \tag{3.22}$$

where

$$\tilde{\beta}^{\text{mech}} = \beta^{\text{mech}} + \frac{2\lambda_w A M_s}{\gamma\alpha} \tag{3.23}$$

and

$$\tilde{\alpha} = \alpha + \frac{2\lambda_w A M_s}{\gamma\beta^{\text{mech}}}. \tag{3.24}$$

The magnetomechanical coupling creates an apparently increased damping of the magnetization dynamics and/or the mechanical motion that is proportional to the number of spins in the domain wall. When β^{mech}, the mechanical damping parameter, becomes large the mechanical motion is quenched and $\tilde{\alpha} \to \alpha$, *i.e.* the excess Gilbert damping is suppressed.

The Onsager response function derived above contains the mechanical damping parameter β^{mech} and the Gilbert damping constant α as phenomenological constants. The latter, however, has been determined microscopically by scattering

theory [15]. Using the conventional notation in terms of transmission $(\hat{t}, \hat{t}')$ and reflection $(\hat{r}, \hat{r}')$ matrices, the scattering matrix in the space of the transport channels to and from the wire at an energy E and spin indices σ, σ' reads

$$\hat{S}_{\sigma,\sigma'}(E) = \begin{pmatrix} \hat{r}_{\sigma,\sigma'}(E) & \hat{t}_{\sigma,\sigma'}(E) \\ \hat{t}_{\sigma,\sigma'}(E) & \hat{r}_{\sigma,\sigma'}(E) \end{pmatrix}. \tag{3.25}$$

The energy pumped out of the system with a parametric time-dependence of the scattering matrix [16] is given by

$$J_E = \frac{\hbar}{4\pi}\mathrm{Tr}_s\frac{\partial\hat{S}}{\partial t}\frac{\partial\hat{S}^\dagger}{\partial t} = \frac{\hbar}{4\pi}(\dot{r}_w)^2\mathrm{Tr}_s\frac{\partial\hat{S}}{\partial r_w}\frac{\partial\hat{S}^\dagger}{\partial r_w}, \tag{3.26}$$

where Tr_s denotes the sum over all states in the left and right leads (including spin). This expression was used by Brataas et al. [17] to derive the Gilbert damping constant microscopically. The energy pumped out of the system due to the moving domain wall is also given by (see Eq. (3.4))

$$J_E = \frac{(\dot{r}_w)^2}{L_{ww}} \tag{3.27}$$

and thus it follows from (3.26)

$$L_{ww} = \left(\frac{\hbar}{4\pi}\mathrm{Tr}_s\frac{\partial\hat{S}}{\partial r_w}\frac{\partial\hat{S}^\dagger}{\partial r_w}\right)^{-1}. \tag{3.28}$$

Comparing this to the previously obtained expression for L_{ww}, Eq. (3.22), we recover the Gilbert damping parameter as calculated by Hals *et al.* [16] in the absence of rotation:

$$\alpha = \frac{\gamma\hbar\lambda_w}{8\pi AM_s}\mathrm{Tr}_s\frac{\partial\hat{S}}{\partial r_w}\frac{\partial\hat{S}^\dagger}{\partial r_w}. \tag{3.29}$$

3.4   NUMERICAL ESTIMATES

Elias *et al.* [18] have grown single-crystalline FeCo wires inside multiwall carbon nanotubes. In this system, the outer wall nantubes form almost ideal bearings for the rotation of the inner tubes [19]. This system could be a possible realization of the model discussed in this chapter. For the magnetic parameters we use values close to that of permalloy, namely $\alpha = 0.01$, $\lambda_w = 100$ nm and $M_s = 10^6$ A/m. Furthermore, we choose a wire area cross section of $A = 100$ nm^2 and the magnetic wire to be of length $l = 1\ \mu$m. The mechanical damping parameter β_{mech} was found to be $\beta_{\mathrm{mech}}/l = 0.044$ u·nm/ps, where 1 u = $1.66\cdot10^{-27}$ kg is the atomic mass

unit, in [20] for a $(4,4)$ nanotube rotating in a $(9,9)$ nanotube bearing. With these values we find

$$\begin{pmatrix} \frac{\tau_{\text{ext}}}{10^{-21}\,\text{Nm}} \\ -\frac{H_{\text{ext}}}{0.1\,\text{T}} \end{pmatrix} = \begin{pmatrix} 0.07 & 10^5 \\ -0.05 & 0.5 \end{pmatrix} \begin{pmatrix} \frac{\dot{\phi}}{1\,\text{GHz}} \\ \frac{\dot{r}_w}{10^5\,\frac{\text{m}}{\text{s}}} \end{pmatrix}. \tag{3.30}$$

The strong coupling between the mechanical degree of freedom and the magnetization dynamics is caused by the small friction of the nanotube-lubricated rotation.

3.5 Summary and Extensions

In this chapter, we have discussed the coupled magneto-mechanical dynamics of a mounted ferromagnetic wire containing a domain wall. As we have discussed above, the mechanical motion induced by the magnetic field is quantified by the Onsager coefficient $L_{\phi w}$ (Einstein-de Haas effect), which is identical with the Barnett response function $-L_{w\phi}$, which describes the magnetization dynamics induced by mechanical rotation.

A possible extension of the system discussed here, albeit beyond the scope of this thesis, is the introduction of temperature and voltage gradients across the magnetic nanowire, which are linked to their corresponding fluxes, namely heat $J_Q = \dot{U}$ and charge currents $J_c = \dot{q}$. The linear response matrix then reads $\vec{J} = \hat{L}\vec{X}$, where

$$\vec{X} = \left(-\Delta V, -\frac{\Delta T}{T}, \tau_{\text{ext}}^{\text{ext}}, -2AM_s H_{\text{ext}} \right) \tag{3.31}$$

and

$$\hat{L} = \begin{pmatrix} L_{cc} & L_{cQ} & L_{c\phi} & L_{cw} \\ L_{Qc} & L_{QQ} & L_{Q\phi} & L_{Qw} \\ L_{\phi c} & L_{\phi Q} & L_{\phi\phi} & L_{\phi w} \\ L_{wc} & L_{wQ} & L_{w\phi} & L_{ww} \end{pmatrix}. \tag{3.32}$$

According to Onsager symmetry, $L_{xw}(\vec{m}) = L_{wx}(-\vec{m}) = L_{wx}(\vec{m})$ as well as $L_{x\phi}(\vec{m}) = L_{\phi x}(-\vec{m}) = -L_{\phi x}(\vec{m})$ for $x = (c, Q)$ if the system is mirror symmetric with respect to a plane normal to the wire. Onsager symmetry also allows us to draw further conclusions: We know that a temperature gradient can induce a spin-transfer torque [21], which is represented by L_{wQ}. According to Onsager symmetry, an opposite effect exists, *i.e.* a heat current induced by magnetization dynamics. Furthermore, since $L_{\phi c} = -L_{c\phi}$ the magnetic wire can be employed as both electromotor [5] and electric generator.

References

[1] G. E. W. Bauer, S. Bretzel, A. Brataas, and Y. Tserkovnyak, *Nanoscale magnetic heat pumps and engines*, Phys. Rev. B **81**, 024427 (2010).

[2] A. Einstein and J. W. de Haas, *Experimental Proof of the Existence of Ampere's Molecular Currents*, Proceedings of the Koninklijke Akademie van Wetenschappen te Amsterdam **18 I**, 696 (1916).

[3] S. J. Barnett, *Magnetization by Rotation*, Phys. Rev. **6**, 239 (1915).

[4] L. Landau and E. Lifshitz, *Electrodynamics of Continous Media* (Pergamon Press, Oxford, 1984).

[5] A. A. Kovalev, G. E. W. Bauer, and A. Brataas, *Magnetovibrational coupling in small cantilevers*, Appl. Phys. Lett. **83**, 1584 (2003).

[6] A. A. Kovalev, G. E. W. Bauer, and A. Brataas, *Nanomechanical Magnetization Reversal*, Phys. Rev. Lett. **94**, 167201 (2005).

[7] A. A. Kovalev, G. E. W. Bauer, and A. Brataas, *Magnetomechanical Torques in Small Magnetic Cantilevers*, Japanese Journal of Applied Physics **45**, 3878 (2006).

[8] P. Fulde and S. Kettemann, *Spin-flip torsion balance*, Annalen der Physik **510**, 214 (1998), ISSN 1521-3889.

[9] T. M. Wallis, J. Moreland, and P. Kabos, *Einstein-de Haas effect in a NiFe film deposited on a microcantilever*, Appl. Phys. Lett. **89**, 122502 (2006).

[10] G. Zolfagharkhani, A. Gaidarzhy, P. Degiovanni, S. Kettemann, P. Fulde, and P. Mohanty, *Nanomechanical detection of itinerant electron spin flip*, Nature Nanotechnology **3**, 720 (2008).

[11] R. A. Beth, *Mechanical Detection and Measurement of the Angular Momentum of Light*, Phys. Rev. **50**, 115 (1936).

[12] L. D. Landau and E. M. Lifshitz, *Statistical Physics, Part 1* (Pergamon Press, 1980), 3rd ed.

[13] L. Onsager, *Reciprocal Relations in Irreversible Processes. I.*, Phys. Rev. **37**, 405 (1931).

[14] N. L. Schryer and L. R. Walker, *The motion of* 180° *domain walls in uniform dc magnetic fields*, Journal of Applied Physics **45**, 5406 (1974).

[15] A. Brataas, Y. Tserkovnyak, and G. E. W. Bauer, *Scattering Theory of Gilbert Damping*, Phys. Rev. Lett. **101**, 037207 (2008).

[16] K. M. D. Hals, A. K. Nguyen, and A. Brataas, *Intrinsic Coupling between Current and Domain Wall Motion in (Ga,Mn)As*, Phys. Rev. Lett. **102**, 256601 (2009).

[17] A. Brataas, Y. Tserkovnyak, and G. E. W. Bauer, *Scattering Theory of Gilbert Damping*, Phys. Rev. Lett. **101**, 037207 (2008).

[18] A. L. Elías, J. A. Rodríguez-Manzo, M. R. McCartney, D. Golberg, A. Zamudio, S. E. Baltazar, F. López-Urías, E. Muñoz Sandoval, L. Gu, C. C. Tang, et al., *Production and Characterization of Single-Crystal FeCo Nanowires Inside Carbon Nanotubes*, Nano Letters **5**, 467 (2005).

[19] A. M. Fennimore, T. D. Yuzvinsky, W.-Q. Han, M. S. Fuhrer, J. Cumings, and A. Zettl, *Rotational actuators based on carbon nanotubes*, Nature **424**, 408 (2003).

[20] J. Servantie and P. Gaspard, *Rotational Dynamics and Friction in Double-Walled Carbon Nanotubes*, Phys. Rev. Lett. **97**, 186106 (2006).

[21] M. Hatami, G. E. W. Bauer, Q. Zhang, and P. J. Kelly, *Thermal Spin-Transfer Torque in Magnetoelectronic Devices*, Phys. Rev. Lett. **99**, 066603 (2007).

4

ALIGNMENT OF RAPIDLY ROTATING GRAINS OF COSMIC DUST

Starlight polarimetry is presently the only method to observe the magnetic field texture on a cosmic length scale. The polarization of starlight is universally attributed to the anisotropic extinction by the alignment of anisotropic dust grains with respect to the magnetic fields. We discuss the alignment dynamics of a single dust grain by the Landau-Lifshitz-Gilbert equation, taking the Barnett and Einstein-de Haas effects (conservation of angular momentum) into account.

4.1 INTRODUCTION

More than sixty years ago it was discovered that starlight can be polarized [1, 2]. To date this observation is universally attributed to the anisotropic extinction arising when irregularly shaped dust grains are aligned with respect to a preferred direction. Cosmic magnetic fields provide such a preferred direction, thus allowing their mapping by starlight polarimetry.

Over the years, many mechanisms have been proposed in order to explain the alignment of dust grains. Davis and Greenstein [3] introduced paramagnetic relaxation as a mechanism of energy dissipation: Unless its angular momentum is aligned with the magnetic field, a grain "feels" an oscillating magnetic field in its restframe, which induces a time-dependent magnetization and therefore energy dissipation. After Spitzer and Tukey [4] had argued that dust grains may contain ferromagnetic inclusions, this mechanism was extended to ferromagnetic particles [5]. It is now accepted that paramagnetic relaxation rates are enhanced by small ferromagnetic inclusions that display "superparamagnetism" [6, 7]. Purcell [8] introduced two new concepts to the grain alignment problem: First, he showed that grains can rotate suprathermally, *i.e.* their mean rotational energy can be much higher than the particle lattice temperature and even that of the surrounding gas, which can lead to rotation frequencies of up to 100 kHz, presumably by the recoil during the desorption of hydrogen molecules. Second, Purcell introduced the Barnett effect [9] – rotation by magnetization – to the problem and showed that it leads to faster relaxation and alignment. More recently, radiative torques have been found to cause rapid rotation of particles with a diameter above 0.1 μm and align the grain with the magnetic field [10].

A remaining conundrum is the observation that dust grains smaller than 0.05 μm do not polarize starlight [10, 11]. Mathis [6] suggested that with decreasing size of the particle, it becomes statistically less likely that the particle contains superparamagnetic, ferromagnetic or ferrimagnetic impurities, thus making Davis-Greenstein type of relaxation mechanisms less efficient for small grains. For grains smaller than a critical size, thermal fluctuations may play an important role: Due to the degradation of H_2 formation sites, the Purcell torques will occasionally change their direction and the particle will thus spin down to thermal rotation frequencies, flip and spin up again [12]. For grains smaller than a critical radius of 0.1 μm, thermal trapping takes place [13]: For sufficiently small modulus of angular momentum, the flipping rate due to thermal fluctuations becomes large and the Purcell torque is no longer able to spin the grain up to suprathermal rotation before the next flipping event takes place.

In summary, the grain alignment process involves the following components: Grains are subject to two systematic torques that may drive the grain to suprather-

mal rotation, H_2 formation torques and torques due to starlight. The latter play only an important role for grains with radii $\gtrsim 0.1\,\mu$m. Achieving suprathermal rotation speeds may be suppressed by thermal flipping events and random collisions. Once the grain rotates suprathermally, the grain dynamics becomes immune from disalignment by random collisions. In this situation, alignment will be accomplished from the combined effect of starlight torques and (para)magnetic dissipation.

When magnetic damping is invoked as an alignment mechanism, the time-scales derived by Davis-Greenstein [3] and subsequent works, *e.g.* [5] for ferromagnetic particles, are usually employed, which do not consider the contribution of the Barnett effect. The Barnett effect is so far employed in grain-alignment discussions in order to justify why the major axis of inertia aligns itself with the axis given by the total angular momentum on a time-scale much faster than the alignment of the angular momentum vector with the magnetic field [14].

In this Chapter, we contribute to the discussion by computing the relaxation time for a single oblate ellipsoid that contains ferromagnetic inclusions. In our approach, we do not make any assumptions about the relative orientation of total angular momentum and major axis of inertia, contrary to aforementioned previous work. We assume that the dynamics can be described by the coupled mechanical and magnetic degrees of freedom. We fully take the Barnett and Einstein-de Haas effects (conservation of angular momentum) into account. Furthermore, we argue that energy is dissipated only by magnetization damping as already in previous works, e.g. [3, 5]. In our approach, we model the magnetization dynamics with a modified Landau-Lifshitz-Gilbert equation, which takes the rotation of the crystal lattice into account.

Our approach obeys the conservation of the total angular momentum $J_\parallel$ along the magnetic field. However, a rotating magnetic moment looses angular momentum and energy by electromagnetic radiation, thus rendering $J_\parallel$ time-dependent. In the treatment presented here, however, we assume that viscous magnetization damping is more efficient than radiative losses. The estimate justifying this assumption can be found in Appendix B.

Heating effects due to the viscous magnetization damping that might lead to a temperature-dependent magnetization and thus possibly to longer time-scales are disregarded, since we assume that the lattice is efficiently equilibrated with the cosmic radiation field. In addition, we assume that the modulus of the magnetization remains constant at all times as it is the case with ferromagnetic inclusions. This is compatible with the estimate that 10% of atoms in interstellar dust are iron [4, 15], of which up to 5% may form iron clusters [16]. Furthermore, mixed MgO-FeO-SiO are assumed to exist and exhibit ferromagnetic behaviour [17]. Thus dust grains with ferromagnetic ordering are a reasonable assumption for certain types

of cosmic clouds.

4.2 EQUATIONS OF MOTION

In this section, we set up the coupled magneto-mechanical equations of motion of a dust grain that contains a magnetic cluster with constant magnetic moment $|\vec{M}| =: M_s$. To this end, we first introduce the Euler angles ϕ, Θ ψ, that let us distinguish a laboratory frame of reference and a frame of reference co-rotating with the particle. With the Landau-Lifshitz-Gilbert (LLG) equation, we model the dynamics of the magnetic moment. A change in the magnetization will affect the rotational state of the particle (Einstein-de Haas effect), which will lead us to the equations of motion for the mechanical angular momentum.

In the following we distinguish the body frame of reference, which rotates with the particle, from the laboratory frame of reference. We assume that the origins of both frames of reference are located at the center of mass of the particle. The reference frames are related by the Euler angles ϕ, Θ and ψ (see Fig. 4.1 for a definition) [18]. A vector $\vec{q}_{\text{lab}}$ in the laboratory frame is related to its projection in the rotating frame by $\vec{q}_{\text{body}} = \mathbf{R}\vec{q}_{\text{lab}}$, where $\mathbf{R}$ denotes the rotation matrix linking the body and laboratory frames of reference. The rotation matrix that rotates the system by an angle η around the x- resp. z-axis is given by

$$
\begin{aligned}
\mathbf{R}_{x,z}(\eta) \quad = \quad & \vec{e}_{x,z}\vec{e}_{x,z}^T + \cos\eta \left[\vec{e}_y\vec{e}_y^T + \vec{e}_{z,x}\vec{e}_{z,x}^T \right] \\
& \mp \sin\eta \left[\vec{e}_{z,x}\vec{e}_y^T - \vec{e}_y\vec{e}_{z,x}^T \right],
\end{aligned}
\tag{4.1}
$$

where $\vec{e}_x^T = (1,0,0)$, $\vec{e}_y^T = (0,1,0)$ and $\vec{e}_z^T = (0,0,1)$ and the superscript T denotes the vector transpose. The rotation matrix that links the body and laboratory frames of reference is then given by $\mathbf{R} = \mathbf{R}_z(\psi)\mathbf{R}_x(\Theta)\mathbf{R}_z(\phi)$, where ψ, Θ and ϕ are the Euler angles defined in Fig. 4.1. The time-derivatives in the laboratory and body frame of references are related by the identity

$$
\dot{\vec{q}}_{\text{lab}} = \mathbf{R}^{-1} \left[\dot{\vec{q}}_{\text{body}} + \vec{\omega}_{\text{body}} \times \vec{q}_{\text{body}} \right],
\tag{4.2}
$$

where

$$
\vec{\omega}_{\text{body}} = \dot{\phi}\begin{pmatrix} \sin\Theta\sin\psi \\ \sin\Theta\cos\psi \\ \cos\Theta \end{pmatrix} + \dot{\Theta}\begin{pmatrix} \cos\psi \\ -\sin\psi \\ 0 \end{pmatrix} + \dot{\psi}\begin{pmatrix} 0 \\ 0 \\ 1 \end{pmatrix}
\tag{4.3}
$$

is the angular velocity in the body frame of reference.

The magnetization dynamics of sufficiently small ferromagnets can be described in the macrospin spin model by the Landau-Lifshitz-Gilbert (LLG) equation [19,
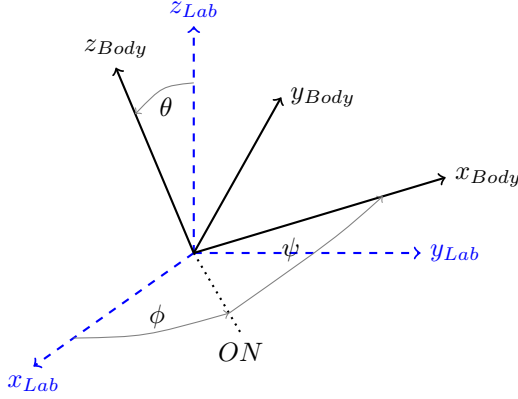
FIGURE 4.1: Definition of the Euler angles. The coordinate system Σ_{lab} (blue axes) denotes the system of inertia, whereas the coordinate system Σ_{body} is the rotating coordinate system (black axes), whose coordinate axis are parallel to the moments of inertia $I_{x,y,z}$. θ denotes the angle between z_{lab} and z_{body}. ϕ is the angle between x_I and ON, where ON denotes the line of intersection between the $x_{\text{lab}} - y_{\text{lab}}$ and $x_{\text{body}} - y_{\text{body}}$ planes. ψ is the angle between ON and the x_{body} axis.

20]

$$\dot{\vec{M}}_{\text{lab}} = \vec{M}_{\text{lab}} \times \gamma \vec{B}_{\text{lab}}^{\text{eff}} - \frac{\alpha \hat{\gamma}}{M_s} \left. \vec{M}_{\text{lab}} \times \dot{\vec{M}}_{\text{lab}} \right|_{\text{body}}, \qquad (4.4)$$

where $\vec{B}_{\text{lab}}^{\text{eff}}$ is the effective magnetic field, $\vec{M}_{\text{lab}}$ is the magnetization vector, $\alpha > 0$ the dimensionless Gilbert damping constant, M_s the modulus of the total magnetic moment, γ the gyromagnetic ratio and $\hat{\gamma} = \gamma/|\gamma|$ denotes its sign, which is positive for protons and negative for electrons. The microscopic origin of the magnetization damping is the spin-orbit interaction, by which the energy in the magnetic system can leak to the lattice. This implies that the damping term in Eq. (4.4) is governed by the magnetization motion relative to the lattice, viz. [21, 22]

$$\left. \vec{M}_{\text{lab}} \times \dot{\vec{M}}_{\text{lab}} \right|_{\text{body}} = \mathbf{R} \left(\vec{M}_{\text{body}} \times \dot{\vec{M}}_{\text{body}} \right). \qquad (4.5)$$

Transforming Eq. (4.4) to the body frame of reference:

$$\dot{\vec{M}}_{\text{body}} = \vec{M}_{\text{body}} \times \left[\gamma \vec{B}_{\text{body}}^{\text{eff}} + \vec{\omega}_{\text{body}} \right] - \frac{\hat{\gamma}\alpha}{M_s} \vec{M}_{\text{body}} \times \dot{\vec{M}}_{\text{body}}. \qquad (4.6)$$

Rotation is seen to induce a (Barnett) gauge field $\vec{\omega}_{\text{body}}/\gamma$ acting on the magnetization in the body frame [22]. In the laboratory frame, the LLG equation of a

magnetic moment in a rotating particle is given by

$$
\begin{aligned}
\dot{\vec{M}}_{\text{lab}} \;\; = \;\; & \vec{M}_{\text{lab}} \times \gamma \vec{B}_{\text{lab}}^{\text{eff}} - \frac{\alpha \hat{\gamma}}{M_s} \vec{M}_{\text{lab}} \times \dot{\vec{M}}_{\text{lab}} \\
& - \frac{\alpha \hat{\gamma}}{M_s} \vec{M}_{\text{lab}} \times (\vec{M}_{\text{lab}} \times \vec{\omega}_{\text{lab}}) \, .
\end{aligned}
\tag{4.7}
$$

We observe that the Barnett field is not apparent, but that the rotation of the lattice manifests itself as an additional damping term in the laboratory system.

The interplay between the Einstein-de Haas effect (rotation by magnetization) and the Barnett effect (magnetization by rotation) is schematically depicted in Fig. 4.2. By virtue of Noether's theorem, the total angular momentum $\vec{J}$ is conserved in the direction of the external magnetic field. This implies that in the laboratory frame the total angular momentum $\vec{J}_{\text{lab}} = \vec{L}_{\text{lab}} + \vec{M}_{\text{lab}}/\gamma$, where $\vec{L}_{\text{lab}}$ denotes the mechanical angular momentum, experiences a torque by the external magnetic field $\vec{B}_{\text{lab}}^{\text{ext}}$

$$
\dot{\vec{J}}_{\text{lab}} = \vec{M}_{\text{lab}} \times \vec{B}_{\text{lab}}^{\text{ext}} \, .
\tag{4.8}
$$

In what follows, we assume that the effective magnetic field equals the external one, *i.e.* we disregard internal magnetic fields associated with crystal anisotropies or dipolar interactions. Then:

$$
\dot{\vec{L}}_{\text{lab}} = \frac{\alpha}{M_s |\gamma|} \left[\vec{M}_{\text{lab}} \times \dot{\vec{M}}_{\text{lab}} + \vec{M}_{\text{lab}} \times \left(\vec{M}_{\text{lab}} \times \vec{\omega}_{\text{lab}} \right) \right] \, .
\tag{4.9}
$$

Eqs. (4.7), (4.8) and (4.9) provide the full set of equations that describes the motion of a rotating magnetic particle in an external magnetic field, taking fully into account the conservation of total angular momentum. The free energy of the whole system reads

$$
F = \frac{1}{2} \vec{\omega}_{\text{body}}^{T} \mathbf{I} \vec{\omega}_{\text{body}} - \vec{M}_{\text{body}} \left(\vec{B}_{\text{body}}^{\text{ext}} + \frac{\vec{\omega}_{\text{body}}}{\gamma} \right) ,
\tag{4.10}
$$

where $\mathbf{I}$ denotes the moment of inertia tensor. We consider in the following symmetric tops and chose the body frame such that $\mathbf{I} = \text{diag}(I_\perp, I_\perp, I_\parallel)$. The problem defined by the equations above is non-linear and an exact solution cannot be obtained analytically. Our numerical simulations on rotating spheres with magnetic inclusions show that the dynamics immediately following initialization of a fast rotation is usually erratic. However, the time scale of orientation of the rotation axes to weak external magnetic fields is governed by a deterministic slow approach to a stable steady state. We therefore proceed by first determining stationary stable states in a magnetic field and then finding the relaxation times associated with small deviations from these steady states.
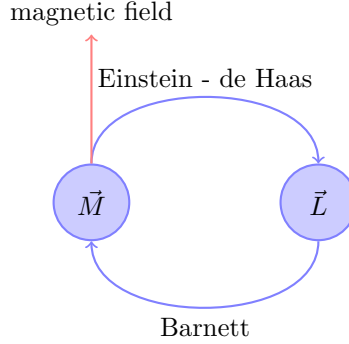
FIGURE 4.2: Schematic interplay between Barnett and Einstein-de Haas effect in a rotating magnetic grain: A change in the magnetization $\vec{M}$ affects the mechanical angular momentum $\vec{L}$ via the Einstein-de Haas effect. *Vice versa,* the mechanical state affects the magnetic state via the Barnett effect. In the presence of an external magnetic field, the component of the total angular momentum parallel to the external field is conserved, while the other experience torques.

4.3 STEADY STATES

In the previous section, section 4.2, we have set up coupled magneto-mechanical equations of motion for a dust grain with constant magnetic moment $|\vec{M}|$. Since the resulting equations of motion, Eqs. (4.7), (4.8) and (4.9), are non-linear, we need to linearize the equations of motion around the steady state in order to recover the time-scales governing the alignment process. The first step in this direction is to determine the steady states, which is the focus of this section.

We assume that the lattice of the dust grain is in thermal equilibrium with the universe via electromagnetic interactions except for the rigid body motion, *i.e.* translations and rotations. We focus here on the relaxation of the rotational modes in the presence of magnetic moments. When $\dot{\vec{M}}_{\text{body}} \neq 0$ energy and angular momentum leak to the lattice by viscous damping. In a steady state, therefore, $\dot{\vec{M}}_{\text{body}} = 0$. Eq. (4.6) requires then that $\vec{M}_{\text{body}} \times (\gamma \vec{B}^{\text{ext}}_{\text{body}} + \vec{\omega}_{\text{body}}) = 0$, *i.e.*, the magnetization must be (anti)parallel to the combined external and Barnett fields. Therefore

$$\vec{M}_{\text{lab,body}} = \pm \frac{M_s}{|\vec{\omega}_{\text{lab,body}} + \gamma \vec{B}^{\text{ext}}_{\text{lab,body}}|} \left(\vec{\omega}_{\text{lab,body}} + \gamma \vec{B}^{\text{ext}}_{\text{lab,body}} \right), \qquad (4.11)$$

where M_s denotes the saturation magnetization and "lab,body" means that Eq. (4.11) holds in either reference frame. Since the external magnetic field in the labo-

ratory frame is constant in time, it follows from Eq. (4.2) that $\dot{\vec{B}}_{\mathrm{body}}^{\mathrm{ext}} = \vec{B}_{\mathrm{body}}^{\mathrm{ext}} \times \vec{\omega}_{\mathrm{body}}$. Since in the steady state the sum of external and Barnett fields in the body frame of reference is constant in time leads to $\dot{\vec{\omega}}_{\mathrm{body}} = \vec{\omega}_{\mathrm{body}} \times \gamma \vec{B}_{\mathrm{body}}^{\mathrm{ext}}$ and thus $\dot{\vec{\omega}}_{\mathrm{lab}} = \vec{\omega}_{\mathrm{lab}} \times \gamma \vec{B}_{\mathrm{lab}}^{\mathrm{ext}}$. This is a constant precession around the external field, which might be chosen along the x-axis. We can parametrize that motion and compare it with the expression in terms of the Euler angles as

$$\vec{\omega}_{\mathrm{lab}} = \Omega \begin{pmatrix} \cos G \\ \sin G \sin A \\ \sin G \cos A \end{pmatrix} = \begin{pmatrix} \dot{\Theta}\cos\phi + \dot{\psi}\sin\Theta\sin\phi \\ \dot{\Theta}\sin\phi - \dot{\psi}\cos\phi\sin\Theta \\ \dot{\phi} + \dot{\psi}\cos\Theta \end{pmatrix}, \quad (4.12)$$

where Ω is the constant rotation frequency, G the constant angle between $\vec{\omega}_{\mathrm{lab}}$ and the external magnetic field and $\dot{A} = \gamma B_{\mathrm{ext}}$ is the frequency of the precession of $\vec{\omega}_{\mathrm{lab}}$ around the external magnetic field, which can have either sign to indicate the chirality. Introducing the angle Γ between the axis defined by the direction of $I_\parallel$ (the z-axis of the body frame of reference) and $\vec{B}^{\mathrm{ext}}$, we find

$$\cos\Gamma := \sin\Theta\sin\phi. \quad (4.13)$$

From Eq. (4.2) and $\dot{\vec{M}}_{\mathrm{body}} = 0$ it follows that

$$\dot{\vec{M}}_{\mathrm{lab}} + \vec{M}_{\mathrm{lab}} \times \vec{\omega}_{\mathrm{lab}} = 0, \quad (4.14)$$

which according to Eq. (4.9) means $\dot{\vec{L}}_{\mathrm{lab}} = 0$, *i.e.* in the steady state the mechanical angular momentum is constant in time and thus cannot precess. In the body frame the moment of inertia tensor is diagonal:

$$\vec{L}_{\mathrm{body}} = \mathbf{I}_{\mathrm{body}}\vec{\omega}_{\mathrm{body}} = \begin{pmatrix} I_\perp & 0 & 0 \\ 0 & I_\perp & 0 \\ 0 & 0 & I_\parallel \end{pmatrix}\vec{\omega}_{\mathrm{body}}. \quad (4.15)$$

We can introduce a new Cartesian axes

$$\vec{v}_1 = \begin{pmatrix} \sin\Theta\sin\phi \\ -\sin\Theta\cos\phi \\ \cos\Theta \end{pmatrix}, \quad \vec{v}_2 = \begin{pmatrix} \cos\Theta\sin\phi \\ -\cos\Theta\cos\phi \\ -\sin\Theta \end{pmatrix}, \quad \vec{v}_3 = \begin{pmatrix} \cos\phi \\ \sin\phi \\ 0 \end{pmatrix}. \quad (4.16)$$

Since $\vec{q}_{\mathrm{body}} = \mathbf{R}_z(\psi)\mathbf{R}_x(\Theta)\mathbf{R}_z(\phi)\vec{q}_{\mathrm{lab}}$, we see that the moment of inertia tensor in the laboratory frame of reference can be written as

$$\mathbf{I}_{\mathrm{lab}} = I_\perp \mathbb{1} + \Delta I \left(\vec{v}_1 \vec{v}_1^T\right), \quad (4.17)$$

where $\Delta I = I_\parallel - I_\perp$ and T denotes the vector transpose so that $\vec{v}_1 \vec{v}_1^T$ is a 3×3 matrix. We have $\dot{\vec{L}}_{\text{lab}} = \dot{\mathbf{I}}_{\text{lab}} \vec{\omega}_{\text{lab}} + \mathbf{I}_{\text{lab}} \dot{\vec{\omega}}_{\text{lab}} = 0$, where

$$\dot{\mathbf{I}}_{\text{lab}} = \Delta I \left[\dot{\Theta} \vec{v}_2 \vec{v}_1^T + \dot{\phi} \sin\Theta \vec{v}_3 \vec{v}_1^T + \dot{\Theta} \vec{v}_1 \vec{v}_2^T + \dot{\phi} \sin\Theta \vec{v}_1 \vec{v}_3^T \right], \qquad (4.18)$$

and $\vec{\omega}_{\text{lab}}$ is given by Eq. (4.12). The coefficients of $\vec{v}_{1,2,3}$ in $\dot{\vec{L}}_{\text{lab}} = 0$ results in a set of three equations,

$$0 = I_\parallel \gamma B_0 \Omega \sin G \left[\sin\Theta \cos\phi \cos A + \sin A \cos\Theta \right], \quad (4.19)$$

$$\Delta I \dot{\Theta} (\vec{v}_1^T \vec{\omega}_{\text{lab}}) = -I_\perp \gamma B_0 \Omega \sin G \left(\vec{v}_2^T \begin{pmatrix} 0 \\ \cos A \\ -\sin A \end{pmatrix} \right), \qquad (4.20)$$

$$\Delta I \dot{\phi} \sin\Theta (\vec{v}_1^T \vec{\omega}_{\text{lab}}) = -I_\perp \gamma B_0 \Omega \sin G \left(\vec{v}_3^T \begin{pmatrix} 0 \\ \cos A \\ -\sin A \end{pmatrix} \right). \qquad (4.21)$$

With Eq. (4.12) it follows that Eqs. (4.19) to (4.21) are true for $\Omega = 0$, *i.e.* a particle at rest. Multiplying $\vec{\omega}_{\text{lab}}$, Eq. (4.12), by $\vec{v}_3^T$ yields

$$\dot{\Theta} = \vec{v}_3^T \vec{\omega}_L = \Omega \left[\cos\phi \cos G + \sin G \sin A \sin\phi \right] \qquad (4.22)$$

while multiplying $\vec{\omega}_{\text{lab}}$ by $\vec{v}_1^T$ yields

$$\dot{\phi} \sin\Theta = -\vec{v}_2^T \vec{\omega}_L = \Omega \left[-\cos\Theta \cos G \sin\phi + \sin G (\sin\Theta \cos A + \cos\phi \cos\Theta \sin A) \right]. \qquad (4.23)$$

For $\sin G = 0$, Eq. (4.19) is fulfilled and Eq. (4.20) resp. Eq. (4.21) become

$$0 = \Delta I \Omega^2 \cos\phi \cos\Gamma \qquad (4.24)$$

and

$$0 = \Delta I \Omega^2 \cos\Gamma \cos\Theta, \qquad (4.25)$$

where we used Eq. (4.22) resp. (4.23). Since $\cos\Gamma = \sin\Theta \sin\phi$ these two conditions imply that for $\Omega \neq 0$ either $\cos\Gamma = 0$, *i.e.* $I_\parallel$ is oriented perpendicular to the magnetic field, or $|\cos\Gamma| = 1$, *i.e.* $I_\parallel$ is parallel to it.

If $\sin G \neq 0$, Eq. (4.19) requires that

$$\sin\Theta \cos\phi \cos A + \sin A \cos\Theta = 0. \qquad (4.26)$$

This can be achieved when both $\cos\phi$ and $\cos\Theta$ are constant and equal to zero. Then Eq. (4.22) yields

$$\dot{\Theta} = \pm\Omega \sin G \sin A \overset{!}{=} 0, \qquad (4.27)$$

which is only true for $\Omega = 0$, *i.e.* the particle is at rest, or $\sin G = 0$ – the latter contradicting our initial assumption of $\sin G \neq 0$. Since $\sin A$ and $\cos A$ are periodic in time, Eq. (4.26) may be fulfilled as well when $\sin \Theta \cos \phi$ and $\cos \Theta$ are periodic with the same period. To find those solutions, we may expand $\sin \Theta \cos \phi$ and $\cos \Theta$ in a Fourier series. Taking into account only the first harmonic $\sin \Theta \cos \phi = c_0 + c_1 \sin A + c_2 \cos A$ and $\cos \Theta = d_0 + d_1 \sin A + d_2 \cos A$, with coefficients $c_{0,1,2}$ and $d_{0,1,2}$. Using this ansatz in Eq. (4.26) one finds that $d_2 = -c_1$ and all other coefficients vanish. Therefore $\Theta = \pm A$ and $\cos \phi = \mp 1$ also fulfills Eq. (4.26). With $\dot{\Theta} = \pm \gamma B_{\text{ext}}$ Eq. (4.20) yields

$$\Delta I \Omega \sin G \Omega = -I_\perp \Omega \sin G. \tag{4.28}$$

For $\Omega \neq 0$ this relation is only fulfilled for $\sin G = 0$, contrary to our initial assumption.

   We conclude that in the steady state the axis defined by the moment of inertia $I_\parallel$ is either perpendicular or parallel to the direction defined by the external magnetic field, whereas the axis of rotation and the magnetic moment are (anti)parallel to it. The energy of Eq. (4.10) for these steady states read

$$F = \frac{J_\parallel^2}{2 I_s} + \frac{3}{2} \frac{M_s^2}{\gamma^2 I_s} - 2\sigma \frac{M_s}{\gamma} \frac{J_\parallel}{I_s} - \sigma M_s B_0, \tag{4.29}$$

where $\sigma = \substack{+ \\ (-)} 1$ denotes the (anti)parallel orientation of $\vec{M}$ with $\vec{B}^{\text{ext}}$, $J_\parallel$ the total angular momentum in direction of $\vec{B}^{\text{ext}}$ and $I_s = I_{\parallel,\perp}$ for $|\cos \Gamma| = 1$ respectively $\cos \Gamma = 0$. The steady state with major axis of inertia oriented along the magnetic has lower kinetic energy. In addition, we find the steady state rotation frequency of the particle

$$\Omega = \frac{J_\parallel - \sigma \frac{M_s}{\gamma}}{I_s}. \tag{4.30}$$

4.4 LINEARIZED EQUATIONS OF MOTION

In the previous section, we have determined the steady states of a rotating dust grain containing a constant magnetic moment M_s. We now proceed to linearize the magneto-mechanical equations of motion obtained in section 4.2 in the vicinity of the steady states.

   So far, our treatment holds for arbitrary ellipsoids. The subsequent treatment for prolate ellipsoids is complicated, since the steady state conditions only determine the angle ϕ while leaving the other two Euler angles unspecified. Furthermore, observational data suggests that cosmic dust grains are of oblate shape [23].

For these reasons, we consider the linearized equations of motion for an oblate particle, *i.e.* $I_\parallel > I_\perp$ (pancake like), in what follows.

As in the previous section we assume that $\vec{B}_\text{lab}^\text{ext} \parallel \vec{x}_\text{lab}$. We choose this orientation of the magnetic field deliberately, since choosing the magnetic field along the $\vec{z}_\text{lab}$-axis and with our choice of Euler angles would lead to the problem of "gimbal lock", *i.e.* in the steady state $\dot{\phi}$ (rotation around z_lab-axis) and $\dot{\psi}$ (rotation around figure axis z_body) would coincide. In the steady state $\mathbf{R}^{-1}\vec{z}_\text{body} = \vec{x}_\text{lab}$. This is the case for $\phi = (n+1/2)\pi$, $\Theta = (k+1/2)\pi$ where $n, k \in \mathbb{Z}$, *i.e.* we distinguish two steady states with $\cos\Gamma = \pm 1$. Considering small deviations of $\vec{\omega}_\text{lab}$ and $\vec{L}_\text{lab}$ from the steady state,

$$\vec{\omega}_\text{lab} = \begin{pmatrix} \Omega + (-1)^{n+k}\delta\dot{\psi} \\ (-1)^n\delta\dot{\Theta} + \Omega\delta\phi \\ \delta\dot{\phi} - (-1)^n\Omega\delta\Theta \end{pmatrix} = \begin{pmatrix} \Omega + \delta\omega_x \\ \delta\omega_y \\ \delta\omega_z \end{pmatrix} \tag{4.31}$$

and

$$\vec{L}_\text{lab} = \begin{pmatrix} I_\parallel(\Omega + \delta\omega_x) \\ I_\perp\delta\omega_y + \Delta I\Omega\delta\phi \\ I_\perp\delta\omega_z - \Delta I(-1)^n\Omega\delta\Theta \end{pmatrix}, \tag{4.32}$$

where $\Delta I = I_\parallel - I_\perp$ and Ω is the rotation frequency in the steady state. Similarly, deviations of the magnetization and total angular momentum can be written as

$$\vec{M}_\text{lab} = \sigma \begin{pmatrix} M_s \\ \delta m_y \\ \delta m_z \end{pmatrix} \quad \text{and} \quad \vec{J}_\text{lab} = \begin{pmatrix} J_\parallel \\ \delta J_y \\ \delta J_z \end{pmatrix}. \tag{4.33}$$

With $\vec{J}_\text{lab} = \vec{L}_\text{lab} + \vec{M}_\text{lab}/\gamma$, $\delta\omega_x = 0$, $\Omega = J_\parallel/I_\parallel - \sigma M_s/(\gamma I_\parallel)$:

$$\vec{\omega}_\text{lab} = \frac{1}{I_\perp} \begin{pmatrix} \frac{I_\perp}{I_\parallel}J_\parallel \\ \delta J_y \\ \delta J_z \end{pmatrix} - \frac{\sigma}{\gamma I_\perp} \begin{pmatrix} \frac{I_\perp}{I_\parallel}M_s \\ \delta m_y \\ \delta m_z \end{pmatrix} + \frac{\Delta I}{I_\perp}\Omega \begin{pmatrix} 0 \\ -\delta\phi \\ (-1)^n\delta\Theta \end{pmatrix}. \tag{4.34}$$

Introducing

$$\delta m_s = \delta m_y + is\delta m_z, \quad \delta J_s = \delta J_y + is\delta J_z, \tag{4.35}$$

with chirality $s = \pm 1$, and comparing Eqs. (4.31) and (4.34), we obtain an equation of motion for $\delta\Gamma_s = (-1)^n\delta\Theta + is\delta\phi$:

$$\delta\dot{\Gamma}_s = -\frac{\sigma}{\gamma}\frac{1}{I_\perp}\delta m_s + \frac{1}{I_\perp}\delta J_s + is\frac{I_\parallel}{I_\perp}\Omega\delta\Gamma_s. \tag{4.36}$$

Using Eq. (4.34) in Eq. (4.7) yields the linearized equation of motion for δm_s,

$$
\begin{aligned}
\dot{\delta m_s} \quad = \quad & -\frac{\alpha\hat{\gamma}\frac{J_{\parallel}}{I_{\parallel}} + i s \sigma \gamma B_0 + \alpha\hat{\gamma}\frac{\Delta I}{I_{\perp}}\frac{\sigma M_s}{\gamma I_{\parallel}}}{A_s^*}\delta m_s \\
& + \frac{\alpha\hat{\gamma}}{A_s^*}\frac{M_s}{I_{\perp}}\delta J_s + \frac{i s \alpha\hat{\gamma}}{A_s^*}M_s\Omega\frac{\Delta I}{I_{\perp}}\delta\Gamma_s,
\end{aligned}
\tag{4.37}
$$

where $A_s = \sigma - i s \hat{\gamma}\alpha$. Furthermore, linearizing Eq. (4.8) yields

$$
\dot{\delta J_s} = -i s \sigma B_0 \delta m_s.
\tag{4.38}
$$

In conclusion, Eqs. (4.36) to (4.38) provide a linearized set of equations for the motion of the particle near the steady state. The motion of the grain in the vicinity of the steady state can be decomposed in a linear combination of eigenmodes $\vec{e}_k e^{E_k t}$, where $\vec{e}_k$, E_k are eigenvectors resp. eigenvalues given by a coefficient matrix defined by Eqs. (4.36) to (4.38). The real part of the eigenvalues E_k is the time-scale with which each eigenmode decays (when $\mathrm{Re} E_k < 0$) or increases (when $\mathrm{Re} E_k > 0$). In order to obtain the time-scales of the alignment process, we thus need to obtain these eigenvalues. Unfortunately, however, we have not been able to find an analytical expression for the eigenvalues, so that we need to employ a perturbative approach. In the following section, we discuss the limit of the damping constant $\alpha \ll 1$, whereas in section 4.6 we discuss the limit in which the magnetic moment in the particle is negligible compared to the mechanical angular momentum component along the direction of the magnetic field.

4.5   TIME SCALES IN THE LIMIT OF VANISHING DAMPING

Only in specially engineered materials the damping constant for magnetic motion $\alpha \gg 0.01$. For local magnetic moments in an insulating matrix the magnetization dynamics may be damped even less. So the regime of weak damping appears to be appropriate for the particles believed to be found in cosmic clouds. Eqs. (4.36) to (4.38) constitute a system of coupled differential equations for the vector $\vec{x}_s^T = (\delta m_s/M_s, \delta J_s/J_{\parallel}, \delta\Gamma_s)$ with

$$
\dot{\vec{x}}_s = \left(\mathbf{R}_0 - \alpha\hat{\gamma}\mathbf{R}_1 + \mathcal{O}(\alpha^2)\right)\vec{x}_s,
\tag{4.39}
$$

where

$$\mathbf{R}_0 = \frac{J_{\parallel}}{I_{\parallel}} \begin{pmatrix} -isp & 0 & 0 \\ -ispm & 0 & 0 \\ -mI_{\parallel}/I_{\perp} & I_{\parallel}/I_{\perp} & is(1-m)I_{\parallel}/I_{\perp} \end{pmatrix}, \tag{4.40}$$

$$\mathbf{R}_1 = \sigma \frac{J_{\parallel}}{I_{\parallel}} \begin{pmatrix} 1+p+m\frac{\Delta I}{I_{\perp}} & -\frac{I_{\parallel}}{I_{\perp}} & -is(1-m)\frac{\Delta I}{I_{\perp}} \\ 0 & 0 & 0 \\ 0 & 0 & 0 \end{pmatrix}, \tag{4.41}$$

with $m = \sigma M_s/\gamma J_{\parallel}$ and $p = \gamma B_0 I_{\parallel}/J_{\parallel}$, and $\mathcal{O}(\alpha^2)$ denotes terms of order α^2 and higher that are assumed to be negligibly small. Solutions of Eq. (4.39) are given by $\vec{x}_s = \sum_i c_i \vec{e}_i e^{E_i t}$, where c_i are coefficients determined by the initial conditions, $\vec{e}_i$ and E_i the eigenvectors resp. eigenvalues of the matrix $\mathbf{R}_0 - \hat{\gamma}\alpha\mathbf{R}_1$. Since typically $\alpha \ll 1$, we can employ the perturbation theory outlined in appendix A. We now discuss the two leading terms in this expansion.

To zeroth order in α the eigenvalues and eigenvectors are given by

$$\vec{e}_1^0 = \begin{pmatrix} 1 \\ m \\ 0 \end{pmatrix} \quad \text{with} \quad E_1^0 = -is\gamma B_0, \tag{4.42}$$

$$\vec{e}_2^0 = \begin{pmatrix} 0 \\ -is(1-m) \\ 1 \end{pmatrix} \quad \text{with} \quad E_2^0 = 0, \tag{4.43}$$

$$\vec{e}_3^0 = \begin{pmatrix} 0 \\ 0 \\ 1 \end{pmatrix} \quad \text{with} \quad E_3^0 = is\frac{J_{\parallel}}{I_{\perp}}(1-m). \tag{4.44}$$

The eigenmode associated with $\vec{e}_1^0$ describes an undamped precession of both magnetization and total angular momentum vector around the magnetic field, the eigenmode associated with $\vec{e}_2^0$ a static deflection of the total angular momentum vector and major axis of inertia from the steady state and the $\vec{e}_3^0$-eigenmode is an undamped rotation of the major axis of inertia around the direction given by the magnetic field.

The positive-definite Hermitian matrix

$$K = \frac{1}{1-m} \begin{pmatrix} 1-m+\frac{2m^2}{1-m} & -\frac{2m}{1-m} & -ism \\ -\frac{2m}{1-m} & \frac{2}{1-m} & is \\ ism & -is & 1-m \end{pmatrix} \tag{4.45}$$

allows us to define a scalar product $\langle \vec{a}|\vec{b}\rangle \equiv \vec{a}^\dagger K \vec{b}$ such that $(\vec{e}_i^0)^\dagger K \vec{e}_j^0 = \delta_{i,j}$, where $\delta_{i,j}$ is the Kronecker δ. With K given by Eq. (4.45) and using Eq. (A.13), we obtain

the first-order correction in α for the eigenvalues $E_{1,2,3}$, the real-parts of whose are the inverse time-scales for the alignment processes:

$$\text{Re} E_1 = -\frac{1}{\tau_{\vec{M},\vec{J}\to\vec{B}}} = -\alpha\hat{\gamma}\sigma\left(\frac{J_\parallel}{I_\parallel} + \gamma B_0 - \frac{\sigma M_s}{\gamma I_\parallel}\right), \tag{4.46}$$

$$\text{Re} E_2 = -\frac{1}{\tau_{\vec{J},I_\parallel\to\vec{B}}} = -\alpha\hat{\gamma}\frac{M_s}{\gamma I_\parallel}, \tag{4.47}$$

$$\text{Re} E_3 = -\frac{1}{\tau_{I_\parallel\to\vec{B}}} = -\alpha\hat{\gamma}\frac{\Delta I}{I_\perp}\frac{M_s}{\gamma I_\parallel}. \tag{4.48}$$

The inverse time-scale $\text{Re} E_1 = -1/\tau_{\vec{J},\vec{M}\to\vec{B}}$, describing the alignment of total angular momentum and magnetization with the external magnetic field, is determined by the magnitude of the combined Barnett- and external magnetic fields. For a stable steady state, the real parts of the eigenvalues must be negative. This allows us to determine σ, the orientation of the magnetization with respect to the magnetic field: $\text{Re} E_1 < 0$ implies that $\hat{\gamma}\sigma = -1$ if $J_\parallel/I_\parallel + \gamma B_0 - \sigma M_s/(\gamma I_\parallel) > 0$ and vice versa.

4.6 TIME SCALES IN THE LIMIT OF SMALL MAGNETIC MOMENT

Similarly, we can investigate the time-scales in the limit of small magnetic moment but possibly large damping. To this end, we introduce the small parameter $\sigma M_s/(\gamma J_\parallel)$, thereby assuming that the magnetic moment is sufficiently smaller than the mechanical angular momentum parallel to the magnetic field, *i.e.* $|I_\parallel\omega| \gg |M_s/\gamma|$.

Eqs. (4.36) to (4.38) may then be written as a matrix differential equation for the vector $\vec{x}_s^T = (\delta m_s/M_s, \delta J_s/J_\parallel, \delta\Gamma_s)$:

$$\dot{\vec{x}}_s = \left[\mathbf{R}_0 + \frac{\sigma M_s}{\gamma I_\parallel}\mathbf{R}_1\right]\vec{x}_s, \tag{4.49}$$

where

$$\mathbf{R}_0 = \frac{J_\parallel}{I_\parallel}\frac{1}{1+\alpha^2}\begin{pmatrix} -A_s(\alpha\hat{\gamma} + is\sigma p) & \alpha\hat{\gamma}\frac{I_\parallel}{I_\perp}A_s & is\alpha\hat{\gamma}\frac{\Delta I}{I_\perp}A_s \\ 0 & 0 & 0 \\ 0 & \frac{I_\parallel}{I_\perp}|A_s|^2 & is|A_s|^2\frac{I_\parallel}{I_\perp} \end{pmatrix}, \tag{4.50}$$

$$\mathbf{R}_1 = \begin{pmatrix} -\frac{\Delta I}{I_\perp}\frac{\alpha\hat{\gamma}}{1+\alpha^2}A_s & 0 & -\frac{\alpha\hat{\gamma}is}{1+\alpha^2}A_s\frac{\Delta I}{I_\perp} \\ -isp & 0 & 0 \\ -\frac{I_\parallel}{I_\perp} & 0 & -is\frac{I_\parallel}{I_\perp} \end{pmatrix}, \tag{4.51}$$

$A_s = \sigma - i s \hat{\gamma} \alpha$ and $p = \gamma B_0 I_\parallel / J_\parallel$.

In the absence of magnetism $\sigma M_s / \gamma I_\parallel = 0$ the solution of (4.49) is given by $\vec{x}_s = \sum_i c_i \vec{e}_i^0 e^{E_i^0 t}$, where c_i are coefficients determined by the initial conditions, $\vec{e}_i^0$ and E_i^0 are the eigenvectors *resp.* eigenvalues of the matrix $\mathbf{R}_0$ given by Eq. (4.50). We find the eigenvalues resp. eigenvectors of $\mathbf{R}_0$ to be

$$
E_1^0 = is\frac{J_\parallel}{I_\perp} \quad \text{with} \quad \vec{e}_1^0 = \begin{pmatrix} -Q_1 \\ 0 \\ 1 \end{pmatrix},
$$

$$
E_2^0 = -\frac{J_\parallel}{I_\parallel} \frac{A_s(\alpha\hat{\gamma} + is\sigma p)}{1 + \alpha^2} \quad \text{with} \quad \vec{e}_2^0 = \begin{pmatrix} 1 \\ 0 \\ 0 \end{pmatrix},
$$

$$
E_3^0 = 0 \quad \text{with} \quad \vec{e}_3^0 = \begin{pmatrix} isQ_0 \\ -is \\ 1 \end{pmatrix}, \tag{4.52}
$$

where

$$
Q_1 = \frac{-is\alpha\hat{\gamma}A_s\left(\frac{\Delta I}{I_\perp}\right)}{is\left(\frac{I_\parallel}{I_\perp}\right)|A_s|^2 + A_s(\alpha\hat{\gamma} + is\sigma p)} \tag{4.53}
$$

and

$$
Q_0 = -\frac{\alpha\hat{\gamma}}{\alpha\hat{\gamma} + is\sigma p}. \tag{4.54}
$$

The eigenmode associated with $\vec{e}_1^0$ describes an undamped precessional motion of the magnetization and the axis with main moment of inertia around the magnetic field. The eigenmode associated with $\vec{e}_2^0$ is a damped magnetization precession. The eigenmode associated with the eigenvalue $E_3^0 = 0$ is just a static deflection from the steady state orientation: The axis with moment of inertia $I_\parallel$ lies in the $x_{lab} - z_{lab}$-plane, as does the total angular momentum vector. In addition, the magnetization is not fully aligned with the direction given by the magnetic field.

We now derive the eigenvalues for these eigenmodes to the next order in our small parameter, which provide the time scale of the alignment of the grain with the magnetic field. The matrix

$$
K = \begin{pmatrix} 1 & Q_0 - isQ_1 & Q_1 \\ Q_0^* + isQ_1^* & k_1 & Q_1 Q_0^* + isk_2 \\ Q_1^* & Q_1^* Q_0 - isk_2 & k_2 \end{pmatrix}, \tag{4.55}
$$

with $k_1 = 2 + |Q_1|^2 + |Q_0|^2 + 2s\mathrm{Im}(Q_1 Q_0^*)$ and $k_2 = 1 + |Q_1|^2$, is a positive-definite Hermitian matrix that defines a scalar product with $(\vec{e}_i^0)^\dagger K \vec{e}_j^0 = \delta_{ij}$, where δ_{ij} is

the Kronecker delta. In first order in $\sigma M_s / \gamma J_\parallel$, we obtain with Eq. (A.13)

$$
\begin{aligned}
\mathrm{Re}E_3 &= -\frac{1}{\tau_{\vec{J} \to \vec{B}}} = \frac{\sigma M_s}{\gamma I_\parallel} \mathrm{Re}\left[(\vec{e}_3^{\,0})^\dagger K R_1 \vec{e}_3^{\,0} \right] \\
&= \left(\frac{\sigma M_s}{\gamma I_\parallel} \right) p \,\mathrm{Re}(i s Q_0) \\
&= -\left(\frac{\sigma M_s}{\gamma I_\parallel} \right) \frac{\sigma p^2 \alpha \hat{\gamma}}{\alpha^2 + p^2}\, ,
\end{aligned}
\tag{4.56}
$$

which is the inverse time-scale $1/\tau_{\vec{J} \to \vec{B}}$ of the $\vec{J}_{\mathrm{lab}}$ alignment. Similarly,

$$
\begin{aligned}
\mathrm{Re}E_1 &= -\frac{1}{\tau_{I_\parallel \to \vec{B}}} = \frac{\sigma M_s}{\gamma I_\parallel} \mathrm{Re}\left[(\vec{e}_1^{\,0})^\dagger K R_1 \vec{e}_1^{\,0} \right] \\
&= \left(\frac{\sigma M_s}{\gamma I_\parallel} \right) \left(\frac{\Delta I}{I_\perp} + 1 + p \right) \mathrm{Re}Q_1 \\
&= -\frac{\alpha \hat{\gamma} \sigma \left(\frac{\sigma M_s}{\gamma I_\parallel} \right) \left(\frac{\Delta I}{I_\perp} \right) \left(\frac{\Delta I}{I_\perp} + 1 + p \right)^2}{\alpha^2 \left(\frac{\Delta I}{I_\perp} \right)^2 + \left(1 + \frac{\Delta I}{I_\perp} + p \right)^2}\, ,
\end{aligned}
\tag{4.57}
$$

which is the inverse time-scale $1/\tau_{I_\parallel \to \vec{B}}$ for the alignment the main axis of inertia with $\vec{B}_{\mathrm{lab}}^{\mathrm{ext}}$.

4.7   Order of magnitude estimates

In this section we estimate the time-scales for the regimes described above. In evaluating our time-scales and putting them into perspective with previously found time-scales, we assume the particle to be of oblate shape with half axes $b > a$ and thus $I_\parallel = 2mb^2/5$ and $I_\perp = m(a^2 + b^2)/5$, where m denotes the mass of the grain. The grain has a volume of $V = (4\pi/3)ab^2 = (4\pi/3)r_{\mathrm{eff}}^3$, where r_{eff} is the effective radius of the grain.

An insecurity of our estimates is the permanent magnetic moment residing in the particle. Observational data suggests that up to 5% of the atoms in cosmic dust grains are iron forming clusters [16]. An upper bound for the magnetic moment residing in a dust grain being given by

$$
N = \frac{M_s}{\mu_B} = \frac{4 \cdot 0.05 \rho V N_A}{0.95 \cdot m_{\mathrm{H_2 0}} + 0.05 \cdot m_{\mathrm{Fe}}} \approx 8 \cdot 10^6 \cdot \left(\frac{r_{\mathrm{eff}}}{0.1\ \mu\mathrm{m}} \right)^3 \left(\frac{\rho}{3\ \frac{\mathrm{g}}{\mathrm{cm}^3}} \right),
\tag{4.58}
$$

with Avogadro constant $N_A = 6 \cdot 10^{22}\ \mathrm{mol}^{-1}$, density ρ, volume $V = (4\pi/3)r_{\mathrm{eff}}^3$ and the molar masses $m_{\mathrm{H_2O}}$ and m_{Fe} for water and iron, when employing the assumption that the dust grain mainly consists of ice and iron, the latter forming one

cluster with uniform magnetic moment. Furthermore, we assumed that each iron atom supplies a magnetic moment of $4\mu_B$, as the electron configuration of the iron atom suggests.

In section 4.6 we considered the time-scales for alignment in the regime when $|M_s/(\gamma J_\parallel)| \ll 1$, *i.e.* when the magnetic moment is negligible compared to the total angular momentum in direction of the external field. $|M_s/(\gamma J_\parallel)| \ll 1$ implies that $|M_s/(\gamma I_\parallel)| \ll |\Omega|$, where Ω is the steady state rotation frequency. For $M_s = N\mu_B$, with N given by Eq, (4.58), our estimates remain valid when

$$|\Omega| \gg 8 \text{ kHz} \cdot \left(\frac{r_{\text{eff}}}{0.1 \ \mu\text{m}}\right)^{-2} \left(\frac{a}{b}\right)^{\frac{2}{3}} . \tag{4.59}$$

Considering that dust grains may rotate suprathermally [8] with frequencies up to 100 kHz, Eq. (4.59) is a good estimate for particles $r_{\text{eff}} \gtrsim 0.1 \ \mu\text{m}$.

One mechanism that randomizes the alignment of dust grains is collisions with surrounding gas molecules. The time-scale for this process was found to be [24]

$$\tau_{\text{drag}} = \frac{3 I_\parallel}{4\sqrt{\pi} n_{H_2} m_{H_2} v_{\text{th}} r_{\text{eff}}^4 \Gamma_\parallel \left(\sqrt{1 - \left(\frac{a}{b}\right)^2}\right)} , \tag{4.60}$$

where $v_{\text{th}} = \sqrt{2 k_B T_g / m_{H_2}}$ is the thermal speed of the surrounding H_2 molecules, n_{H_2} is the number density, m_{H_2} the mass of a hydrogen molecule and $\Gamma_\parallel$ is a geometric factor,

$$\Gamma_\parallel(e) = \frac{3}{16} \left(3 + 4(1 - e^2) g(e) - \frac{1}{e^2} \left(1 - (1 - e^2)^2 g(e)\right)\right) \tag{4.61}$$

and $g(e) = (2e)^{-1} \ln[(1 + e)/(1 - e)]$. One finds

$$\tau_{\text{drag}} \sim 1.6 \cdot 10^6 \text{ yr} \cdot \left(\frac{r_{\text{eff}}}{0.1 \ \mu\text{m}}\right) \left(\frac{T_g}{20 \text{ K}}\right)^{-\frac{1}{2}} \left(\frac{n_{H_2}}{30 \ \frac{1}{\text{cm}^3}}\right) . \tag{4.62}$$

The time-scales $\tau_{I_\parallel \to \vec{B}}$ and $\tau_{\vec{J}, I_\parallel \to \vec{B}}$ in section 4.5 as well as $\tau_{\vec{J} \to \vec{B}}$ and $\tau_{I_\parallel \to \vec{B}}$ in section 4.6 are the time-scales on which the alignment of both the total angular momentum $\vec{J}$ and the major axis of inertia with the magnetic field occurs. To put them into perspective, we compare these time-scales with the time-scales for the same processes derived by Davis and Greenstein [3] for paramagnetic relaxation and the one derived by Henry [5] for ferromagnetic relaxation as well as the time-scale τ_{drag} on which the orientation of the grain gets randomized by collisions with gas molecules (Eq. (4.62)).

The time scales $\tau_{I_\parallel \to \vec{B}}$ and $\tau_{\vec{J}, I_\parallel \to \vec{B}}$ in section 4.5 as well as $\tau_{\vec{J} \to \vec{B}}$ and $\tau_{I_\parallel \to \vec{B}}$ in section 4.6, are proportional to the parameter $(\gamma I_\parallel)/(M_s \alpha)$. We also observe that the time scales we obtained in section 4.6 coincide with those derived in section 4.5 in the limit $\alpha \ll 1$. The alignment time-scales are then proportional to

$$\tau = \frac{I_\parallel |\gamma|}{M_s \alpha} \sim 1.3 \cdot 10^{-4} \text{ s} \cdot \left(\frac{r_{\text{eff}}}{0.1 \ \mu\text{m}} \right)^2 \frac{1}{\alpha} \left(\frac{b}{a} \right)^{\frac{2}{3}}, \qquad (4.63)$$

when the magnetic moment of the grain is $N\mu_B$ with N given by Eq. (4.59). We see that in our model, grain alignment happens instantaneously compared to the time-scale due to gas-grain collisions, Eq. (4.62). This implies, that an ensemble of grains will be almost perfectly aligned.

The time-scale for paramagnetic alignment was determined by Davis and Greenstein [3] to be

$$\tau_{\text{DG}} = \frac{I_\parallel}{KVB_0^2}. \qquad (4.64)$$

K is related to the imaginary part of the magnetic susceptibility χ by $\text{Im}(\chi) = K\omega$ and is estimated to be $K \approx 1.2 \cdot 10^{-13} \text{s} \cdot (20 \text{ K}/T)$ [10], with T being the grain temperature. Thus, the time-scale for paramagnetic alignment can be estimated to be

$$\tau_{DG} \approx 1.2 \cdot 10^6 \text{ yr} \cdot \left(\frac{\rho}{3 \frac{\text{g}}{\text{cm}^3}} \right) \left(\frac{r_{\text{eff}}}{0.1 \ \mu\text{m}} \right)^2 \left(\frac{B_0}{5 \ \mu\text{G}} \right)^{-2} \left(\frac{b}{a} \right)^{\frac{2}{3}}. \qquad (4.65)$$

We observe that τ_{DG} is quadratic in r_{eff}, whereas τ_{drag} is linear. This implies that for large grains the time-scale for disalignment by gas collisions may be shorter than the alignment time, thus leading to imperfect alignment.

Henry [5] investigated the alignment process of ferromagnetic grains with uniform magnetization density and assuming that the shape anisotropy, given by the geometry of the grain, is the dominant contribution to the effective magnetic field. This is different from our approach, where we have assumed that shape anisotropy is negligible since we imagine a spherical magnetic cluster embedded in a much larger grain. The time-scale governing the alignment process was found to be the same as in Eq. (4.64), with K being now given by

$$K = \frac{2\gamma^2 (M_s/V)^2 (N_\perp - N_\parallel)}{T_2 \omega_0^4} \qquad (4.66)$$

with demagnetization factors $N_\parallel$, $N_\perp$, resonance frequency ω_0 and relaxation time T_2. For Fe $K = 3 \cdot 10^{-7}$ s at low temperature and when the ratio of long and short
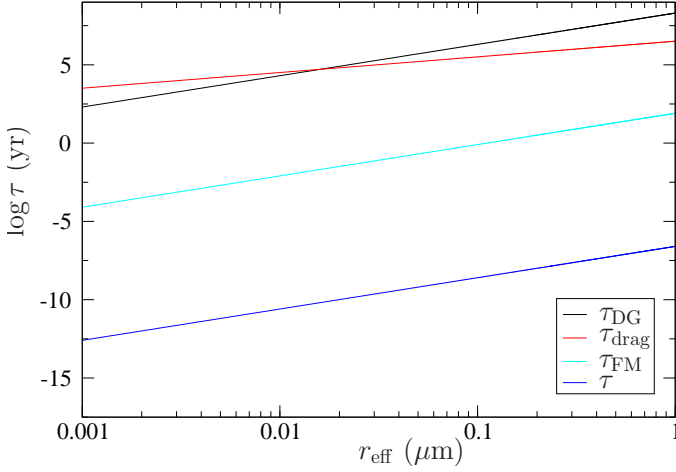
FIGURE 4.3: Comparison of τ, the time-scale for alignment of the major axis of inertia and total angular momentum with the magnetic field, with the time-scales derived by Davis and Greenstein (τ_{DG}) resp. Henry (τ_{FM}) for the same process for paramagnetic resp. ferromagnetic grains. τ_{drag} is the time-scale on which the grains get randomized due to collisions with surrounding gas. We observe, that the time-scale derived in this chapter are much shorter than the previously derived time-scales for grain alignment. We chose $\rho = 3\ \mathrm{g/cm}^3$, $a/b = 0.5$, $B_0 = 5\ \mu\mathrm{G}$, $T_g = 20\ \mathrm{K}$, $n_{H_2} = 30\ \mathrm{cm}^{-3}$ and $\alpha = 10^{-2}$.

axis of the particle is two [5], leading to

$$\tau_{\mathrm{FM}} \approx 0.5\ \mathrm{yr} \cdot \left(\frac{\rho}{3\ \frac{\mathrm{g}}{\mathrm{cm}^3}}\right)\left(\frac{r_{\mathrm{eff}}}{0.1\ \mu\mathrm{m}}\right)^2 \left(\frac{B_0}{5\ \mu\mathrm{G}}\right)^{-2} \left(\frac{b}{a}\right)^{\frac{2}{3}} \approx 4 \cdot 10^{-7} \tau_{DG}. \qquad (4.67)$$

As with the alignment time-scale τ derived by us, τ_{FM} is instantanous compared to the time-scale given by gas-grain collisions.

In Fig. 4.3 we summarize the different time-scales. We observe, that the time-scales we have obtained for the alignment process are much shorter than the time-scale due to paramagnetic damping, due to magnetic damping in a uniformly ferromagnetic grain or the time-scale on which gas-grain collisions take place. We can attribute the smallness of our time-scale in comparison to the τ_{DG} to the fact, that a permanent magnetic moment of just some μ_B is larger than the paramagnetism induced by the weak magnetic field present in the grain alignment problem. In comparison to τ_{FM}, we have rapid alignment due to our disregarding of effective fields due to anisotropy, leading to quicker energy dissipation due to magnetization damping.

4.8 CONCLUSIONS AND OUTLOOK

We studied the alignment of rotating magnetic grains with respect to an external magnetic field, carefully taking the conservation of angular momentum into account. The magnetization dynamics was modelled with the Landau-Lifshitz-Gilbert equation with a modified damping term in the laboratory frame in order to account for the viscous magnetization damping due to the motion of the magnetization relative to the lattice. We identified possible steady states, and calculated the time-scales for alignment in the special case of an oblate spheroid. We find that the time-scales determining the alignment of the long axis of inertia depend only on the magnetic moment and the shape and size of the particle but not on the rotation frequency resp. mechanical angular momentum of the particle. The time-scale for the alignment of the major axis of inertia are proportional to the magnetic moment of the particle. If small particles have consistently a smaller magnetic moment, their alignment process will take longer resp. they might get randomized by, *e.g.*, collisions before they reach alignment.

We disregarded the contribution of crystal anisotropies to the effective magnetic field. When the anisotropy field dominates over both Barnett and external magnetic fields, the magnetic moment is locked to a specific direction in the lattice frame of reference. Then the damping term vanishes and the particle will not align itself with the direction of the magnetic field but carries out a precessional motion, that is damped only by other processes such as radiative losses. Our estimated alignment time scales are therefore a lower bound to the expected ones. More work is needed to narrow down the alignment time scales in the presence of magnetic anisotropies.

In the present chapter, we only focused on an isolated particle, thus neglecting collisions with other particles or interactions with surrounding gas molecules. Such interaction adds stochastic torques to the problem. As a result, the time-evolution of the probability distribution of an ensemble of particles becomes the important quantity, whose time-evolution may be described by the Fokker-Planck equation [25]. The probability distribution then yields a mean axial alignment of the dust grains, which is the experimentally accessible quantity.

REFERENCES

[1] J. S. Hall, *Observations of the Polarized Light From Stars*, Science **109**, 166 (1949).

[2] W. A. Hiltner, *Polarization of Light From Distant Stars by Interstellar Medium*, Science **109**, 165 (1949).

[3] L. Davis, Jr. and J. L. Greenstein, *The Polarization of Starlight by Aligned Dust Grains.*, Astrophysical Journal **114**, 206 (1951).

[4] L. Spitzer, Jr. and J. W. Tukey, *A Theory of Interstellar Polarization.*, Astrophysical Journal **114**, 187 (1951).

[5] J. Henry, *Polarization of Starlight by Ferromagnetic Particles.*, Astrophysical Journal **128**, 497 (1958).

[6] J. S. Mathis, *The alignment of interstellar grains*, Astrophysical Journal **308**, 281 (1986).

[7] R. V. Jones and L. Spitzer, Jr., *Magnetic Alignment of Interstellar Grains*, Astrophysical Journal **147**, 943 (1967).

[8] E. M. Purcell, *Suprathermal rotation of interstellar grains*, Astrophysical Journal **231**, 404 (1979).

[9] S. J. Barnett, *Magnetization by Rotation*, Phys. Rev. **6**, 239 (1915).

[10] B. Draine, in *The Cold Universe: Saas-Fee Advanced Course 32*, edited by D. Pfenniger (Springer, 2004).

[11] D. C. B. Whittet, in *Astrophysics of Dust*, edited by A. N. Witt, G. C. Clayton, & B. T. Draine (2004), vol. 309 of *Astronomical Society of the Pacific Conference Series*, pp. 65–+.

[12] L. Spitzer, Jr. and T. A. McGlynn, *Disorientation of interstellar grains in suprathermal rotation*, Astrophysical Journal **231**, 417 (1979).

[13] A. Lazarian and B. T. Draine, *Thermal Flipping and Thermal Trapping: New Elements in Grain Dynamics*, The Astrophysical Journal Letters **516**, L37 (1999).

[14] A. Lazarian, *Tracing magnetic fields with aligned grains*, Journal of Quantitative Spectroscopy and Radiative Transfer **106**, 225 (2007), ISSN 0022-4073.

[15] P. G. Martin, *On the value of GEMS (glass with embedded metal and sulphides)*, Astrophysical Journal - Letters **445**, L63 (1995).

[16] B. T. Draine and A. Lazarian, *Magnetic Dipole Microwave Emission from Dust Grains*, The Astrophysical Journal **512**, 740 (1999).

[17] W. W. Duley, *Magnetic alignment of interstellar grains*, Astrophysical Journal - Letters **219**, L129 (1978).

[18] L. D. Landau and E. M. Lifshitz, *Mechanics* (Butterworth Heinemann, 1976), 3rd ed.

[19] T. Gilbert, *A Lagrangian formulation of the gyromagnetic equation of the magnetic field (Abstract Only)*, Physical Review **100**, 1243 (1955).

[20] T. Gilbert, *A phenomenological theory of damping in ferromagnetic materials*, Magnetics, IEEE Transactions on **40**, 3443 (2004).

[21] A. A. Kovalev, G. E. W. Bauer, and A. Brataas, *Nanomechanical Magnetization Reversal*, Phys. Rev. Lett. **94**, 167201 (2005).

[22] S. Bretzel, G. E. W. Bauer, Y. Tserkovnyak, and A. Brataas, *Barnett Effect in Magnetic Thin Films and Nanostructures*, Applied Physics Letters **95**, 122504 (2009).

[23] R. H. Hildebrand and M. Dragovan, *The Shapes and Alignment Properties of Interstellar Dust Grains*, Astrophysical Journal **450**, 663 (1995).

[24] A. Lazarian and W. G. Roberge, *Barnett Relaxation in Thermally Rotating Grains*, The Astrophysical Journal **484**, 230 (1997).

[25] W. G. Roberge and A. Lazarian, *Davis-Greenstein alignment of oblate spheroidal grains*, Monthly Notices of the Royal Astronomical Society **305**, 615 (1999), ISSN 1365-2966.

5

THE BARNETT VS. LANDAU LEVELS IN THE ROTATING FREE ELECTRON GAS

The Barnett effect – the reorientation of the electron spin induced by rotation – was discovered at the dawn of quantum mechanics and provided first evidence for an anomalous g -factor of the electron. In recent years, there has been a renewed interest in systems, that couple magnetic and mechanical degrees of freedom. However, most of this research has focused on the Einstein - de Haas effect, i.e., rotation induced by magnetization. Here we consider the orbital Barnett effect in the rotating electron gas. We find rotationally induced paramagnetism in a spin-free system, quite different from the diamagnetic response to an external magnetic field.

5.1 INTRODUCTION

A close relationship between ferromagnetism and angular momentum was first proposed by Ampère and later elaborated in detail by Weber [1]. However, the so-called molecular current hypothesis remained unproven until 1915, when Barnett [2, 3] managed to induce a net magnetization of a demagnetized ferromagnetic body by mechanical rotation. Shortly thereafter, Einstein and de Haas [4] observed a mechanical rotation induced by the change of magnetization of a suspended ferromagnetic body.

The Barnett effect – magnetization induced by rotation – can be understood by classical mechanics: A gyroscopic wheel aligns its angular momentum with the axis of an impressed rotation in order to minimize energy. Modelling a magnetic moment as a gyroscopic wheel, one finds that rotation is equivalent to a "Barnett gauge field" [3] in the rotating frame,

$$\vec{B}_g = -\frac{\vec{\omega}}{\gamma}, \tag{5.1}$$

where $\vec{\omega}$ denotes the rotation axis and $\gamma = g|e|/(2m)$. In this chapter, we demonstrate that this Barnett gauge field not only acts on the electron spin but has effects on the orbital degrees of motion that differ from a conventional magnetic field. We illustrate this by comparing the eigenstates of the rotating two-dimensional electron gas, which we call "Barnett levels", with the Landau in an external magnetic field.

Related to the Barnett effect is the Sagnac effect [5], originally devised for light: a beam of light is split and the two resulting beams are made to enclose a closed area. Rotating the interferometer, one observes shifts in the interference pattern at the exit point, since the light beams in both arms experience different path lengths under rotation. In matter wave interferometers, the Sagnac effect can be understood by means of the Barnett gauge field. It was observed experimentally for electrons in vacuum [6] and atoms [7]. The Sagnac effect has also been studied theoretically in mesoscopic quantum rings [8].

Superseded by electron spin resonance to measure g-factors, gyromagnetic methods have been largely forgotten in the last decades. However, the miniaturization of electric circuits and mechanical systems revived some interest. An Einstein-de Haas type of experiment was discussed in a mesoscopic cantilever with a ferromagnetic tip [9–11]. We previously studied the Barnett effect [12] in ferromagnets by the Landau-Lifshitz-Gilbert equation. For a model system consisting of a suspended magnetic wire we demonstrated the equivalence of Barnett and Einstein-de Haas effects by invoking the Onsager reciprocity relations [13]. Matsuo *et al.* [14] derived the Pauli-Schrödinger equation in a rotating frame, using the covari-

ant Dirac equation as a starting point. The resulting Hamiltonian contains a spin-orbit interaction term augmented by a term due to mechanical rotation. With this Pauli-Schrödinger equation the mechanical generation of spin currents in systems rotating at non-relativistic speeds was predicted [14, 15].

5.2 ROTATING FRAME OF REFERENCE

Rotation of a quantum state $|\psi\rangle$ by an angle ϕ is represented by a unitary operator $\hat{R}$,

$$|\psi(\phi)\rangle = \hat{R}(\phi)|\psi(0)\rangle, \tag{5.2}$$

while operators transform as

$$\hat{A}(\phi) = \hat{R}(\phi)\hat{A}(0)\hat{R}^{\dagger}(\phi), \tag{5.3}$$

since rotating both states and operator by the same angle must leave the expectation value unchanged. For rotations around the z-axis [16],

$$\hat{R}(\phi) = e^{-\frac{i}{\hbar}\hat{J}_z\phi}, \tag{5.4}$$

where $\hat{J}_z = \hat{L}_z + \hat{s}_z$ is the total angular momentum operator in the z-direction, with $\hat{L}_z$ being the orbital and $\hat{s}_z$ the spin angular momentum operator.

Rotation introduces a time-dependence into the Hamiltonian, which can be removed by switching to the rotating frame of reference. Let us denote the orbital coordinate as $\Theta(t) = \Theta_{\text{Rot}} + \phi(t)$, where $\phi(t)$ is the angle by which the system has been rotated and Θ_{Rot} denotes the orbital variable in the rotating frame of reference. We can remove an explicit time dependence by transforming to the rotating frame of reference using Eqs. (5.3) and (5.2). The Schrödinger equation in the rotating frame then reads

$$i\hbar\frac{\mathrm{d}}{\mathrm{d}t}|\psi(\Theta_{\text{Rot}})\rangle = \left(\hat{H}_0(\Theta_{\text{Rot}}) - \hat{J}_z\frac{\mathrm{d}\phi(t)}{\mathrm{d}t}\right)|\psi(\Theta_{\text{Rot}})\rangle, \tag{5.5}$$

in which $\hat{H}_0$ and the eigenstates no longer depend on the time-dependent coordinates. The total Hamiltonian $\hat{H}_0 - \hat{J}_z\mathrm{d}\phi(t)/\mathrm{d}t$ may still be time-dependent when the angular velocity is not constant. In the following, we denote $|\psi(\Theta_{\text{Rot}})\rangle$ as $|\psi_{\text{Rot}}\rangle$ and $|\psi(\Theta_{\text{Rot}} + \phi(t))\rangle$ as $|\psi_{\text{Lab}}\rangle$.

5.3 EIGENSTATES OF A ROTATING TWO-DIMENSIONAL EL-ECTRON GAS

Consider a two-dimensional free electron gas (2DEG) with radius R residing in the $x-y$-plane that is rotated around the z-axis with angular frequency ω. The Hamil-

tonian in the rotating frame of reference is that of a free electron, i.e.,

$$\hat{H}_{\text{Rot}} = \frac{\hbar^2 \vec{\hat{k}}^2}{2m} - \omega \hat{J}_z.$$

(5.6)

Exploiting the axial symmetry, we can rewrite (5.6): In polar coordinates (r, θ) and with the boundary condition $\psi(r = R) = 0$, we obtain the normalized eigenstates that we refer to as *Barnett levels*:

$$\psi_{n,k,\sigma}(r,\theta) = \frac{e^{in\theta}}{\sqrt{\pi} R J_{|n|+1}(j_{|n|,k})} J_{|n|}\left(\frac{j_{|n|,k}}{R} r\right) |\sigma\rangle$$

(5.7)

with eigenenergies

$$E_{n,k,\sigma} = \frac{\hbar^2 j_{|n|,k}^2}{2mR^2} - \hbar\omega\left(n + \frac{\sigma}{2}\right),$$

(5.8)

where $|\sigma = \pm 1\rangle$ denote the spin wave functions with $s_z|\sigma\rangle = (\sigma\hbar/2)|\sigma\rangle$ and J_n is the nth-order Bessel function of the first kind with zeros at $x = j_{n,k}$. We see that rotation shifts the energy by $-\hbar\omega(n + \sigma/2)$, but leaves the eigenstates in comparison to a non-rotating electron gas unchanged.

According to Eq. (5.8) that rotation lifts the degeneracy of states with opposite spin and orbital angular momentum with respect to the axis of rotation. At the Fermi surface, the electron velocity is $v = \hbar k_F/m \approx 10^4$ m/s for $k_F = 10^6$ cm^{-1}, which is much larger than the velocity of the outer edge of the 2DEG, which is given by $\omega R = 1$ m/s for a 2DEG with radius $R = 1$ μm rotating with 1 MHz. For electrons on classical trajectories at $r = R$ the velocity in azimuthal direction is given by $v_\Theta = L_z/(mR)$. In the eigenstates $L_z = \hbar n$ and using $|n| < j_{|n|,k}$, one finds

$$\frac{\hbar^2 j_{|n|,k}^2}{mR^2} \gg \hbar\omega|n|,$$

(5.9)

implying that the Barnett splitting is a minute correction to the eigenenergies if $\omega \ll \hbar k_F/(mR) = v_F/R$. In fact, for $\omega = 1$ MHz $\hbar\omega \approx 7 \cdot 10^{-10}$ eV, which is almost three orders of magnitude below the hyperfine splitting of hydrogen [17].

Comparing the Hamiltonian of a 2DEG in a magnetic field B_0 along the z-axis,

$$\hat{H}_{\text{LL}} = \frac{\vec{\hat{p}}^2}{2m} + \frac{|e|}{2m} B_0 \left(\hat{L}_z + g_s \hat{s}_z\right) + \frac{|e|^2}{2m} \frac{B_0^2}{4} \hat{r}^2,$$

(5.10)

with Eq. (5.6), we realize that $\vec{B}$ and $\vec{\omega}$ act quite differently on the electrons: applying a magnetic field causes an effective parabolic confinement which is absent in a rotating electron gas. In contrast to the magnetic field ω couples identically to the spin and orbital degrees of freedom.

The eigenvalues in (5.8) resemble the Landau level spectrum, $E_{n,\sigma}^{LL} = \hbar\omega_c \left(n + \frac{1}{2}\right)$, where $\omega_c = 2\mu_B B_0/\hbar$, with Bohr magneton $\mu_B = |e|\hbar/(2m)$, is the cyclotron frequency. However, Landau levels are characterized by a discrete and highly degenerate energy spectrum, whereas in the case of rotation each orbital mode n is associated with an infinite number of states with different radial components whose energies form a non-degenerate continuum of states.

We illustrate the difference between Barnett and Landau wave functions by perturbation theory when $\lambda = R^4 B_0^2 |e|^2/\hbar^2 \ll 1$. For $R = 1\,\mu$m, $\lambda < 1$ for $B_0 \lesssim 0.5$ mT. The Landau levels then read

$$\psi_{n,k,\sigma}\left(\tilde{r} = \frac{r}{R}, \Theta\right) = \frac{e^{in\Theta}}{\sqrt{\pi}} \left[\frac{J_{|n|}(j_{|n|,k}\tilde{r})}{J_{|n|+1}(j_{|n|,k})} \right.$$
$$\left. - \sum_{s \neq k} \left(\frac{R^2 B_0 |e|}{\hbar}\right)^2 \frac{\sqrt{2} J_{|n|}(j_{|n|,s}\tilde{r})\kappa_{k,s}}{j_{|n|,k}^2 - j_{|n|,s}^2} \right] |\sigma\rangle \quad (5.11)$$

with energies

$$E = \frac{\hbar^2 j_{|n|,k}^2}{2mR^2} + \mu_B B_0 (n + g_s \sigma) + \frac{R^2 m}{\hbar^2} (\mu_B B_0)^2 \kappa_{k,k}, \quad (5.12)$$

where

$$\kappa_{k,q} = \frac{\int_0^1 d\tilde{r}\, \tilde{r}^3 J_{|n|}(j_{|n|,k}\tilde{r}) J_{|n|}(j_{|n|,q}\tilde{r})}{J_{|n|+1}(j_{|n|,k}) J_{|n|+1}(j_{|n|,q})}. \quad (5.13)$$

In a free electron gas with $E_F \gg \hbar^2/(2mR^2)$, states with $n \gg 1$ are occupied. The difference between the probability distributions obtained from Eqs. (5.7) and (5.11) is plotted for angular momentum $100\hbar$, *i.e.* $n = 100$, in Fig. 5.1 for the four lowest energy states and $\lambda = 0.01$. The diamagnetic term acts as an effective confinement, since the probability of finding an electron near the edge of the disk is smaller for Landau than for Barnett levels. Expressed differently, in the rotating case centrifugal forces push the electrons to the outside of the disk that do not act in the case of a magnetic field.

5.4 MAGNETIZATION BY ROTATION – THE BARNETT EFFECT

The magnetization $\langle m_z \rangle$, where $\langle \dots \rangle$ refers to grand-canonical averaging, induced by an applied magnetic field B in the z-direction can be obtained from the grand canonical potential Ω as $\langle m_z \rangle = -(\partial\Omega/\partial B)_{T,\mu}$. For the Barnett magnetization, *i.e.,*
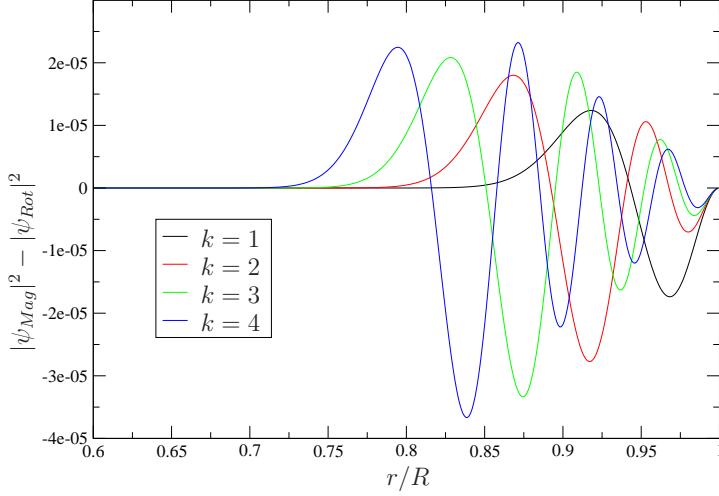
FIGURE 5.1: Difference between the wave functions of a (rotating) two-dimensional electron gas and one in an applied magnetic field for the lowest energy eigenstates with $\langle L_z \rangle = 100\hbar$.

magnetization by rotation, we can establish a similar relation as follows: The work needed to increase the rotation frequency by $d\omega$ is given by

$$\delta W = \langle H(\omega + d\omega) - H(\omega) \rangle = -\langle J_z \rangle d\omega, \tag{5.14}$$

where in the last step we used the Hamiltonian in the rotating frame of reference, Eq. (5.5). The total angular and magnetic momenta are related by

$$\langle m_z \rangle = -\gamma_J \langle J_z \rangle, \tag{5.15}$$

where $\gamma_J = g_J \mu_B / \hbar$ with Bohr magneton μ_B and g_J the Lande g-factor of the total angular momentum. Thus

$$\delta W = \frac{1}{\gamma_J} \langle m_z \rangle d\omega \tag{5.16}$$

and the complete differential of the grand canonical potential becomes

$$d\Omega = -SdT - Nd\mu + \frac{m_z}{\gamma_J} d\omega. \tag{5.17}$$

Therefore,

$$\langle m_z \rangle = \gamma_J \left(\frac{\partial \Omega}{\partial \omega} \right)_{T,\mu}. \tag{5.18}$$

We can now compute the Barnett area magnetization density, $M_z = \langle m_z \rangle / \pi R^2$, in the 2DEG with energy eigenvalues $E_{n,k,\sigma}$ given by Eq. (5.8). Then,

$$
\begin{aligned}
M_z &= -k_B T \frac{\gamma_J}{\pi R^2} \sum_{n,k,\sigma} \frac{\partial}{\partial \omega} \ln\left(1 + e^{-\beta(E_{n,k,\sigma} - \mu)}\right) \\
&= -\frac{\gamma_J \hbar}{\pi R^2} \sum_{n,k,\sigma} \left(n + \frac{\sigma}{2}\right) f(E_{n,k,\sigma}).
\end{aligned}
\tag{5.19}
$$

We can evaluate the sum over states at low temperatures and small rotation frequencies, $\hbar\omega \ll \hbar^2 j^2_{|n|,k}/(2mR^2)$. Since the zeroth order term and terms proportional to σn in the first order term drop out when summing over n and $\sigma = \pm 1$, we can write

$$
M_z = -\frac{\gamma_J}{\pi R^2} \sum_{n,k,\sigma} \delta\left(\frac{\hbar^2 j^2_{|n|,k}}{2mR^2} - \mu\right) \hbar^2 \omega \left(n^2 + \frac{1}{4}\right).
\tag{5.20}
$$

We can identify a term proportional to the energy density of states per unit area of the 2DEG

$$
D(E) := \frac{1}{\pi R^2} \sum_{n,k,\sigma} \delta\left(\frac{\hbar^2}{2mR^2} j^2_{|n|,k} - E\right) = \frac{2}{\pi^2} \frac{m}{\hbar^2}.
\tag{5.21}
$$

We still have to compute the term proportional to n^2 in Eq. (5.20). The Bessel function zeros obey $|n| < j_{|n|,1} < j_{|n|,2} < \cdots < j_{|n|,k}$ and for large $|n|$

$$
j_{n,1} \approx n + cn^{1/3} + \mathcal{O}(n^{-1/3}),
\tag{5.22}
$$

where $c \approx 1.856$ [18]. Denoting the highest occupied angular momentum quantum number with $|n_{max}|$ and using $\mu \gg \hbar^2/(2mR^2)$ we find

$$
|n_{max}| \approx \sqrt{\frac{2mR^2\mu}{\hbar^2}} \gg 1
\tag{5.23}
$$

and

$$
\begin{aligned}
\sum_{n=-\infty}^{\infty} n^2 &\sum_{k=1}^{\infty} \delta\left(\frac{\hbar^2}{2mR^2} j^2_{|n|,k} - \mu\right) \\
&= \sqrt{\frac{2mR^2}{\hbar^2\mu}} \sum_{n=0}^{|n_{max}|} n^2 \sum_{k=1}^{\infty} \delta\left(j_{|n|,k} - \sqrt{\frac{2mR^2\mu}{\hbar^2}}\right).
\end{aligned}
\tag{5.24}
$$

The factor

$$
\rho_n(x) := \sum_{k=1}^{\infty} \delta(j_{n,k} - x)
\tag{5.25}
$$

is the density of zeros of the Bessel function of the first kind in the interval $[x, x + dx]$. For large n [19]

$$\rho_n(x) \approx \frac{1}{\pi}\sqrt{1 - \frac{n^2}{x^2}}. \tag{5.26}$$

and

$$(5.24) = \sqrt{\frac{2mR^2}{\hbar^2\mu}} \sum_{n=0}^{n_{max}} n^2 \frac{1}{\pi}\sqrt{1 - \frac{n^2}{n_{max}^2}}$$

$$= \frac{2mR^2}{\hbar^2}\frac{1}{\pi}\int_0^1 dx\, x^2\sqrt{1-x^2} = \frac{mR^2}{8\hbar^2}. \tag{5.27}$$

Finally,

$$\begin{aligned} M_z &= -\frac{\gamma_J}{2}\hbar^2\omega D(\mu) - \frac{\gamma_J\omega m}{4\pi} \\ &= -\frac{\gamma_J}{\pi^2}m\omega - \frac{\gamma_J\omega m}{4\pi}. \end{aligned} \tag{5.28}$$

The Barnett magnetization is thus purely paramagnetic, *i.e.*, pointing in direction of the Barnett gauge field $-\omega/\gamma_J$. The first term in Eq. (5.28) stems from the coupling of the electron spin with the Barnett gauge field. The coupling of the electron spin with an applied magnetic field manifests itself in Pauli paramagnetism, *i.e.* $M_z = \chi_{\text{Pauli}}B_0$ with [20]

$$\chi_{\text{Pauli}} = \mu_B^2 D(\mu) = \frac{2}{\pi^2}m\left(\frac{\mu_B}{\hbar}\right)^2. \tag{5.29}$$

Using χ_{Pauli} in the first term of Eq. (5.28), we can write it as

$$M_z|_{\text{Pauli}} = \chi_{\text{Pauli}}\left(\frac{g_J}{2}\right)^2\left(-\frac{\omega}{\gamma_J}\right), \tag{5.30}$$

where $g_J = \gamma_J\hbar/\mu_B$. In an free electron gas in an applied magnetic field, the orbital motion of the electron gas gives rise to Landau diamagnetism with a susceptibility of $\chi_{\text{Landau}} = -\chi_{\text{Pauli}}/3$. In the case of a rotating free electron gas the second term in Eq. (5.28) stems from the orbital motion of the electrons, which is also a paramagnetic response to the Barnett gauge field $-\omega/\gamma_J$. The orbital contribution $M_z|_{\text{orbital}}$ to the magnetization M_z of Eq. (5.28) can be written as $M_z|_{\text{orbital}} = \chi_{\text{orbital}}(-\omega/\gamma_J)$ with

$$\chi_{\text{orbital}} = -\frac{3\pi^2}{2}\left(\frac{g_J}{2}\right)^2\chi_{\text{Landau}} = \frac{\pi^2}{2}\left(\frac{g_J}{2}\right)^2\chi_{\text{Pauli}}. \tag{5.31}$$

Since $\gamma_J/g_J \approx 10^{11}$ (Ts)$^{-1}$, the Barnett gauge field $B_{\text{Barnett}} = -\omega/\gamma_J$ is small for rotation frequencies achievable in the laboratory. For $\omega = 1$ MHz, $B_{\text{Barnett}} \approx 10^{-5}$ T. As a consequence, the achievable Barnett area magnetization density can be estimated to be

$$|M_z| \approx \left(\frac{\omega}{1\ \text{MHz}}\right)\left(\frac{m}{m_e}\right) \cdot 10^{-14}\ \text{A}, \tag{5.32}$$

where m_e is the mass of the free electron.

5.5 ROTATION-INDUCED EFFECTS IN A ROTATING ELECTRON GAS WITH SPIN-ORBIT INTERACTION

By taking the non-relativistic limit of the Dirac equation in the rotating frame of reference, Matsuo *et al.* [14] arrived at the Pauli-Hamiltonian for a rotating system:

$$\hat{H} = \frac{\vec{\hat{\pi}}^2}{2m} - \vec{\omega}\cdot(\vec{r}\times\vec{\hat{\pi}}) - \vec{\omega}\cdot\vec{\hat{S}} - \frac{g}{2}\mu_B \vec{B}\cdot\vec{\sigma} - \frac{\lambda|e|}{2\hbar}\left[\vec{\hat{\pi}}\times\vec{E}' - \vec{E}'\times\vec{\hat{\pi}}\right] + \frac{\lambda|e|}{2}\text{div}\vec{E}' + |e|\phi, \tag{5.33}$$

where $\vec{\hat{\pi}} = \vec{p} + |e|\vec{A}$, $|e|$ the elementary charge, $\vec{\hat{S}} = \vec{\hat{\sigma}}\hbar/2$ is the spin angular momentum operator, $\vec{E}' = \vec{E} + (\vec{\omega}\times\vec{r})\times\vec{B}$ is the effective electric field in the rotating frame of reference, ϕ the electric potential, g the electron g-factor and λ is the spin-orbit-coupling constant. $\lambda = \hbar^2/4m^2c^2$ is negligible in vacuum. However, in some condensed matter systems coupling to the lattice can be described by the same Hamiltonian with an effectively enhanced λ [21, 22]. In the previous section we have discussed the rotation-induced magnetization, whereas Matsuo *et al.* focused on the mechanical generation of spin currents in systems described by the Hamiltonian of Eq. (5.33). Another way to explore the effects of mechanical rotation is studying the energy corrections of electronic states. Since for $B_0 = 1$ T $\omega_c \approx 10^{11}$ Hz, we may assume that $|\vec{\omega}| \ll \omega_c$ in almost all practical cases. Therefore, we may treat the effects of mechanical rotation perturbatively. Assuming that both $\vec{B}$ and $\vec{E}$ are constant and oriented along the z-direction as well as assuming that the electron's motion is restricted to the $x-y$-plane, the Hamiltonian of Eq. (5.33) reduces to that of a Rashba 2DEG rotating in a magnetic field:

$$\hat{H} = \hat{H}_0 + \hat{H}_{\text{pert}}, \tag{5.34}$$

where

$$\hat{H}_0 = \frac{\vec{\hat{\pi}}^2}{2m} - \frac{\lambda|e|}{\hbar}\vec{\hat{\sigma}}(\vec{\hat{\pi}}\times\vec{E}) + \frac{g}{2}\mu_B \vec{\hat{\sigma}}\cdot\vec{B}. \tag{5.35}$$

and

$$\hat{H}_{\text{pert}} = -\frac{\hbar\omega}{2}\hat{\sigma}_z - \omega(\hat{x}\hat{\pi}_y - \hat{y}\hat{\pi}_x) + \frac{\lambda|e|}{\hbar}\omega B_0\hat{\sigma}_z(\hat{x}\hat{\pi}_y - \hat{y}\hat{\pi}_x) + \omega B_0\lambda|e| \tag{5.36}$$

is the perturbation due to rotation. In the following discussion, we follow an approach outlined in [23] that does not make use of any particular gauge. Observing that

$$[\hat{\pi}_x, \hat{\pi}_y] = -i\hbar|e|B_0 \tag{5.37}$$

for all gauges allows us to define the lowering operators

$$\hat{a} = \frac{\hat{\pi}_x - i\hat{\pi}_y}{\sqrt{2m\hbar\omega_c}} \quad \text{and} \quad \hat{b} = i\hat{a}^\dagger + \sqrt{\frac{m\omega_c}{2\hbar}}(\hat{x} + i\hat{y}), \tag{5.38}$$

where $\omega_c = |e|B_0/m$ is the cyclotron frequency. One sees that

$$[\hat{a}, \hat{a}^\dagger] = [\hat{b}, \hat{b}^\dagger] = 1 \quad \text{and} \quad [\hat{a}, \hat{b}] = [\hat{a}^\dagger, \hat{b}] = 0. \tag{5.39}$$

We can introduce the ground state $|0\rangle$ with $\hat{a}|0\rangle = \hat{b}|0\rangle = 0$. By using the properties of the ladder operators $\hat{a}$ and $\hat{b}$ one sees

$$\langle 0|\hat{b}^n\hat{a}^m(\hat{a}^\dagger)^k(\hat{b}^\dagger)^l|0\rangle = \delta_{k,m}\delta_{l,n}k!l!\langle 0|0\rangle. \tag{5.40}$$

Using Eqs. (5.37) and (5.38), the unperturbed Hamiltonian can be written as

$$H_0 = \hbar\omega_c\left(\hat{a}^\dagger\hat{a} + \frac{1}{2}\right) + \frac{\hbar\omega_c g}{4}\sigma_z - \frac{\lambda|e||\vec{E}|}{\hbar}\sqrt{2m\hbar\omega_c}\begin{pmatrix} 0 & i\hat{a} \\ -i\hat{a}^\dagger & 0 \end{pmatrix} \tag{5.41}$$

with eigenvalues [24]

$$E_{k>0,l,\sigma} = \hbar\omega_c(k + \sigma\delta), \tag{5.42}$$

and corresponding eigenstates

$$|k > 0, l, \sigma\rangle = \frac{1}{\sqrt{2k!l!\langle 0|0\rangle}}\begin{pmatrix} -i\chi_\sigma(\hat{a}^\dagger)^{k-1}(\hat{b}^\dagger)^l \\ (\hat{a}^\dagger)^k(\hat{b}^\dagger)^l \end{pmatrix}|0\rangle, \tag{5.43}$$

where $\sigma = \pm 1$,

$$\delta = \sqrt{\frac{1}{4}\left(\frac{g}{2} - 1\right)^2 + \frac{2k\lambda^2|e|^2|\vec{E}|^2}{\omega_c^2 l_B^2\hbar^2}} \tag{5.44}$$

(with $l_B = \sqrt{\hbar/(|e|B_0)}$) and

$$\chi_\sigma = \frac{\hbar\omega_c l_B}{\sqrt{2}\lambda|e||\vec{E}|}\left(\sigma\delta - \frac{1}{2}\left(1 - \frac{g}{2}\right)\right). \tag{5.45}$$

The Rashba spinorbit parameter in thin films $\alpha = \lambda|e||\vec{E}|$, where $|\vec{E}|$ is the electric field confining the electrons to a two-dimensional system. For a gold film on a silver substrate [25] a spin orbit splitting of $\Delta k = 0.025$ Å corresponding to $\alpha = 0.4$ eV

was found. With this, we can estimate $\hbar\omega_c l_B / (\lambda |e| |\vec{E}|) \ll 1$, assuming that $B_0 = 1$ T. As a result, we have in good approximation

$$\delta \approx \sqrt{2k} \frac{\lambda |e| |\vec{E}|}{\hbar\omega_c l_B} \quad \text{and} \quad \chi_\sigma \approx \sqrt{k}. \tag{5.46}$$

For $k = 0$

$$E_{0,l} = \frac{\hbar\omega_c}{2} \left(1 - \frac{g}{2} \right) \quad \text{and} \quad |0, l\rangle = \frac{(\hat{b}^\dagger)^l}{\sqrt{l!}} \begin{pmatrix} 0 \\ 1 \end{pmatrix} |0\rangle. \tag{5.47}$$

We note that the unperturbed eigenstates are degenerate in the quantum number l. Therefore, the first order energy corrections are given by the eigenvalues of a matrix with entries $\langle k, \tilde{l}, \sigma | H_{\text{pert}} | k, l, \sigma \rangle$, where H_{pert} is given by Eq. (5.36). With the eigenstates given by Eq. (5.43) and Eq. (5.40) one easily sees that

$$\langle k, \tilde{l}, \sigma | \sigma_z | k, l, \sigma \rangle = 0. \tag{5.48}$$

The angular momentum operator can be expressed in terms of the operators a, b, $a^\dagger$ and $b^\dagger$ as

$$\hat{L}_z = \hat{x}\hat{\pi}_y - \hat{y}\hat{\pi}_x = \hbar \left(\hat{a}^\dagger \hat{a} + \hat{a}\hat{a}^\dagger + i\hat{b}\hat{a} - i\hat{b}^\dagger \hat{a}^\dagger \right). \tag{5.49}$$

and one obtains

$$\langle k, \tilde{l}, \sigma | \hat{L}_z | k, l, \sigma \rangle = \frac{\delta_{\tilde{l},l} \hbar}{|\chi_\sigma|^2 + k} \left(|\chi_\sigma|^2 (2k-1) + k(2k+1) \right) \approx 2\hbar k \delta_{\tilde{l},l} \tag{5.50}$$

and

$$\langle k, \tilde{l}, \sigma | \sigma_z \hat{L}_z | k, l, \sigma \rangle = \frac{\delta_{l,\tilde{l}} \hbar}{|\chi_\sigma|^2 + k} \left(|\chi_\sigma|^2 (2k-1) - k(2k+1) \right) \approx -\hbar \delta_{\tilde{l},l}. \tag{5.51}$$

We see with Eqs. (5.50) and (5.51) that the matrix with entries $\langle k, \tilde{l}, \sigma | H_{\text{pert}} | k, l, \sigma \rangle$ is diagonal and that in first order perturbation theory rotation does not lift the degeneracy in l. The first order energy correction to the eigenstate $|k, l, \sigma\rangle$ is given by

$$\Delta E_{k,l,\sigma} \approx -2\hbar\omega k. \tag{5.52}$$

Similarly, for $k = 0$ we obtain from Eq. (5.47)

$$\Delta E_{k=0,l} = -\frac{\omega\hbar}{2}. \tag{5.53}$$

We note that rotation does not lift the degeneracy with respect to the quantum number l. Furthermore, in first order perturbation theory the result is independent of the spin-orbit coupling constant.

For $B_0 = 1$ T corresponding to $\omega_c \approx 1.8 \cdot 10^{11}$ Hz resp. $\hbar\omega_c \approx 10^{-4}$ eV, we see that the rotation-induced energy-splitting is only a minor correction, since $\hbar\omega \approx 7 \cdot 10^{-10}$ eV for $\omega = 1$ MHz, which is about four orders of magnitude smaller than the hyperfine splitting of hydrogen [17].

5.6 Conclusions

We explored the differences between the "Barnett gauge field" due to rotation and an applied external magnetic field for the two-dimensional electron gas. The "Barnett levels" in the rotating 2DEG differ from the Landau levels in an applied magnetic field, *e.g.*, by the lack of degeneracy: Whereas the Landau levels are highly degenerate, the Barnett levels are not. In addition, mechanical rotation introduces a centrifugal term in the Hamiltonian, which leads – in comparison to the case of an applied magnetic field – to a shift of the expectation value of the radial coordinate towards the edge of the disk.

Rotation may be considered as a Barnett gauge field $B_{\text{Barnett}} = -\omega/\gamma_J$. Spin-polarization due to rotation leads to a paramagnetic response $(g_J/2)^2 \chi_{\text{Pauli}}$, where χ_{Pauli} is the susceptibility found for the usual Pauli paramagnetism of a free electron gas. However, since the Barnett gauge field couples only linearly to the orbital degrees of freedom of the electron, we find not a diamagnetic response – as for an applied field where we have Landau diamagnetism $-\chi_{\text{Pauli}}/3$, but also a paramagnetic response.

Furthermore, we used the Hamiltonian for a rotating Rashba system derived by Matsuo *et al.* [14] in order to discuss the rotation induced energy splitting. The energy correction is small for attainable rotation frequencies, making experimental observation difficult.

References

[1] E. Stoner, *Magnetism and Matter* (Methuen, London, 1934).

[2] S. J. Barnett, *Gyromagnetic and Electron-Inertia Effects*, Rev. Mod. Phys. **7**, 129 (1935).

[3] S. J. Barnett, *Magnetization by Rotation*, Phys. Rev. **6**, 239 (1915).

[4] A. Einstein and J. W. de Haas, *Experimental Proof of the Existence of Ampere's Molecular Currents*, Proceedings of the Koninklijke Akademie van Wetenschappen te Amsterdam **18 I**, 696 (1916).

[5] E. J. Post, *Sagnac Effect*, Rev. Mod. Phys. **39**, 475 (1967).

[6] F. Hasselbach and M. Nicklaus, *Sagnac experiment with electrons: Observation of the rotational phase shift of electron waves in vacuum*, Phys. Rev. A **48**, 143 (1993).

[7] F. Riehle, T. Kisters, A. Witte, J. Helmcke, and C. J. Bordé, *Optical Ramsey spectroscopy in a rotating frame: Sagnac effect in a matter-wave interferometer*, Phys. Rev. Lett. **67**, 177 (1991).

[8] M. Zivkovic, M. Jääskeläinen, C. P. Search, and I. Djuric, *Sagnac rotational phase shifts in a mesoscopic electron interferometer with spin-orbit interactions*, Phys. Rev. B **77**, 115306 (2008).

[9] A. A. Kovalev, G. E. W. Bauer, and A. Brataas, *Magnetovibrational coupling in small cantilevers*, Applied Physics Letters **83**, 1584 (2003).

[10] A. A. Kovalev, G. E. W. Bauer, and A. Brataas, *Nanomechanical Magnetization Reversal*, Physical Review Letters **94**, 167201 (pages 4) (2005).

[11] T. M. Wallis, J. Moreland, and P. Kabos, *Einstein-de Haas effect in a NiFe film deposited on a microcantilever*, Appl. Phys. Lett. **89**, 122502 (2006).

[12] S. Bretzel, G. E. W. Bauer, Y. Tserkovnyak, and A. Brataas, *Barnett Effect in Magnetic Thin Films and Nanostructures*, Applied Physics Letters **95**, 122504 (2009).

[13] G. E. W. Bauer, S. Bretzel, A. Brataas, and Y. Tserkovnyak, *Nanoscale magnetic heat pumps and engines*, Phys. Rev. B **81**, 024427 (2010).

[14] M. Matsuo, J. Ieda, E. Saitoh, and S. Maekawa, *Effects of Mechanical Rotation on Spin Currents*, Phys. Rev. Lett. **106**, 076601 (2011).

[15] M. Matsuo, J. Ieda, E. Saitoh, and S. Maekawa, *Spin-dependent inertial force and spin current in accelerating systems*, Phys. Rev. B **84**, 104410 (2011).

[16] A. Messiah, *Quantum Mechanics, Vol. 1 and 2* (Dover, Mineola, 1999).

[17] L. W. Anderson, F. M. Pipkin, and J. C. Baird, *Hyperfine Structure of Hydrogen, Deuterium, and Tritium*, Phys. Rev. **120**, 1279 (1960).

[18] G. N. Watson, *A Treatise on the Theory of Bessel Functions* (Cambridge University Press, 1922).

[19] M. E. Muldoon, *Approximate Distribution Density of Zeros of Bessel Functions*, Europhysics Letters **20**, 1 (1992).

[20] N. W. Ashcroft and N. D. Mermin, *Solid State Physics* (Harcourt College Publishers, 1976).

[21] S. Takahashi and S. Maekawa, *Spin current, spin accumulation and spin Hall effect*, Science and Technology of Advanced Materials **9**, 014105 (2008).

[22] L. Vila, T. Kimura, and Y. Otani, *Evolution of the Spin Hall Effect in Pt Nanowires: Size and Temperature Effects*, Phys. Rev. Lett. **99**, 226604 (2007).

[23] C. F. Lo, *A gauge-independent formulation of the Landau level problem*, European Journal of Physics **13**, 125 (1992).

[24] W. Yang, K. Chang, X. Wu, H. Zheng, and F. Peeters, *Interplay between s − d exchange interaction and Rashba effect: Spin-polarized transport*, Appl. Phys. Lett. **89**, 132112 (2006).

[25] G. Nicolay, F. Reinert, S. Hüfner, and P. Blaha, *Spin-orbit splitting of the L -gap surface state on Au(111) and Ag(111)*, Phys. Rev. B **65**, 033407 (2001).

A

PERTURBATION THEORY

Here we outline the perturbation theory for the eigenvalue problem of a general matrix **M** as outlined in [1].

The inner product $\langle \vec{x}, \vec{y} \rangle$ of vectors $\vec{x}, \vec{y} \in \mathbb{C}^n$ has the following properties:

1. $\langle \vec{x}, \vec{x} \rangle$ real and non-negative for all $\vec{x} \in \mathbb{C}^n$

2. $\langle \vec{x}, \vec{x} \rangle = 0$ if and only if $\vec{x} = \vec{0}$

3. $\langle \vec{x}, \vec{y} \rangle = \langle \vec{y}, \vec{x} \rangle^*$

4. $\langle \vec{x}, \alpha \vec{y} + \beta \vec{z} \rangle = \alpha \langle \vec{x}, \vec{y} \rangle + \beta \langle \vec{x}, \vec{z} \rangle$

A possible definition of the inner product is

$$\langle \vec{x}, \vec{y} \rangle := \vec{x}^\dagger \mathbf{K} \vec{y}, \tag{A.1}$$

where **K** is a Hermitian, positive-definite matrix and $\vec{x}^\dagger$ denotes the Hermitian conjugate of $\vec{x}$. Two vectors $\vec{x}$ and $\vec{y}$ are said to be **K**-orthogonal if $\langle \vec{x}, \vec{y} \rangle = \vec{x}^\dagger \mathbf{K} \vec{y} = 0$.

In a linear vector space with an inner product, we call $\mathbf{A}^\#$ the adjoint of the matrix **A** if $\langle \vec{x}, \mathbf{A} \vec{y} \rangle = \langle \mathbf{A}^\# \vec{x}, \vec{y} \rangle$ for all $\vec{x}, \vec{y}$ in this space. It follows from the inner product defined by Eq. (A.1), that

$$\mathbf{A}^\# = \mathbf{K}^{-1} \mathbf{A}^\dagger \mathbf{K}. \tag{A.2}$$

A is called **K**-normal if it commutes with its **K**-adjoint, i.e. when $\mathbf{A}\mathbf{A}^\# = \mathbf{A}^\#\mathbf{A}$. Let us consider a complete set of vectors $\vec{u}_i$ which are pairwise **K**-orthogonal and maximally normalized, *i.e.*

$$\vec{u}_i^\dagger \mathbf{K} \vec{u}_j = \begin{cases} 0 & \text{if} \quad j \neq i \\ 1 & \text{if} \quad j = i \end{cases} . \tag{A.3}$$

The normalized **K**-dyads $E_{i,j}$ are defined as

$$\mathbf{E}_{ij} \equiv \vec{u}_i \vec{u}_j^\dagger \mathbf{K}. \tag{A.4}$$

Since the set of $\vec{u}_i$ was assumed to be complete, the set of **K**-dyads E_{ij} must be complete as well and may serve as a basis for the expansion of square matrices. An arbitrary square matrix **A** can be thus written as

$$\mathbf{A} = \sum_{ij} a_{ij}\mathbf{E}_{ij} = \sum_{ij} a_{ij}\vec{u}_i \vec{u}_j^\dagger \mathbf{K}. \tag{A.5}$$

Multiplying by $\vec{u}_m^\dagger \mathbf{K}$ from the left and by $\vec{u}_m$ from the right the expansion coefficients read

$$a_{mn} = \vec{u}_m^\dagger K A \vec{u}_n. \tag{A.6}$$

If the $\vec{u}_i$ are eigenvectors of the matrix **A**, one finds for $m = n$ that $a_{m,n} = \lambda_n$, where λ_n is an eigenvalue of **A**, while $a_{mn} = 0$ in all other cases.

Suppose now that

$$\mathbf{A} = \mathbf{A}_0 + \epsilon\mathbf{A}_1, \tag{A.7}$$

where ϵ is a small parameter. We assume that $\mathbf{A}_0$ is **K**-normal and that the eigenvalue problem of $\mathbf{A}_0$ has been solved. Furthermore, the eigenvalues λ_i of $\mathbf{A}_0$ are non-degenerate and the eigenvectors $\vec{u}_i$ are pairwise **K**-orthogonal and maximally normalized (*i.e.* normalized with respect to the inner product defined by **K**). Following (A.5) we can expand

$$\mathbf{A}_0 = \sum_i \lambda_i \mathbf{E}_{ii} = \sum_i \lambda_i \vec{u}_i \vec{u}_i^\dagger \mathbf{K} \tag{A.8}$$

where all λ_i are distinct. Following (A.5) and (A.6), we can also write

$$\mathbf{A}_1 = \sum_{i,j} (\vec{u}_i \mathbf{K}\mathbf{A}_1 \vec{u}_j) E_{i,j}. \tag{A.9}$$

In order to obtain the exact eigenvectors and eigenvalues, we make the ansatz $\vec{u}_i' = \vec{u}_i + \epsilon\vec{v}_i + \epsilon^2 \vec{w}_i + \mathcal{O}(\epsilon^3)$ and $\lambda_i' = \lambda_i + \epsilon\mu_i + \epsilon^2 \nu_i + \mathcal{O}(\epsilon^3)$. Collecting the first order terms yields

$$\mathbf{A}_1 \vec{u}_i + \mathbf{A}_0 \vec{v}_i = \mu_i \vec{u}_i + \lambda_i \vec{v}_i. \tag{A.10}$$

Since the set of eigenvectors is complete, we can expand

$$\vec{v}_i = \sum_j a_{ij}\vec{u}_j. \tag{A.11}$$

With (A.8) and (A.9) and the relation

$$\mathbf{E}_{ij}\vec{u}_k = \vec{u}_i\,\vec{u}_j^\dagger\mathbf{K}\vec{u}_k = \begin{cases} 0 & \text{if} \quad k \neq j \\ \vec{u}_i & \text{if} \quad k = j \end{cases} \tag{A.12}$$

by comparing the coefficients of the eigenvectors in (A.10) for $i = j$ we obtain the first order correction of the eigenvalue,

$$\mu_i = \vec{u}_i^\dagger\mathbf{K}\mathbf{A}_1\,\vec{u}_i\,. \tag{A.13}$$

REFERENCES

[1] M. C. Pease III, *Methods of Matrix Algebra* (Academic Press, 1965).

B

DAMPING BY RADIATION

In this chapter we discuss radiative losses and estimate their strength compared to Gilbert damping.

We first discuss the multipole fields created by a precessing magnetic moment following the presentation in [1]. When a time-dependence of $e^{-i\omega t}$ is assumed, Maxwell's equations in a source free region read

$$\nabla \times \vec{E} = i k \vec{B}, \qquad \nabla \times \vec{E} = 0 \tag{B.1}$$

$$\nabla \times \vec{B} = -i k \vec{E}, \qquad \nabla \times \vec{B} = 0, \tag{B.2}$$

where $k = \omega/c$. A general solution for electromagnetic fields in a source free region is given by

$$\vec{E} = \sum_{l,m} \left[a_E(l,m) f_l(kr) \vec{X}_{l,m} - \frac{i}{k} a_M(l,m) \nabla \times g_l(kr) \vec{X}_{l,m} \right], \tag{B.3}$$

$$\vec{B} = \sum_{l,m} \left[\frac{i}{k} a_E(l,m) \nabla \times f_l(kr) \vec{X}_{l,m} + a_M(l,m) \nabla \times g_l(kr) \vec{X}_{l,m} \right], \tag{B.4}$$

where $\vec{X}_{l,m}$ denote the normalized vector spherical harmonics. These are defined as

$$\vec{X}_{l,m} = \frac{1}{\sqrt{l(l+1)}} \vec{L} Y_{l,m}, \tag{B.5}$$

with angular momentum operator $\vec{L} = -i\vec{r} \times \nabla$ and spherical harmonics $Y_{l,m}$. The functions f_l and g_l are both linear combinations of the spherical Hankel func-

tions of first and second kind $h^{1,2}(kr)$. The multipole moments created by a time-varying magnetic moment $\vec{M}e^{-i\omega t}$, where we take the real part as the physical quantity, are given by [1]

$$a_E(l, m) = -\frac{4\pi k^3}{\sqrt{l(l+1)}} \int \mathrm{d}^3x Y_{l,m}^* \left[\nabla \cdot \left(\vec{r} \times \vec{M}\right) j_l(kr)\right] \qquad \text{(B.6)}$$

and

$$a_M(l, m) = \frac{4i\pi k^4}{\sqrt{l(l+1)}} \int \mathrm{d}^3x Y_{l,m}^* (\vec{r} \cdot \vec{M}) j_l(kr), \qquad \text{(B.7)}$$

where j_l denotes spherical Bessel functions. The power radiated away by a source is given by

$$P = \frac{c}{8\pi k^2} \sum_{l,m} \left[|a_E(l, m)|^2 + |a_M(l, m)|^2\right]. \qquad \text{(B.8)}$$

We now consider a magnetic moment that precesses with frequency ω and at an angle $\tilde{\Theta}$ around the z-axis. Assuming that the magnetization density m_0/V is nonzero in a source region of radius a, we can write

$$\vec{M}e^{-i\omega t} = \Theta(r-a) \frac{m_0}{V} \sin\tilde{\Theta} \begin{pmatrix} i \\ 1 \\ 0 \end{pmatrix} e^{-i\omega t}. \qquad \text{(B.9)}$$

One immediately sees from Eq. (B.6) that $a_E(l, m) = 0$, since the magnetization density is assumed to be constant in the source region. By parametrizing the position vector $\vec{r}$ as $\vec{r} = r(\sin\Theta\sin\phi, \sin\Theta\cos\phi, \cos\Theta)^T$ one finds

$$a_M(l, m) = -4\pi i k^4 \sqrt{\frac{4\pi}{3}} \frac{m_0}{V} \sin\tilde{\Theta} \delta_{1,l}\delta_{m,1} \int_0^a \mathrm{d}r r^3 j_l(kr), \qquad \text{(B.10)}$$

where we exploited the orthogonality of the spherical harmonics. In the limit $ka \rightarrow 0$, one finds

$$\frac{k^4}{V} \int_0^a \mathrm{d}r r^3 j_1(kr) \overset{ka \rightarrow 0}{=} -\frac{3}{4\pi} k^3 \qquad \text{(B.11)}$$

and thus

$$a_M(l, m) = i\sqrt{12\pi} m_0 \sin\tilde{\Theta} k^3 \delta_{1,m}\delta_{1,l}. \qquad \text{(B.12)}$$

As only the magnetic multipole moment with $l = m = 1$ is nonzero, using Eqs. (B.8) and (B.12) we find for the power radiated away by the precessing magnetic moment m_0

$$P = \frac{3}{2} c k^4 m_0^2 \sin^2\tilde{\Theta}. \qquad \text{(B.13)}$$

A rotating magnetic moment rotating with frequency ω has the potential energy $-m_0\omega/\gamma$. Thus we can estimate the time τ_R in which this energy is radiated away as

$$\tau_R = \left| \frac{m_0 \frac{\omega}{\gamma}}{P} \right| = \frac{2}{3} \frac{1}{|m_0\gamma k^3 \sin\tilde\Theta|} \, . \tag{B.14}$$

The time scale at which Gilbert damping leads to the alignment of a rotating magnetic moment with the rotation axis is given by $\tau_G = (\alpha\omega)^{-1}$. Thus

$$\frac{\tau_R}{\tau_G} = \frac{2}{3} \frac{\alpha c^3}{m_0\omega^2|\gamma|\sin\tilde\Theta} \approx 10^{32} \frac{\alpha}{N(\omega/(1\text{ Mhz}))} \, , \tag{B.15}$$

where we have used $m_0 = N\mu_B$. We may thus conclude that radiative losses are negligible in comparison to Gilbert damping.

REFERENCES

[1] J. D. Jackson, *Classical Electrodynamics* (John Wiley & Sons, Inc., 1962).

SUMMARY

The first technological application of magnetic phenomena has been the compass, which ultimately enabled the colonization of the world by Europeans in the late middle ages and thus shaped the early modern era. A compass is also an example for a magneto-mechanical device, i.e. a device in which the magnetic and mechanical degrees of freedom are coupled. There had been no conclusive theory on the origin of magnetism until the advances in electrodynamics in the 19th century led to the formulation of the molecular current theory of ferromagnetism. In order to test this theory, gyromagnetic experiments were devised: The Barnett effect, i.e. magnetization by rotation, and the Einstein-de Haas effect, where a mechanical rotation induced by a change of magnetization is studied. These two experiments, in particular Barnett's work, provided first evidence of the anomalous g-factor and thus a hint at the quantum nature of the electron spin.

The most notable technological developments of the last decades have been in microelectronics. Advances in fabrication techniques and an ever increasing control of materials enabled the microelectronics industry to comply with Moore's law, i.e. that the number of transistors on an integrated circuit doubles roughly every two years by continuously shrinking the size of the building blocks of the integrated circuits. Not only did the sizes of electric elements on integrated circuits shrink, but by employing the same techniques the sizes of mechanical elements, such as cantilevers, were miniaturized in similar fashion, giving rise to the field of micro-electro-mechanical devices (MEMS) and eventually nano-electro-mechanical devices (NEMS).

In line with the emergence of the fields of MEMS and NEMS, the interest in gyromagnetic experiments has revived. In particular, the Einstein-de Haas effect in a cantilever with ferromagnetic tip has been studied previously both experimentally and theoretically. In this thesis, we focused on the Barnett effect and the interplay of this effect with its close relative, the Einstein-de Haas effect. In Chapter 1 of this thesis we introduce the field by reviewing the classical Einstein-de Haas and Barnett effect as well as the Landau-Lifshitz-Gilbert equation, which we use extensively in the following chapters.

In Chapter 2, we perform a feasibility study concerning the Barnett effect in magnetic nanostructures and thin films. To this end, we introduce a modification in the damping term of the Landau-Lifshitz-Gilbert equation, which takes into

account the viscous damping of the magnetization motion relative to the frame of reference defined by the lattice. This gives rise to a Barnett gauge field in the Landau-Lifshitz-Gilbert equation in the lattice frame of reference. We study the effect of this gauge field on the magnetization density and estimate the mechanical rotation frequencies required to observe the Barnett effect in a thin film by, *e.g.*, the magneto-optical Kerr effect. In addition, we discuss the feasibility of moving domain walls by mechanical rotation of a ferromagnetic wire.

In Chapter 3 we continue our discussion of the Barnett effect in magnetic nanostructures in terms of the magneto-mechanical dynamics of a suspended quasi one-dimensional magnetic wire containing a tail-to-tail domain wall. The system may be driven out of equilibrium by a mechanical torque and/or an applied magnetic field. Applying Onsager's reciprocity relation, we find a unified description of the Barnett effect – magnetization by rotation – and Einstein-de Haas effect – mechanical rotation induced by magnetization.

In Chapter 4, we focus on the dynamics of rapidly rotating cosmic dust grains. The polarization of starlight passing through clouds of cosmic dust is attributed to the fact that the dust grains align their large axis of inertia with respect to the direction provided by cosmic magnetic fields. As the exact mechanisms of this alignment and the magnitude of the relevant time-scales remain under discussion, we investigate the alignment of particles with ferromagnetic inclusions by formulating the coupled magneto-mechanical equations of motion. To this end, we use the Landau-Lifshitz-Gilbert equation, modified to take into account the effects of mechanical rotation, in order to model the magnetization dynamics. We find that the relevant time-scales for the alignment of the major axis of inertia with the external magnetic field is independent from the mechanical angular momentum of a particle in contrast to previous works.

In Chapter 5, we discuss the effects of mechanical rotation on a free electron gas. By taking into account the orbital degrees of freedom of the electrons in the rotating frame of reference, we find eigenstates that resemble the Landau levels in a free electron gas subjected to an external magnetic field. However, in the case of rotation, the electron's spectrum in the plane perpendicular to the rotation axis is not degenerate as is the case with the electrons in Landau levels and the plane perpendicular to the applied magnetic field. Furthermore, we find the Barnett magnetization induced in a free electron gas to be a purely paramagnetic effect in contrast to the response to a magnetic field.

SAMENVATTING

De eerste technologische toepassing van magnetische effecten was het kompas, dat uiteindelijk de kolonisatie van de wereld door Europeanen in de late Middeleeuwen mogelijk maakte, en daarmee vorm gaf aan het begin van de Moderne Tijd. Een kompas is ook een voorbeeld van een magneto-mechanisch apparaat, d.w.z. een apparaat waarin de magnetische en mechanische vrijdheidsgraden gekoppeld zijn. Er was geen sluitende theorie van de oorsprong van het magnetisme totdat de voortschrijdende inzichten in electrodynamica in de 19e eeuw leidden tot de theorie van ferromagnetisme op basis van moleculaire stromen. Om deze theorie te testen werden gyromagnetische experimenten bedacht: het Barnett effect, wat neerkomt op magnetisatie door rotatie enerzijds, en het Einstein-de Haas effect, waar een mechanische rotatie wordt veroorzaakt door een veranderende magnetisatie anderzijds. Deze twee experimenten, het werk van Barnett in het bijzonder, vormden het eerste bewijs van de afwijkende g-factor en gaven daarmee een hint van het kwantum karakter van de elektronspin.

De meest opmerkelijke technologische vooruitgangen van de afgelopen decennia hebben zich voorgedaan in de micro-electronica. Vooruitgang in fabricagetechnieken en een steeds betere beheersing van materiaaleigenschappen hebben de micro-electronica industrie het mogelijk gemaakt om de wet van Moore bij te benen, wat wil zeggen dat het aantal transistoren op een geïntegreerde schakeling ruwweg elke twee jaar verdubbelt, door de bouwstenen van de circuits continu te verkleinen. Niet alleen de afmetingen van de elektrische componenten zijn verkleind, maar door dezelfde technieken toe te passen op mechanische componenten, zoals buigbare balken, zijn deze op soortgelijke wijze verkleind. Dit leidde tot de opkomst van het vakgebied van de micro-elektromechanische systemen (MEMS), kort daarna gevolgd door de nano-elektromechanische systemen (NEMS).

In lijn met de opkomst van onderzoek aan MEMS en NEMS is er hernieuwde belangstelling voor gyromagnetische experimenten ontstaan. In het bijzonder is er zowel theoretisch als experimenteel onderzoek gedaan aan het Einstein-de Haas-effect in een buigende balk met een ferromagnetische tip. In dit proefschrift hebben wij ons gericht op het Barnett effect, en het samenspel met het nauw verwante Einstein-de Haas effect. In hoofdstuk 1 introduceren we het vakgebied door een overzicht van de klassieke Einstein-de Haas en Barnett effecten, tesamen met

de Landau-Lifschitz-Gilbert-vergelijking te geven, waar we in de daaropvolgende hoofdstukken uitvoerig gebruik van maken.

In hoofdstuk 2 voeren we een haalbaarheidsstudie uit over het Barnett-effect in magnetische nanostructuren en dunne films. Hiertoe introduceren we een modificatie van de dempingsterm van de Landau-Lifschitz-Gilbert vergelijking, om rekening te houden met de visceuze demping van de beweging van de magnetisatie relatief aan het referentie-assenstelsel van het kristalrooster. Dit veroorzaakt een Barnett ijkveld in de Landau-Lifschitz-Gilbert vergelijking. We bestuderen het effect van dit ijkveld op de magnetisatiedichtheid en schatten de mechanische rotatiefrequenties die benodigd zijn om het Barnett-effect te meten in een dunne film, bijvoorbeeld door gebruik te maken van het magneto-optische Kerr effect. Daarnaast bespreken we de mogelijkheid om domeingrenzen te verschuiven door mechanische rotatie van een ferromagnetisch draadje.

In hoofdstuk 3 zetten we onze discussie van het Barnett-effect in magnetische nanostructuren voort in termen van de magneto-mechanische dynamica van een vrijhangend quasi 1-dimensionaal draadje die een staart-op-staart domeingrens bevat. Het systeem kan uit evenwicht gedreven worden door een mechanische koppel en/of een aangelegd magneetveld. Door Onsager's reciprociteitsrelatie toe te passen vinden we een verenigde beschrijving van het Barnett-effect (magnetisatie door rotatie) en het Einstein-de Haas-effect (rotatie door magnetisatie).

In hoofdstuk 4 richten wij ons op de dynamica van snel roterende kosmische stofkorrels. De polarisatie van sterlicht dat door wolken kosmische stof schijnt wordt toegeschreven aan het feit dat de stofkorrels hun dominante traagheidsas uitlijnen op de richting van de kosmische magneetvelden. Aangezien de precieze mechanismen van deze uitlijning en de relevante tijdschalen nog steeds onderwerp van discussie zijn, onderzoeken wij de uitlijning van ferromagnetische stofkorrels door de gekoppelde magneto-mechanische bewegingsvergelijkingen te formuleren op basis van een Landau-Lifschitz-Gilbert-vergelijking die aangepast is om rekening te houden met de effecten van mechanische rotatie, teneinde de magnetisatiedynamica te modelleren. Ons resultaat is dat de relevante tijdschalen voor de uitlijning van de dominante traagheidsas op het extern magneetveld onafhankelijk zijn van het mechanisch impulsmoment van een deeltje, in tegenstelling tot eerder werk.

In hoofdstuk 5 bespreken we de effecten van mechanische rotatie op een vrije-elektronengas. Door rekening te houden met de orbitale vrijheidsgraden van de elektronen in het roterende assenstelsel vinden we eigentoestanden die lijken op de Landau niveaus van een vrije-elektronengas in een extern magneetveld. Maar, in het geval van rotatie, zien we dat het spectrum van het elektron in het vlak loodrecht op de rotatie-as niet ontaard is, in tegenstelling tot het spectrum van elektronen in Landau niveaus (in het vlak loodrecht op het aangelegde magneetveld).

Verder zien we dat de Barnett-magnetisatie geïnduceerd in een vrije-elektronengas een louter paramagnetisch effect is, in tegenstelling tot de respons op een aangelegd magneetveld.

CURRICULUM VITAE

Stefan BRETZEL

26-04-1979	Born in Friedrichshafen, Germany.
1990–1999	Highschool Graf-Zeppelin-Gymnasium, Friedrichshafen, Germany
2000–2007	Diplom in Physics University of Konstanz, Konstanz, Germany Thesis supervisor: Prof. Dr. Wolfgang Belzig
2003/2004	Graduate exchange student University of Western Ontario, London, Ontario, Canada
2007–2011	PhD research Delft University of Technology Promoter: Prof. dr. ir. G.E.W. Bauer

LIST OF PUBLICATIONS

1. S. Bretzel, G. E. W. Bauer, Y. Tserkovnyak and A. Brataas, *Barnett Effect in Thin Magnetic Films and Nanostructures*, Applied Physics Letters **95**, 122504 (2009).

2. G. E. W. Bauer, S. Bretzel, Y. Tserkovnyak and A. Brataas, *Nanoscale magnetic heat pumps and engines*, Physical Review B **81**, 0244427 (2010).

3. S. Bretzel, G. E. W. Bauer and A. G. G. M. Tielens, *Alignment of rapidly rotating grains of cosmic dust*, in preparation.

4. S. Bretzel, G. E. W. Bauer, A. Brataas and Y. Tserkovnyak, *The Barnett vs. Landau levels in the rotating free electron gas*, in preparation.

ACKNOWLEDGEMENTS

In fall 2006 I started wondering what to do after receiving my Diplom in Physics. Somehow, it occured to me that living a bit further West of my hometown than Konstanz might be fun – "further West" I imagined being somewhere in Canada or the US. By some reasoning I fail to reconstruct right now, I soon convinced myself that the Netherlands might be an improved version of Kansas (flatter and having additional canals and windmills) and that Delft might be worth a shot. And so, just before Christmas 2006, I sent an email to *Gerrit* applying for a position as PhD student. I was pleasantly surprised to find a reply in my in-box within less than half an hour inviting me to Delft for a talk, ideally on the day after tomorrow. During my interview, we discussed aspects of my thesis, whether non-beerdrinking Germans exist, travelling and whether I was the missing half of *Wetzel's Bretzels*. From *Gerrit* I learned not only a lot about Physics and how to discuss it via email, but also lots about Japan and exotic foods – his other two obsessions.

One of *Gerrit*'s aims during my PhD was to infect me with his love for travelling. Right at the start of my PhD, I visited *Yaroslav T.* in Los Angeles. Apart from helping me getting started with my work, we also had long – often wikipedia-fueled – discussions about politics, history and everything else. A year later, I went to visit *Arne* in Trondheim, where I had a near-Robinson Crusoe experience by missing the last boat from Munkholmen Island. My furthest trip took me to Sendai: *Prof. Maekawa* invited me to spend two weeks there in 2009, often discussing physics with me long after I would normally call it a day.

When I moved into F328, I found a friendly Dutch guy sitting there: *Marnix*. In order to thank him for being my guide to everything Dutch as well as serving as my chauffeur whenever I needed one, I propose that the following empirical sociological law should be named after him:

> If a conversation only lasts long enough, Marnix will inevitably comment on Stefan's biblical age and/or ask for the return of his grandfather's stolen bicycle.

Without *Chris*, I would probably have never realized that there is not only a speed limit on highways but also on treadmills – the latter not being police but fuse enforced. Speaking about gym, I also need to mention *Ciprian*, who for a long time

was only our theoretical gym partner before moving to the experimental side, and *Giorgi*. Thanks to *Giorgi*, I also learned how to open front doors without keys.

With both *Fabian* and *Mihajlo* I share a previous supervisor. In fact, *Mihajlo* used to be my "virtual" office mate in Konstanz until he suddenly materialized one day. I owe thanks to *Fabian* for creatively decorating our office in my absence, but I will probably never forgive him for putting the most interesting poster at a place not visible from my desk. Soon after *Alina* joined the group, we realized a remarkable correlation between hers and *Fabian*'s absence (the rest of that story is left to the reader as an exercise). I owe my first exposure to poker – a game I usually loose but still love playing – to *Jeroen* who ran the "Casino Flamingstraat" at the start of my PhD. The first common adventure *Rakesh* and I had, was resetting the language preferences on *Fabian*'s computer from Hungarian to something more understandable – a traumatic experience we analyzed at regular Wednesday-evening sessions at t'Klooster.

I thank *Xuhui* not only for giving me ample opportunity to dissassemble IKEA furniture, but also making me his paranymf. I still have troubles distinguishing his prononciations of Floyd and Freud, thus I always want to ask "Do you mean Pink or Siegmund?" whenever he talks about one of them (my guess is that he usually refers to the latter). There is a lot I have to thank *Jiang* for: Not only was he a valuable source of advice during his stay in Delft, but he also invited me for a six week visit to Fudan University, where he is now a faculty. In addition, he hosted our group's poker evenings for a long time and he was a good business partner – for offering a place to stay during his last weeks in Delft, I received whatever he couldn't sell or take with him to China. Among that such valuable items as numerous Chinese bowls and an odd number of chopsticks. Now, *Yan-Tin*, *Hu-Jun* and *Peng* represent "China" in our group.

In 2009 I had enough of living in downtown Delft and thus started looking for new accomodation. Incidentally, so did *Mireia* and *Joost*. We ended up renting the probably safest place in Delft – just opposite of the police, fire and ambulance stations. I should thank *Mireia* not only for organizing a vast amount of kitchen equipment but also for throwing a number of (surprise – at least they were surprising to me) parties at our place. Without *Joost* I would never have learned that eating fla after dinners is mandatory in this country and that there are about 264 different kinds of stamppot. After a couple of months *Mireia* moved out and *Nestor* in. With *Nestor* I had many interesting discussions about almost everything ranging from politics to the endless topic "Spain compared to Germany resp. the Netherlands". There is one more Spanish I have to mention: *Toni*, who diligently served as my Spanish-English translator whenever I was the only non-Spanish present. *Rodridgo* – so it seems – joined the group for the sole purpose of reminding *Toni* of Spain's or Barcelona's most recent defeat in soccer matches.

Without *Tungky* I would have never learned that there are three levels of spicyness in Indonesian cuisine: Spicy, insanely spicy and some degree of spicyness that can be considered chemical warfare. Thanks to his frequent invitations for dinners, I learned to eat food of the second spicyness degree without turning too red. To *Kim* and *Erin* I am indebted for reviving my long neglected infatuation with board games. Almost two years into my PhD, *Fatemeh J.* came for an interview to Delft. I still remember that after her interview I had to give her – at *Moosa*'s insistence – extremely detailed instructions on how to get from Delft to the doorstep of a hotel in Konstanz, her next destination. Thanks to her, I now know that dried peppermint leaves can be used for more than making infusions, that "The Big Bang Theory" is an accurate depiction of real life (as long as academia can be considered "real life") and just about everything I ever wanted to know about Iran. The latest addition to our group is *Akash*. At the start of his PhD, I was his cooking-hotline ("I bought Frankfurters. Now what?"). However, he has since then progressed far beyond my cooking skills – at least when it comes to Indian-style dishes. I need to thank *Frans* for giving me opportunity to do anthropological field work concerning "Dutch weddings" and to *Fatemeh M.* for providing essential BBQ equipment.

One riddle I could not solve during my PhD is from where *Miriam* takes her constant joyfullness and liveliness, which I not only witnessed during the two semesters I taught for her but also whenever she came to see my office mates. I will remember *Yaroslav* for his stories about travelling, in particular border checks, and for being the human backup of wikipedia (I guess he'll even know the current population of Langenargen – it is 7803). *Yuli* is somewhat of an oracle to me: He often would remark something during coffee breaks that proved hard to understand first, but eventually turned out to be something very deep. He also demonstrated, that Siberian wilderness skills can be easily transferred to Colorado. *Jos* is one of the few true Dutch in the theory group, although his accent suggests he's British. When our previous secretary *Yvonne* retired, the question who would now make coffee and fetch the mail erupted. After a couple of months of heated discussion we were finally saved by *Marjolein*, who has replaced "coffee anarchy" with a "coffee making schedule" and is also extremely good at organizing things more important.

During my years in Konstanz, I shared an apartment and a research assitantship with *Michael*, who became my partner in countless Skype marathons during the last years. Furthermore, I need to thank him for his heroic effort to comment just about every article on my blog. Going even further home, I need to mention my Friedrichshafen friends: *Oli*, with whom my scientific career started as our high school's chemistry nerds, is the other member of "PhD students anonymous, section Friedrichshafen" and my cross-country skiing buddy every winter. *Annette* has pretty much kept me up to date the last years with everything Friedrichshafen related that did not make it to the newspapers as well as being a patient listener

whenever I needed one. My oldest friends are *Wolfgang* and *Andi*, whom I met in a sandbox during our early kindergarden days. They have been my cycling companions (undefeatable opponent would be closer to truth for *Wolfgang*, however) during my summer vacations in Oberschwaben.

Last but not least, I'd like to thank my family. Since space is limited, a general "huge thank you" goes to all my cousins, aunts, uncles and so on. In particular, I'd like to thank *Christian*, *Ingrid* and *Christopher* for their continous efforts to convince me that a "real job" might be indeed something worthwhile. In addition, I'd like to thank my uncle *Georg*, who was always there for advice when I needed one and for hooking me up with a drug called "cycling" – one of my earliest childhood memories is when he carried me on his bicycle all the way to Waldburg somewhen in the early 1980s.

As a small child, I must have been a nuisance since I continously asked a never ending stream of questions – or so my parents tell me. Anyway, Mama, Papa, danke dass ihr meine Wissbegierigkeit gefördert habt – das Ergebnis haltet ihr gerade in den Händen. I also owe you a lot for their support when doing a PhD proved to be everything but a joyride – without you and your love I wouldn't have made it. I also have to thank my mother for being the mysterious artist designing this thesis' cover, while thanks goes to my father for distracting me from hard PhD student life with a continous stream of emails with fun stuff he came up with.

Speaking about emails: For the first half of my PhD I received periodically emails with subject lines like "For the search party" or "Current location" – my brother *Thomas*' way of making me envious of his backpacker life in South-East Asia and Australia. I need to thank him for letting me crash his couch last Easter as well as his continous efforts to improve my musical taste, which – so far – proved to be futile. When I started studying, *Karin* and *Lisa* were still in primary school. Now, at the end of my PhD studies, they are students themselves – time must have progressed in leaps. I owe thanks to *Lisa* for giving me a running tour – in the literal sense of the word – of her university's campus as well as letting me crash her place in Cologne. Thanks to *Karin*'s nosy questions I learned how to explain physics at a kindergarden, primary and high school level. I hope one day she reciprocates by explaining me what this "life" thing is the biologists are constantly talking about.